

BIODEGRADATION OF POLYCYCLIC AROMATIC HYDROCARBONS COMMONLY FOUND IN
COAL SLURRY USING WHITE ROT FUNGI ISOLATED FROM EAST KALIMANTAN



A Dissertation Submitted in Partial Fulfillment of the Requirements
for the Degree of Doctor of Philosophy in Biological Sciences

Common Course

FACULTY OF SCIENCE

Chulalongkorn University

Academic Year 2020

Copyright of Chulalongkorn University

การย่อยสลายทางชีวภาพของพอลิไซคลิกแอโรแมติกไฮโดรคาร์บอนที่มักพบในเลนถ่านหินโดยใช้รา
ไวท์รอตที่แยกจากอีสต์คาลิมันตัน



วิทยานิพนธ์นี้เป็นส่วนหนึ่งของการศึกษาตามหลักสูตรปริญญาวิทยาศาสตรดุษฎีบัณฑิต
สาขาวิชาวิทยาศาสตร์ชีวภาพ ไม่สังกัดภาควิชา/เทียบเท่า
คณะวิทยาศาสตร์ จุฬาลงกรณ์มหาวิทยาลัย
ปีการศึกษา 2563
ลิขสิทธิ์ของจุฬาลงกรณ์มหาวิทยาลัย

Thesis Title BIODEGRADATION OF POLYCYCLIC AROMATIC HYDROCARBONS
COMMONLY FOUND IN COAL SLURRY USING WHITE ROT FUNGI
ISOLATED FROM EAST KALIMANTAN

By Mrs. Retno Wulandari

Field of Study Biological Sciences

Thesis Advisor Associate Professor SEHANAT PRASONGSUK, Ph.D.

Thesis Co Advisor Professor HUNSA PUNNAPAYAK, Ph.D.

Accepted by the FACULTY OF SCIENCE, Chulalongkorn University in Partial Fulfillment
of the Requirement for the Doctor of Philosophy

..... Dean of the FACULTY OF SCIENCE
(Professor POLKIT SANGVANICH, Ph.D.)

DISSERTATION COMMITTEE

..... Chairman
(Assistant Professor JITTRA PIAPUKIEW, Ph.D.)

..... Thesis Advisor
(Associate Professor SEHANAT PRASONGSUK, Ph.D.)

..... Thesis Co-Advisor
(Professor HUNSA PUNNAPAYAK, Ph.D.)

..... Examiner
(Associate Professor PONGTHARIN LOTRAKUL, Ph.D.)

..... Examiner
(Professor ALISA VANGNAI, Ph.D.)

..... Examiner
(SUPAWIN WATCHARAMUL, Ph.D.)

..... Examiner
(Professor Rudianto Amirta, Ph.D.)

..... External Examiner
(Associate Professor Siripong Premjet, Ph.D.)

เรตโน วุแลนตารี :

การย่อยสลายทางชีวภาพของพอลิไซคลิกแอโรแมติกไฮโดรคาร์บอนที่มีกพบในเลนถ่านหินโดยใช้ราไวท์รอตที่แยกจากอีสต์คาไลมันตัน. (BIODEGRADATION OF POLYCYCLIC AROMATIC HYDROCARBONS COMMONLY FOUND IN COAL SLURRY USING WHITE ROT FUNGI ISOLATED FROM EAST KALIMANTAN) อ.ที่ปรึกษาหลัก : สีหนาท ประสงค์สุข, อ.ที่ปรึกษาร่วม : ทรรษา ปุณณะพยัคฆ์

เชื้อราเน่าขาวจำนวน 50 ตัวอย่าง สามารถจำแนกได้เป็น 6 วงศ์ 30 ชนิด พบเชื้อราชนิดแบนราบติดไปกับพื้น (Resupinate) ในวงศ์ Basidiomycota ที่ไม่เคยมีรายงานในอินโดนีเซียมาก่อน (New record) จำนวน 2 ชนิด ได้แก่ *Ceriporia inflata* และ *Ceriporia lacerata* งานวิจัยนี้ได้เสนอวิธีในการคัดแยกเชื้อราเน่าขาว 4 ขั้นตอน และคัดเลือก *Trametes polyzona* PBURU 12 โดยพิจารณาจากประสิทธิภาพการผลิตแลคเคส ซึ่งเป็นเอนไซม์ในกลุ่ม LMEs ได้สูงที่สุดจากตัวอย่าง 30 ไอโซเลต และวางแผนการทดลองด้วย Plackett-Burman design เพื่อคัดเลือกปัจจัยที่เกี่ยวข้องในการผลิตเอนไซม์ พบว่า กลูโคส เบงโทน CuSO_4 และ pH ส่งเสริมให้ PBURU 12 ผลิตแลคเคสได้สูงที่สุด นอกจากนี้ เมื่อใช้เทคนิคพื้นผิวตอบสนอง (Response surface methodology) เพื่อศึกษาภาวะของอาหารที่เหมาะสม สามารถชักนำกิจกรรมของแลคเคสให้เพิ่มขึ้นได้เกือบ 3 เท่า เมื่อเปรียบเทียบกับอาหารพื้นฐาน โดยมี pH ที่เหมาะสมและมีความเสถียรที่ pH 4.5 และ 5.0 ตามลำดับ ซึ่ง PBURU 12 แสดงกิจกรรมของเอนไซม์ได้ในช่วงอุณหภูมิกว้าง ระหว่าง 20-70°C และคงตัวที่ 20-40°C เป็นเวลา 60 นาที การเติม Cu^{2+} กระตุ้นการทำงานของแลคเคส ในขณะที่ Fe^{2+} และ NaN_3 เป็นตัวยับยั้งที่มีศักยภาพ การใช้เอนไซม์หยาบ (1 U/ml) ที่ผลิตโดย PBURU 12 สามารถย่อยสลาย PAHs ได้สูงถึงร้อยละ 50 ภายใน 24 ชั่วโมง การเติม ABTS เพิ่มอัตราการย่อยสลายเป็น 1 เท่า และเพิ่มขึ้นเป็น 2 เท่า เมื่อเพิ่มความเข้มข้นของแลคเคสเป็น 10 U/ml เอนไซม์หยาบของแลคเคสสามารถย่อยสลาย PAHs แบบผสมได้สูงถึงร้อยละ 70 การทดสอบความเป็นพิษต่อยีนด้วย *Allium cepa* L. แสดงให้เห็นว่าการบำบัด PAHs ด้วยแลคเคสสามารถลดความเป็นพิษได้ ในขณะที่ผลการทดสอบ AMES โดยใช้ *Salmonella typhimurium* พบว่า สายพันธุ์ TA 98 และ TA 100 แสดงฤทธิ์ก่อการกลายพันธุ์ที่แตกต่างกันต่อการไม่บำบัดและบำบัด PAHs

สาขาวิชา วิทยาศาสตร์ชีวภาพ
ปีการศึกษา 2563

ลายมือชื่อนิสิต

ลายมือชื่อ อ.ที่ปรึกษาหลัก

ลายมือชื่อ อ.ที่ปรึกษาร่วม

6072872423 : MAJOR BIOLOGICAL SCIENCES

KEYWORD: Crude enzyme; Degradation; Laccase; PAHs; White-rot fungi

Retno Wulandari : BIODEGRADATION OF POLYCYCLIC AROMATIC HYDROCARBONS COMMONLY FOUND IN COAL SLURRY USING WHITE ROT FUNGI ISOLATED FROM EAST KALIMANTAN. Advisor: Assoc. Prof. SEHANAT PRASONGSUK, Ph.D. Co-advisor: Prof. HUNSA PUNNAPAYAK, Ph.D.

Fifty specimens of white-rot fungi were identified and placed into 6 families and 30 species. Two new records of resupinate fungi (Basidiomycota) were discovered and reported for Indonesia: *Ceriporia inflata* and *Ceriporia lacerata*. Furthermore, a four-step screening protocol to select WRF has been conducted. These stepwise protocols have selected *Trametes polyzona* PBURU 12 based on its superior performance among the 30 isolates tested in this experiment with laccase as the major LMEs produced. Plackett-Burman's design was used for screening multiple factors at a time. The result suggested that the highest positive effects influencing laccase production by PBURU 12 were glucose, peptone, CuSO_4 and pH. Furthermore, the response surface methodology (RSM) showed that the optimized medium induced a nearly 3-folds increase in laccase activity compared to the basal medium. The optimum pH and stability were shown at pH 4.5 and 5.0, respectively. PBURU 12 acted in the broad temperature range of 20-70°C and stable at 20-40°C for 60 minutes. Cu^{2+} was showed a stimulatory effect on laccase activity, while Fe^{2+} and NaN_3 were found to be potent inhibitors. Degradation of PAHs using crude laccase (1 U/ml) of PBURU 12 was able to degrade PAHs up to 50% within 24 hours. PAHs degradation were increased to 1-fold when ABTS was added, and up to 2-fold when laccase concentration was increased to 10 U/ml. The crude laccase was capable to degrade the PAHs mixture up to 70%. The genotoxicity experiment using *Allium cepa* L. revealed that the laccase-treated PAHs were less toxic compared to untreated. While the results of the AMES test with *Salmonella typhimurium* revealed that strain TA98 and TA100 showed different mutagenic activity toward untreated and treated-PAHs.

Field of Study: Biological Sciences

Student's Signature

Academic Year: 2020

Advisor's Signature

Co-advisor's Signature

ACKNOWLEDGEMENTS

I would like to express my deepest and greatest gratitude to:

Allah SWT the mighty for granted and listen to all my prayer.

Assoc. Prof. Sehanat Prasongsuk, Ph.D. my thesis advisor for all the excellent suggestions, guidance, patience and encouragement throughout my study.

Prof. Hunsa Punnapayak, Ph.D. my thesis co-adviser, for his excellent supervision, scholarly guidance, valuable recommendations and support throughout my study.

Prof. Seung Wook Kim, Ph.D. at Department of Chemical and Biological Engineering, Korea University for the opportunity to work in his laboratory and his kindly encouragement during his stay in Chulalongkorn University.

Assoc. Prof. Pongtharin Lotrakul Ph.D. for the guidance, suggestions and inputs throughout my study and as one of my dissertation committee.

Prof. Dr. Rudianto Amirta at Faculty of Forestry, Mulawarman University for all the guidance, support, prayer and patience he demonstrates throughout my study and as one of my dissertation committee.

Assist. Prof. Jittra Piapukiew, Ph.D., Prof. Alisa Vangnai Ph.D., Dr. Supawin Watcharamul and Assoc. Prof. Siripong Premjet Ph.D. from Naresuan University for their valuable comments, suggestions and serving as Chairman, committees and external committee on my dissertation defense.

Benjawan Yanwisetpakdee, Ponglada Permpornsakul, Ritbey Ruga, Sopian Hadi, Sorawit Na Nongkhai, Taufiq Haqiqi, Franxisca Mariani and all the members of Plant Biomass Utilization Research Unit for the help, advice on scientific techniques, i-thesis and friendship during my study.

My parents, sisters and brothers for their prayer, love, care and supports during my study.

Finally, my husband Heru Kusdianto that always shows unconditional care and support, always be patient and understanding during my study. To my children who always show great patience and understanding to all my activities to fulfill my study.

Retno Wulandari

TABLE OF CONTENTS

	Page
ABSTRACT (THAI).....	iii
ABSTRACT (ENGLISH).....	iv
ACKNOWLEDGEMENTS	v
TABLE OF CONTENTS	vi
REFERENCES	135
VITA.....	175



TABLE OF CONTENTS

	PAGE
ABSTRACT IN THAI	iii
ABSTRACT IN ENGLISH	iv
ACKNOWLEDGMENTS	v
TABLE OF CONTENTS	vi
LIST OF TABLES	vii
LIST OF FIGURES	
CHAPTER	
I. INTRODUCTION	1
1.1. Rationales	1
1.2. Objectives	2
1.3. Keywords	3
1.4. Anticipated benefits	3
II. LITERATURE REVIEW	4
2.1. Overview of fungi	4
2.2. Diversity of Polyporales in Indonesia White-rot fungi (WRF)	5
2.3. Wood degrading fungi	8
2.4. White-rot fungi and its lignin-modifying enzymes (LMEs)	10
2.5. LMEs screening and production by white-rot fungi	15
2.6. LMEs characterization	19
2.7. Overview of polycyclic aromatic hydrocarbons (PAHs)	20
2.8. Degradation of PAHs by white-rot fungi	25
2.9. PAHs occurrence in coal	28
III. MATERIALS AND METHODS	32
3.1. Materials and Equipment	32
3.2. Chemicals	33
3.3. Collection and isolation of white rot fungi	34
3.4. Morphological observation	34

3.5. DNA isolation, PCR amplification and nucleotide sequencing	35
3.6. Lignin modifying enzyme screening and determination activities	35
3.6.1. Qualitative screening	35
3.6.2. Quantitative assay	36
3.6.3. Protein determination	36
3.7. PAH degradation test and PAH determination	37
3.7.1. PAH tolerance test	37
3.7.2. PAH degradation in liquid medium	37
3.7.3. PAHs determination	38
3.8. Optimization of laccase production medium	38
3.9. Purification and characterization of a laccase from the selected fungal isolate	40
3.9.1. Laccase production profile	40
3.9.2. Purification of extracellular laccase	41
3.9.3. Characterization of the crude and purified laccases	41
3.10. Degradation of PAHs using crude laccase and live fungal mycelia	42
3.11. Toxicity of PAHs degraded products	43
3.11.2. Genotoxicity test	43
3.11.3. Mutagenicity test	44
3.13. Statistical analysis	44
IV. RESULT AND DISCUSSION	45
4.1. Collection and morphological identification of white rot fungi	45
4.2. Screening of white rot fungi for PAH degradation	79
4.2.1. Guaiacol Assay	79
4.2.2. ABTS assay	82
4.2.3. PAH tolerance	84
4.2.4. PAHs degradation in liquid medium by white-rot fungi	87
4.3. Characterization of selected isolate	91

4.3.1.	Molecular identification of isolate PBURU 12	91
4.3.2.	Optimization and production of laccase from PBURU 12	93
4.3.2.1.	Screening of the medium composition for laccase production using the Plackett-Burman design	94
4.3.2.2.	Medium optimization for laccase production using Response Surface Methodology (RSM)	98
4.3.3.	Purification of laccase from PBURU 12	105
4.3.4.	Characterization of the purified laccases	108
4.3.4.1.	pH optimum and stability of the purified laccase of <i>T. polyzona</i> PBURU 12	108
4.3.4.2.	Thermostability of purified laccase of <i>T. polyzona</i> PBURU 12	110
4.3.4.3.	Effect of metal ions and inhibitors on PBURU 12 purified laccase	112
4.3.4.4.	The effect of substrate specificity and kinetic parameters	115
4.4.	Degradation of PAHs using live mycelia and crude laccase of PBURU 12.	117
4.5.	Phytotoxicity and genotoxicity tests of PAHs and treated-PAHs	124
4.6.	Mutagenicity (Ames) test of degraded PAHs	130
V.	CONCLUSION	134
VI.	REFERENCES	136
VII.	APPENDIX	158

LIST OF TABLES

TABLE		PAGE
Table 2.6.	Some physico-chemical characteristic of optimum condition of purified fungal LMEs	20
Table 2.7	Physical-chemical properties and some relevant information of 16 PAHs enlisted as priority pollutants by US EPA (Ghosal et al., 2016)	22
Table 2.8.	Some of PAHs degradation by different species of WRF	26
Table 2.9.	Characteristic of coal washery effluents	31
Table 3.8.1.	The Plackett–Burman design for screening variables in laccase production.	39
Table 3.8.2.	CCD experiment range and levels of independent variables	40
Table 4.1.1.	Morphological comparison of <i>Ceriporia inflata</i> PBURU R1 and <i>C. lacerata</i> PBURU 141 with the type specimens	49
Table 4.1.2.	White rot isolates collected from three zones of Samarinda botanical garden	51
Table 4.2.1.	White rot isolates and their reaction to guaiacol oxidation	81
Table 4.2.2.1.	Secondary screening of white rot fungi on LME agar supplemented with 1 mM ABTS.	83
Table 4.2.4.	Lignin-modifying enzymes (LMEs) profiles of 4 isolates.	90
Table 4.3.2.1.	The Plackett-Burman experimental design observed and predicted values effected laccase production by PBURU 12.	95

Table 4.3.2.2. Analysis of variance (ANOVA) of PBD for laccase production by PBURU 12	96
Table 4.3.2.3. Central composite design matrix and their observed responses for laccase production by PBURU 12	99
Table 4.3.2.4. Analysis of variance (ANOVA) of the Central Composite Design experimental model developed for laccase production by PBURU 12	100
Table 4.3.3.1. Summary of purification step laccase from PBURU 12	106
Table 4.3.4.3.1. Effect of metal ions, inhibitors and chelating agents on PBURU 12 purified laccase	113
Table 4.3.4.3.2. Effect of solvents on PBURU 12 purified laccase	114
Table 4.3.4.4. Substrate specificity and kinetic constants from PBURU 12	115
Table 4.4.1. Degradation (%) of phenanthrene, fluoranthene and pyrene (100 ppm) after 24 hours of incubation with PBURU 12.	118
Table 4.5.1. Genotoxicity of PAHs (100 ppm) and their laccase-treated degradation products against <i>A. cepa</i> root tip cells.	128
Table 4.6. Mutagenic study of phenanthrene (100 ppm) and its laccase-treated degradation products using <i>S. typhimurium</i> strains TA98 and TA100.	131

LIST OF FIGURES

FIGURES		PAGE
Figure 2.2.	Structure of lignocellulosic biomass	9
Figure 2.3.	Degradation of organic pollutant by white rot fungi (WRF) and their oxidative and extracellular ligninolytic systems	11
Figure 2.4.	Model of the catalytic cluster of the laccase from <i>Trametes versicolor</i> made of four copper atoms	15
Figure 2.7.1.	Structures of 16 PAHs	21
Figure 2.7.2.	Structure of phenanthrene containing bay and K region	23
Figure 2.7.3.	Chemical structures, physical and toxicological characteristics of PAHs. The symbols are: (DA) DNA adducts, (SCE) sister chromatid exchange, (CA) chromosomal aberrations, (Ames) <i>Salmonella typhimurium</i> reversion assay, (UDS) unscheduled DNA synthesis, (-) not genotoxic (Cerniglia, 1992).	25
Figure 2.8.	Generalized pathway for the metabolism of PAHs by fungi and bacteria	27
Figure 2.9.	Occurrence of PAHs in raw coal	29
Figure 4.1.1.	Map of Samarinda botanical garden	46
Figure 4.1.2.	Morphological characteristics of <i>Ceriporia inflata</i> PBURU R1 (1); (A) Basidiocarp, (B) Basidiospore, (C) Cystidia, (D) Basidia, (E) Generative hyphae and <i>C. lacerata</i> PBURU 141 (2). (A) Basidiocarp, (B) Basidia and Basidiospore, (C) Generative hyphae.	48
Figure 4.1.3.	Basidiocarp of <i>Bjerkandera adusta</i>	52

Figure 4.1.4.	Basidiocarp of <i>Ceriporia inflata</i>	53
Figure 4.1.5.	Basidiocarp of <i>Ceriporia lacerata</i>	54
Figure 4.1.6.	Basidiocarp of <i>Coriolopsis sanguinaria</i>	54
Figure 4.1.7.	Basidiocarp of <i>Earliella scabrosa</i>	55
Figure 4.1.8.	Basidiocarp of <i>Fomitopsis</i> sp.	56
Figure 4.1.9.	Basidiocarp of <i>Ganoderma australe</i>	57
Figure 4.1.10.	Basidiocarp of <i>Ganoderma applanatum</i>	58
Figure 4.1.11.	Basidiocarp of <i>Gloeoporus dichrous</i>	59
Figure 4.1.12.	Basidiocarp of <i>Lentinus sajur-caju</i>	60
Figure 4.1.13.	Basidiocarp of <i>Lentinus squarrosulus</i>	60
Figure 4.1.14.	Basidiocarp of <i>Lenzites elegans</i>	61
Figure 4.1.15.	Basidiocarp of <i>Microporellus obovatus</i>	62
Figure 4.1.16.	Basidiocarp of <i>Microporus affinis</i>	63
Figure 4.1.17.	Basidiocarp of <i>Microporus xanthopus</i>	64
Figure 4.1.18.	Basidiocarp of <i>Phellinus fastuosus</i>	65
Figure 4.1.19.	Basidiocarp of <i>Polyporus arcularius</i>	66
Figure 4.1.20.	Basidiocarp of <i>Polyporus badius</i>	67
Figure 4.1.21.	Basidiocarp of <i>Polyporus ostreiformis</i>	67
Figure 4.1.22.	Basidiocarp of <i>Pycnoporus coccineus</i>	68
Figure 4.1.23.	Basidiocarp of <i>Pycnoporus sanguineus</i>	69
Figure 4.1.24.	Basidiocarp of <i>Rigidoporus microporus</i>	70
Figure 4.1.25.	Basidiocarp of <i>Schizophyllum commune</i>	71
Figure 4.1.26.	Basidiocarp of <i>Trametes lactinea</i>	71
Figure 4.1.27.	Basidiocarp of <i>Trametes hirsuta</i>	72
Figure 4.1.28.	Basidiocarp of <i>Trametes menziesii</i>	74
Figure 4.1.29.	Basidiocarp of <i>Trametes polyzona</i>	75
Figure 4.1.30.	Basidiocarp of <i>Trametes versicolor</i>	75
Figure 4.1.31.	Basidiocarp of <i>Trichaptum bifforme</i>	76
Figure 4.1.32.	Basidiocarp of <i>Junghuhnina</i> sp.	77

Figure 4.2.1.	Phenoloxidase agar assay using 0.01% guaiacol sequentially; Control agar; yellowish (Y); light brown (LB); brown (B); dark brown (DB).	80
Figure 4.2.2.	LME agar assay supplemented with 5 mM ABTS after 3 days of cultivation. A. No reaction to ABTS; B. Color zone with limited growth; C. Color zone with growth	82
Figure 4.2.3.	Relative growth (%) of selected WRF isolates against fluoranthene, phenanthrene and pyrene in different concentrations.	86
Figure 4.2.4.	Degradation (%) of 100 ppm PAHs by selected isolates cultivated using basal medium at 30°C, shaking 150 rpm for 15 days. (A) Phenanthrene-100 ppm; (B) Fluoranthene-100 ppm; (C) Pyrene-100 ppm.	88
Figure 4.3.1.	Phylogenetic tree of genus <i>Trametes</i> related to PBURU 12. Bar 0.05 = base substitution. Bootstrap values are shown next to the branches.	92
Figure 4.3.2.1.	Pareto chart of factors effects on laccase production by PBURU 12	94
Figure 4.3.2.5.	Normal probability plot residual of laccase activity (A) and perturbation graph for 4 factors affecting laccase activity.	101
Figure 4.3.2.6.	Three-dimensional response surface plots of the effect combinations on laccase production by <i>T. polyzona</i> PBURU 12	102
Figure 4.3.2.7.	Time course and growth of laccase production by PBURU 12 at room temperature, Shaked at 150 rpm in (A) the basal and (B) optimized medium. Results showed as a mean with standard deviation from three replications.	104

- Figure 4.3.3.2. Chromatographic profile of laccase activity and absorbance at 280 nm after fractionation using HiTrap Q Sepharose Fast Flow (FF) anion-exchange column. 106
- Figure 4.3.3.3. The SDS-PAGE analysis of purified laccase of *T. polyzona* PBURU 12: Lane 1; molecular weight protein marker; 2; purified laccase (10 µg of protein) 107
- Figure 4.3.4.1. Effect of pH on laccase activity (a); stability of laccase after incubation for 60 minutes (b) and stability of laccase after incubation for 24 hours (c). 109
- Figure 4.3.4.2. Effect of temperature on laccase activity (a); stability of laccase after incubation for 60 minutes (b) and stability of laccase after incubation for 24 hours (c). 111
- Figure 4.3.4.4. Lineweaver-Burk plot of the purified laccase from PBURU 12 using different substrates. 116
- Figure 4.4.1. PAHs degradation using crude enzyme of PBURU 12 for 1 and 24 h at 30 °C with continuous shaking at 150 rpm in dark condition. 121
- Figure 4.4.2. HPLC chromatograms of mixed-PAHs degradation by PBURU 12 crude laccase (10 U/ml). The media containing fluorene, phenanthrene, fluoranthene, and pyrene at 100 ppm each. Representative HPLC chromatograms from 24 hours mixture of PAHs (A) mixed-PAHs control and (B) Treated mixed-PAHs. The retention time of phenanthrene, fluoranthene, and pyrene were ± 5.21, 6.16, and 6.88 minutes, respectively. 123
- Figure 4.5.1. Root length of *Allium cepa*. Values are mean ± SD of five samples 125

CHAPTER I

INTRODUCTION

1.1. Rationales

East Kalimantan is the second largest island in Indonesia, covering the total area of 139,461.82 square kilometers. The province is rich in natural resources, especially oils, minerals and tropical forest products (Jepson & van Noord, 2002). Over-exploitation of natural resources by industry and the urban population has caused huge environmental problems such as landslides, floods, deforestation and pollution of the soil, water and air. Following in the footsteps of the forestry industry, coal mining has become a massive industry in East Kalimantan, resulting in a large number of sites contaminated by persistent chemicals from coal dredging and blackwater slurry from coal washing, threatening the already endangered biodiversity. The most commonly found chemicals in coal slurry are heavy metals, acrylamides, polycyclic aromatic hydrocarbons (PAHs) and other chemicals that are categorized as hazardous, carcinogenic and toxic to human health (Doyle et al., 2008). PAHs commonly found in coal slurry include naphthalene, phenanthrene, toluene, benzo (a) anthracene, pyrene, chrysene, xylene, etc. (Valentin et al., 2006). During the past decades, researchers have been focusing on the isolation of white rot fungi that are able to degrade different recalcitrant organic compounds, such as PAHs, in soil and wastewater using the activities of their lignin modifying enzymes (laccases and peroxidases) (Baldrian, 2006; Cabana et al., 2007). Nevertheless, the application of white rot fungi for biodegradation has been limited by their poor competitive growth in the presence of such recalcitrant and toxic compounds (Singh & Kapoor, 2014). Recently, a number of white rot basidiomycetes have been reported for their ability to compete, grow and breakdown the contaminants. However, the studies have been limited only to a few species that show great potential in bioremediation (Singh & Kapoor, 2014). An effort to seek out other species has been conducted in East Kalimantan (Hadibarata et al., 2012). The use of such local isolates is preferred over foreign isolates due to the

ecological cautionary of alien species' introduction. East Kalimantan tropical forest covers 14.651.553 ha and is recognized for its biologically diverse ecosystems, suggesting a high fungal diversity (Yamashita et al., 2009). The study of *Armillaria* sp., *Pleurotus eryngii*, *Polyporus* sp. from East Kalimantan tropical forest on biodegradation of various recalcitrant compounds such as PAHs, dyes and lignin polymers showed comparable results to those of other previously reported foreign species (Hadibarata, 2013; Hadibarata & Kristanti, 2013; Hadibarata & Tachibana, 2010). However, the properties of oxidative enzymes such as laccases from these fungi and their ability to degrade PAHs at higher concentrations like those in coal slurry have not been investigated. Therefore, the purposes of this study are to (i) isolate laccase producing white rot fungi from East Kalimantan, (ii) produce, purify and characterize a laccase from a selected isolate, (iii) investigate the potential of using the enzyme and live fungal culture to degrade selected PAHs commonly found in coal slurry, and (iv) investigate the toxicity effect of PAHs after degradation. The results obtained from this study will contribute to the basic and applied knowledge of white rot fungi from East Kalimantan regarding their diversity and their potential to be used as a remediation agent for coal slurry treatment.

1.2. Objectives

1. To isolate the laccase-producing white rot fungi in Samarinda Botanical Garden, East Kalimantan.
2. To optimally produce, purify and characterize the laccase enzyme from selected fungal isolate.
3. To assess the potential of using the selected laccase in bioremediation of some polycyclic aromatic hydrocarbons commonly found in coal slurry in East Kalimantan.
4. To investigate the phytotoxicity, genotoxicity and mutagenicity effects of PAHs after degradation.

1.3. Keywords

Crude enzyme; degradation; laccase; PAHs; white-rot fungi

1.4. Anticipated benefits

Information obtained from this study will lead to the better understanding in diversity of white rot fungi in East Kalimantan, Indonesia and their potential to be used for bioremediation of polycyclic aromatic hydrocarbons.



CHAPTER II

LITERATURE REVIEWS

2.1. Overview of fungi

Fungi are eukaryotic, spore-producing organisms with absorptive nutrition that generally reproduce both sexually and asexually, usually as filamentous, branched somatic structures known as hyphae (Alexopoulos et al., 1996). Fungi have a significant role in nature and human life, such as decomposers, producers of important antibiotics, enzymes and acting as a biological control (Bilal et al., 2017; Evans et al., 2001; Hyde et al., 2019). On the other hand, fungi also become a foe for nature and human life. They caused food spoilage, plant diseases and produced mycotoxins (Hyde et al., 2019). There are many mushroom species that have yet to be described in the world, properly recorded, especially in tropical regions such as Indonesia. The tropical rain forest in Indonesia covers an area with a high rainfall intensity, as well as wet and humid environmental conditions, making the tropical rain forest an ideal environment for the growth of many organisms, including fungi (Gallery, 2014). It is estimated that there are 1,5 million mushroom species in the world, in which around 28,700 macroscopic mushrooms, 24,000 of microscopic mushrooms, and 13,500 types of lichens have been discovered, whereas 1,433,800 species, both macro and micro, have not been discovered (Laessøe & Lincoff, 2002). Among these species, 1,800 are thought to have beneficial metabolites for treatment, with only about 10% containing toxins. In Indonesia, two hundred thousand (13.3%) of these species are possible (Putra et al., 2019). Most fungi that grow in tropical rain forests are decomposers degrading living foliage on the forest floor, but among many of these fungi are saprophyte fungi that grow by attaching to trees in the tropical rain forest. East Kalimantan is the second largest island in Indonesia, which covers 14.651.553 ha of forest. The tropical rainforest of East Kalimantan is recognized for its biologically diverse ecosystems. Fungal diversity

in East Kalimantan is expected to be relatively high due to the species richness of woody plants, the most important biomass used by the fungi. In addition, an earlier survey conducted by Tropenbos, Mulawarman University and Bogor Agricultural Institute for Gunung Lumut Biodiversity Assessment in Protection Forest in 2005, found more than 100 species of macroscopic fungi (Tropenbos International Indonesia, 2005). This makes the inventory of mushroom variants in Indonesia an important step in efforts to utilize and conserve existing germplasm (Putra et al., 2019).

The most recent fungal taxonomy includes the described diversity of known 'true fungi' (Whittaker, 1969). The following characteristics have been described for true fungi: having β -glucan and (generally) chitin cell wall; mostly unicellular or growing as a mycelium with multinucleated, walled, cylindrical cells of variable size; and flattened mitochondrial cristae (Whittaker, 1969). True fungi are divided into nine major lineages: Opisthokonta, Chytridiomycota, Neocallimastigomycota, Blastocladiomycota, Zoopagomycota, Mucoromycota, Glomeromycota, Ascomycota and Basidiomycota (Naranjo-Ortiz & Gabaldón, 2019).

2.2. Diversity of Polyporales in Indonesia

The Agaricomycetes contain large concentrations of wood decayers, litter decomposers and ectomycorrhizal fungi, along with relatively small numbers of important pathogens of timber (Hibbett, 2006). Agaricomycetes is a Basidiomycota clade that contains approximately 21,000 described species, accounting for one-fifth of all known fungi (Hibbett et al., 2014). However, new taxa are constantly being discovered, being described, and molecular ecologists routinely detect Agaricomycetes DNA sequences that cannot be attributed to known species, implying that the group's actual diversity is far greater than and surpasses the current catalog (Hibbett et al., 2014; Hibbett, 2006). Agaricomycete systematists have traditionally used morphological, biochemical, and ecological characteristics to develop phylogenetic hypotheses and structure classifications. Anatomical features (e.g., shapes and staining reactions of spores, basidia, and cystidia, hyphal systems of fruiting bodies, rhizomorph

structures), macro-morphology of fruiting bodies (including developmental characters), pigment chemistry, cytological characters, wood-decay modes (white rot vs. brown rot), and asexual reproductive forms have all been used to address relationships and provide identification tools (Hibbett, 2006).

The most studied Agaricomycetes belong to the order Polyporales. From 2010 to 2017, there were 577 taxonomic proposals in Polyporales submitted to Mycobank, while during the same time span, PubMed recorded 2183 publications with the keyword 'Polyporales' (Justo et al., 2017). The Polyporales are a large group of macrofungi, which divided into eight families namely *Bondarzewiaceae*, *Coniophoraceae*, *Corticaceae*, *Fistulinaceae*, *Ganodermataceae*, *Hymenochaetaceae*, *Polyporaceae*, and *Thelephoraceae* (Bolhassan et al., 2012). Furthermore, Polyporales are a group of fungi that includes important wood decomposers in forest ecosystems (Hattori, 2017). Polyporales are commonly found in the pantropics, which have higher relative temperatures, humidity, and rainfall frequency (Tianara et al., 2020). According to Dai (2012), 704 polypore species from 132 genera and ten orders were identified, with the majority of them belonging to the orders Polyporales and Hymenochaetales from all forest types in China, with WRF reporting on the majority of Polyporales collected. Furthermore, Hattori (2017) also revealed there were 403 newly described Polyporales from the Malesian and Papuan regions in the 19th and early 20th centuries. *Microporus affinis* (Blume & T. Nees) Kuntze is one of the most frequent species in both the warm temperate to subtropical Castanopsis forests of Japan and the lowland rainforests of Malesia (Hattori, 2017).

Polyporales collection and taxonomy studies have been conducted extensively throughout Indonesia in a variety of areas and provinces. Rahmawati (2018) investigated the diversity of macroscopic fungi (Basidiomycetes) in the Bayur Forest, Landak Regency, West Borneo, and discovered a dominant group of Aphyllorphorales and Polyporales fungi. These include *Pycnoporus sanguineus*, *Polyporus versicolor*, *Polyporus varius*, *Schizophyllum commune*, *Thelephora palmata*, *Earliella scabrosa*,

Lignosus rhinocerus, *Trametes versicolor*, *Heterobasidion annosum* and *Ganoderma applanatum*. Furthermore, eleven new records of polyporales species for Indonesia from Java were listed, documented and morphologically described by Tianara et al. (2020). The lists included *Gloeophyllum subferrugineum*, *Inonotus tabacinus*, *Hymenochaete luteobadia*, *Amauroderma leptopus*, *Ganoderma colossus*, *Rigidoporus ulmarius*, *Cellulariella acuta*, *Cerrena unicolor*, *Funalia caperata*, *Funalia* sp. and *Perreniporia martia*. Additionally, Mardji and Noor (2009) was conducted a research in Gunung Lumut Protection Forest, East Kalimantan and found that 32 species of macrofungi belongs to Polyporales group among them are *Amauroderma* sp., *Coriolopsis* sp., *Elfvigia* sp., *Fomes annosus*, *Ganoderma adpersum*, *Ganoderma applanatum*, *Ganoderma* sp., *Hymenochaete rubiginosa*, *Nigrofomes* sp., *Oxyporus* sp., *Phellinus igniarius*, *Piptoporus betulinus*, *Polyporus* sp., *Polyporus xanthopus*, *Pyrrhoderma sendaiense*, *Rigidoporus* sp., *Trametes* sp., and *Trametes gibbosa*, respectively.

Resupinate fungi are term refers to corticioid and polypore fungi that produce a flat fruiting body that mostly addressed to the substrate (Gates, 2009). The term corticioid refers to something that resembles a member of the genus *Corticium*, which is the type genus for the family *Corticaceae* (Larsson, 2007). The term came into use when Donk (1964) attempted to classify the Aphyllophorales (homobasidiomycetes without gills) into well-defined families. The resupinate fungi are a diverse group of fungi that appear very similar to the naked eye until examined under a microscope, revealing their diverse microscopic structures (Gates, 2009). As efficient wood decomposers, these fungi are common in tropical forests. There are currently up to 1853 resupinate polypore species in 282 genera and 50 putative families: In Asia, 766 species have been reported (Hjortstam & Ryvarde, 2007; Permpornsakul et al., 2016). Taxonomic and systematic studies of resupinate fungi have primarily relied on their morphology because molecular data, particularly from tropic regions, is scarce (Permpornsakul et al., 2016). Studies on resupinate fungi have recently been

conducted in the tropical areas of southern China and Thailand, with many new species described (Jia & Cui, 2013; Jia et al., 2013; Permpornsakul et al., 2016). While limited studies of resupinate fungi have been conducted in Indonesia, A study of resupinate fungi from Sumatra and East Kalimantan *Acacia Mangium* plantation forest has been conducted by Glen et al. (2014). They identified *Peniophora* sp., *Phanerochaete* sp., *Phlebia* sp., and *Phlebiopsis* sp. using molecular approach.

2.3. Wood degrading fungi

Wood and lignified gramineous and other annual plants are generally called lignocellulose because they are composed of the three main natural polymers: cellulose, hemicelluloses and lignin (Hatakka & Hammel, 2010). Cellulose is a linear polymer made up of D-glucose subunits linked together by β -1,4 glycosidic bonds to form the dimer cellobiose. These combine to form long chains (or elemental fibrils) that are held together by hydrogen bonds and van der Waals forces. Cellulose is typically found in crystalline form, with a small amount of non-organized cellulose chains forming amorphous cellulose (Sánchez, 2009). Cellulose comprises 40–50% of lignocellulosic biomass feedstock (Alonso et al., 2012). Hemicellulose, a polysaccharide with a lower molecular weight than cellulose is formed from D-xylose, D-mannose, D-galactose, D-glucose, L-arabinose, 4-O-methyl-glucuronic, D-galacturonic, and D-glucuronic acids which comprise from 15-30% of the biomass (Alonso et al., 2012; Hatakka & Hammel, 2010; Sánchez, 2009). Sugars are held together by β -1,4- and occasionally β -1,3-glycosidic bonds. The main difference between cellulose and hemicellulose is that hemicellulose has branches with short lateral chains made up of various sugars, whereas cellulose is made up of easily hydrolyzed oligomers which are linked together by lignin, forming a physical seal that is an impenetrable barrier in the plant cell wall (Sánchez, 2009). Lignins are formed through the oxidative coupling of p-hydroxycinnamyl alcohol monomers with p-coumaryl, coniferyl, and sinapyl alcohol units, which account for 15-30% of biomass weight (Alonso et al., 2012; Hatakka & Hammel, 2010; Sánchez, 2009). Lignin strengthens plant

cell walls through the adhesion of layers of cellulose microfibrils, allowing plants to significantly expand in body size, improve water transport, resistance to pathogens, and slow the degradation of wood by microorganisms (Janusz et al., 2017).

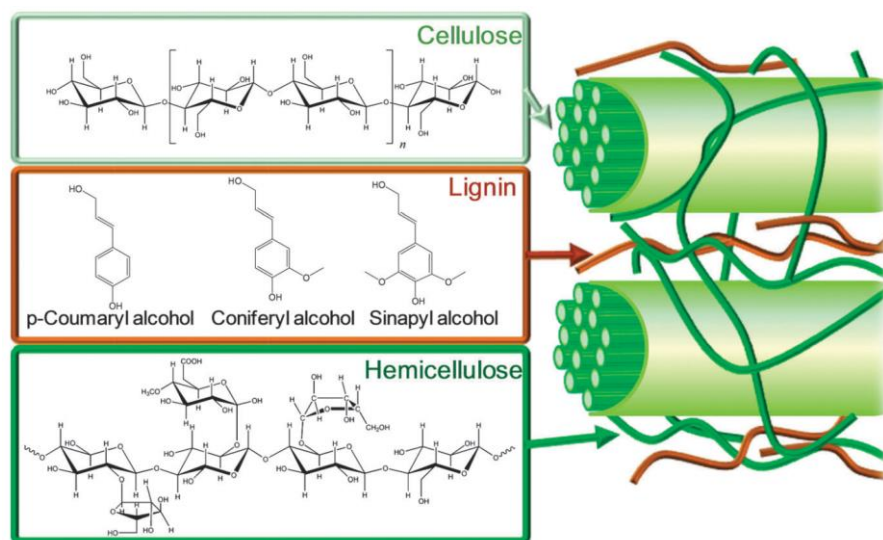


Figure 2.2. Structure of lignocellulosic biomass (Alonso et al., 2012).

Fungi are the organisms most responsible for lignocellulose degradation (Sánchez, 2009). Wood degrading fungi are divided into brown-rot and white-rot fungi (Hatakka & Hammel, 2010). These types of fungi have a well-developed enzymatic system that allows them to grow well on a wide variety of natural and synthetic substrates which are able to produce and secrete extracellular enzymes at a higher rate into their peripheral environment, degrading various substrates to small molecules that are absorbed and metabolized in their cells (Goltapeh et al., 2013). Brown-rot fungi degrade cellulose, hemicellulose and modify lignin. Brown-rotted wood residue is dark, shrinks and is typically broken into cubical fragments. The brown color indicates the presence of modified lignin in wood (Hatakka, 2001). White-rot fungi (WRF), which are primarily a group of Basidiomycota, are a physiological group of basidiomycetes that have a remarkable ability to degrade lignin and lignin-like substances by giving the wood a bleached white appearance (Pointing, 2001). They can degrade both lignin and

cellulose biopolymers within lignocellulose biomass, and they have the unique ability to degrade lignin efficiently by producing synergistic ligninolytic enzymes (Sánchez, 2009). Furthermore, WRF contains distinct oxidative and extracellular ligninolytic systems with low substrate specificity, allowing them to transform or degrade a wide range of environmental contaminants (Zhuo & Fan, 2021). As a result, this study focused on white rot fungi.

2.4. White-rot fungi and its lignin-modifying enzymes (LMEs)

White-rot fungi (WRF) are a physiological rather than taxonomic grouping of fungi capable of degrading lignin (a heterogeneous polyphenolic polymer) within lignocellulosic substrates extensively. The term "white-rot" refers to the appearance of wood attacked by these fungi, in which lignin removal causes the substrate to appear bleached (Pointing, 2001). White-rot fungi, like most fungi, exist primarily as branching threads called hyphae that grow from the tips and are usually 1 to 2 in diameter. Hyphae invade wood cells and lie along the lumen walls after emerging from spores or nearby colonies that secrete enzymes and metabolites that cause the depolymerization of hemicelluloses and cellulose, as well as the fragmentation of lignin (Kirk & Cullen, 1998).

White-rot fungi (WRF) secrete one or more of three extracellular enzymes that are required for lignin degradation and work in tandem with other processes to result in lignin mineralization and also known as lignin-modifying enzymes (LMEs) (Pointing, 2001). These extracellular ligninolytic systems are also effective xenobiotic defenses and are distributed differently among WRF (Zhuo & Fan, 2021). Some researchers have classified WRF into four groups based on their ligninolytic enzyme composition and secretion (Figure 2.3): (i) LiP, MnP, and laccase producing strains; (ii) MnP and laccase producing strains; (iii) LiP and MnP producing strains; and (iv) LiP and laccase producing strains (Bilal et al., 2017). Among the wide diversity of evaluated fungi, *Phanerochaete chrysosporium* was one of the first widely studied WRF (Tortella et al., 2015).

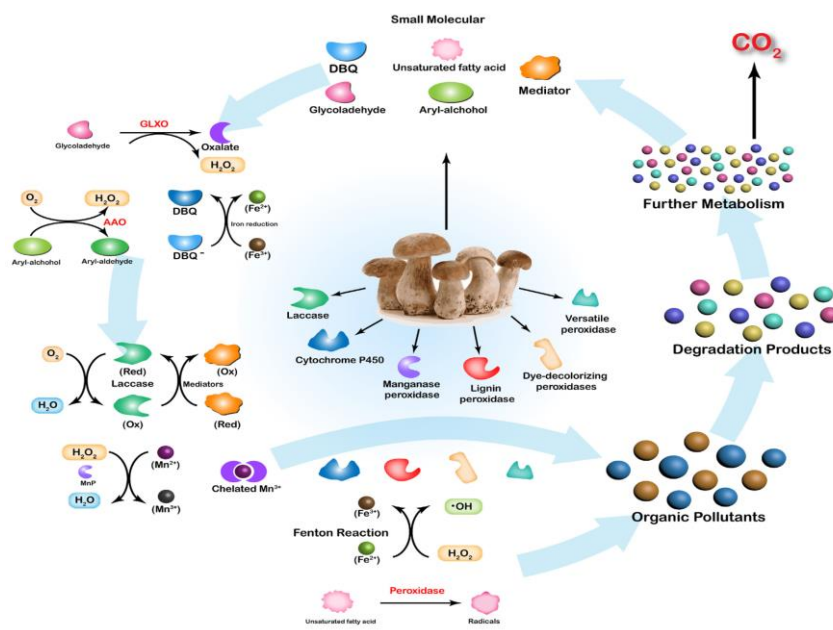


Figure 2.3. Degradation of organic pollutant by white rot fungi (WRF) and their oxidative and extracellular ligninolytic systems (Zhuo & Fan, 2021).

White-rot fungi have a wide variety of enzymes, including extracellular ligninolytic enzymes (lignin peroxidases, manganese peroxidase, and laccase) (Teerapatsakul et al., 2007). White rot fungi secrete one or more extracellular non-specific LMEs that are involved in the degradation of several recalcitrant aromatic compounds, including synthetic dyes, polycyclic aromatic hydrocarbons, plastic, biocides, explosives, inks, perfumes, photographic materials (Tišma et al., 2010).

Lignin peroxidase (LiPs, ligninase, EC 1.11.1.14) catalyzes the H_2O_2 -dependent oxidative depolymerization of lignin (Piontek et al., 2001). LiPs are monomeric hemoproteins with molecular masses of around 40 kDa, and their Fe(III) is pentacoordinated to four heme tetrapyrrole nitrogens and a histidine residue, similar to classical peroxidases such as horseradish peroxidase (HRP). LiP has a peroxidase catalytic cycle that is similar to HRP's (Abdel-Hamid et al., 2013). LiPs are stronger oxidants with a higher redox potential than classical peroxidases, since the iron in the porphyrin ring in LiPs is more electron deficient than in classical peroxidases (Millis et

al., 1989). In the presence of (endogenously generated) H_2O_2 , LiP catalyzes the oxidation of veratryl alcohol, which then undergoes one-electron oxidation of non-phenolic aromatic nuclei in lignin to generate aryl cation radicals (Reddy & D'Souza, 1994). These are then non-enzymatically degraded into aromatic and aliphatic products that are mineralized intracellularly. The radicals produced can undergo a variety of reactions, such as benzylic alcohol oxidation, carbon-carbon bond cleavage, hydroxylation, phenol dimerization/polymerization, and demethylation (Pointing, 2001). *Phanerochaete chrysosporium* is a model ligninolytic microorganism with multiple LiPs genes that secrete the enzymes as isozymes (Biko et al., 2020). *Phanerochaete sordida*, *Phlebia radiata*, *Trametes versicolor*, *Pleurotus eryngii*, *Pleurotus ostreatus*, and *Bjerkandera adusta* are some other notable class II peroxidase producers (Ayuso-Fernández et al., 2017).

Manganese peroxidase (MnP, E.C.1.11.1.13) is glycosylate protein and contains heme as the prosthetic group (Hofrichter, 2002). Manganese peroxidase oxidizes Mn(II) to Mn(III) which then oxidizes phenolic rings to phenoxy radicals, leading to the decomposition of the structures (Hatakka & Hammel, 2010). MnP has a molecular weight (MW) ranging from 38 to 62.5 kDa, but most purified enzymes have MWs around 45 kDa (Hofrichter, 2002). The catalytic cycle of manganese peroxidase is similar to that of lignin peroxidase and other peroxidases but requires the presence of Mn^{2+} to complete the cycle (Hofrichter, 2002). To break the peroxide dioxygen link and create manganese peroxidase compound I, a two-electron transfer from the heme is required. Subsequent reduction is carried out by manganese peroxidase compound II. Compound II is formed by oxidizing Mn^{2+} ion to Mn^{3+} and acting as a one-electron donor. Compound II is reduced by the synthesis of additional Mn^{3+} from Mn^{2+} , which results in the production of native enzyme (Hofrichter, 2002). High concentrations of H_2O_2 cause reversible inactivation of MnP and the formation of compound III (Wariishi et al., 1992). The presence of ligands such as malonate and oxalate assist in the stabilisation of Mn^{3+} ions and promotes their release from the enzyme into the

surrounding environment (Hofrichter, 2002). Manganese peroxidase also catalyses the oxidation of several mono-aromatic phenols, including aromatic dyes. In contrast to LiP, MnPs are widespread among lignin-degrading fungi including both rot and litter-decomposing basidiomycetous species (Hatakka, 2001). The ability to synthesize MnP is found in many different taxonomic groups of basidiomycetes. MnP has been found to be expressed and secreted by typical wood colonizers of phylogenetically older families such as *Meruliaceae*, *Coriolaceae*, and *Polyporaceae*, as well as soil-litter colonizers of Euagaric families such as *Strophariaceae* and *Tricholomataceae* (Hofrichter, 2002).

Laccase (Lac, benzenediol: oxygen oxidoreductase, EC 1.10.3.2) belongs to a group of polyphenol oxidases containing copper atoms in the catalytic center and usually called multicopper oxidases (Baldrian, 2006). Laccases from fungi are frequently found as isoenzymes that oligomerize to form multimeric complexes. The monomer's molecular mass ranges between 50 and 100 kDa. A covalently linked carbohydrate moiety (10–45%) is an important feature that may contribute to the enzymes' high stability (Claus, 2004). A minimum of four copper atoms per active protein unit are required for catalytic activity (Figure 2.4): Type 1: paramagnetic 'blue' copper with 610 nm absorbance; Type 2: non-blue paramagnetic copper; Type 3: diamagnetic spin-coupled copper-copper pair with 330 nm absorbance (Claus, 2004). Laccase catalysis is believed to comprise three major steps: 1. Type 1 Cu reduction by reducing substrate; 2. Internal electron transfer from type 1 Cu to type 2 and type 3 Cu trinuclear cluster; 3. O₂ reduction (to water) at type 2 and type 3 Cu (Gianfreda et al., 1999). Although laccase is commonly found in wood-degrading basidiomycetes, their redox potentials are low, allowing only the oxidation of phenolic lignin units (which often account for less than 10% of the polymer) (Hatakka, 1994). A lower oxidation potential of the substrate or a higher redox potential of the laccase (type 1 site) frequently results in a faster rate of substrate oxidation, indicating that the electron transfer (from the substrate to the laccase) corresponds to Marcus' "outer-

sphere" mechanism type (Gianfreda et al., 1999). Camarero et al. (2005), stated that the broad substrate specificity of laccases together with the use of molecular oxygen as the final electron acceptor make these enzymes highly interesting for industrial and environmental applications. However, the redox potential of laccases is low (>1 V) compared to the other peroxidase enzymes which only allow laccases to degrade only low-redox-potential compounds. Therefore, the presence of certain small-molecular weight compounds that act as redox mediators is able to expand the catalytic activity of the laccase towards more recalcitrant compounds such as non-phenolic compounds (Camarero et al., 2005). ABTS (2,2'-azino-bis(3-ethylbenzothiazoline-6-sulfonic acid), TEMPO(2,2,6,6-tetramethylpiperidin-1-yl)Oxyl) and 1-hydroxybenzotriazole (HBT) are well-known laccase redox mediators (Bourbonnais & Paice, 1990; Cañas & Camarero, 2010). Despite the demonstrated efficacy of case-mediator systems, the use of these synthetic mediators is hampered by their high cost and the generation of potentially toxic compounds. Therefore, a number of studies on the alternative mediators which naturally occur in the environment have been conducted (Camarero et al., 2005). Of such natural mediators, 3-hydroxyanthranilic acid (3-HAA), 4-hydroxybenzoic acid and acetosyringone are a few examples (Cañas & Camarero, 2010). In spite of such limitations, laccases have been broadly used in biotechnological and environmental applications. In environmental applications, laccase has been used as an enzyme that is responsible for the degradation of lignin, polycyclic aromatic hydrocarbons (PAHs), phenols, humic acid, pesticides, synthetic dyes and endocrine disrupting chemicals (EDCs) (Cabana et al., 2007; Gianfreda et al., 1999).

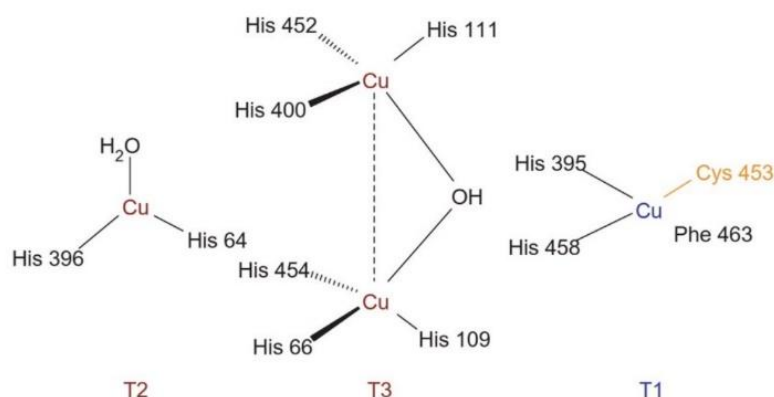


Figure 2.4. Model of the catalytic cluster of the laccase from *Trametes versicolor* made of four copper atoms (Riva, 2006).

2.5. LMEs screening and production by white-rot fungi

The primary purpose of screening is to identify fungi with desirable properties for use in a variety of applications, such as bioremediation of industrial wastewater and contaminated sites and lignocellulolytic enzyme production (Ang et al., 2011). Most screenings classify ligninolytic enzyme activities as either present or absent in specific fungi, while very few studies link fungal growth to ligninolytic enzyme activities (Viswanath et al., 2010). The activities of ligninolytic enzymes are closely related to fungal growth. The association of ligninolytic activities with growth has the advantage of providing a good indication of fungal growth based on colony size determined from screening plates. Thus, by interpreting the ratio of halo to fungal colony against the incubation period, a quantitative method for measuring ligninolytic enzyme activity can be developed (Ang et al., 2011). Common screening reagents used are guaiacol, 2,2-azino-bis (3-ethylbenzthiazoline-6-sulphonic acid) (ABTS), syringaldazine and polymeric dyes like Remazol brilliant blue-R (RBB-R) (D'Souza et al., 1999; Kameshwar & Qin, 2017). The colorless guaiacol and ABTS are oxidized in the presence of phenol oxidases to form reddish-brown and green compounds, respectively (Afrida et al., 2009; Thongkred et al., 2011). In the presence of laccase, the pale yellow syringaldazine is

oxidized to a purple-colored compound, whereas the blue RBB-R dye is decolorized by the combined action of peroxidases and hydrogen peroxide-producing oxidases (Ang et al., 2011).

Solid-state fermentation (SSF) is defined as the growth of filamentous fungi on a solid substrate in the absence of free water, but with enough water present to support their growth and metabolism (Fazenda et al., 2008). However, it is frequently a slow process. In addition, SSF is difficult to monitor, control, and scale-up. As a result, submerged fermentation (SMF) has emerged as the preferred fermentation method for commercial applications. Submerged fermentation involves the nurturing of microorganisms in a high oxygen concentrated liquid nutrient medium (Shraddha et al., 2011). SMF is less problematic by definition (heat and oxygen mass transfer are much better, and culture homogeneity is usually superior), making it more reliable and reproducible, easier to monitor and control key operational parameters, and more flexible (Fazenda et al., 2008). In general, lignocellulosic agro-industrial residues stand out as substrates for mycelial growth in various culture media, whether solid-state fermentation (SSF) or submerged fermentation (SMF), because they contain significant amounts of nitrogen, carbohydrates, minerals, and vitamins, in addition to the typical cellulose, hemicellulose, and lignin composition (da Silva Vilar et al., 2021).

White-rot fungi have evolved to exploit a wide range of habitats. As a result, different species necessitate different conditions for optimal growth. Fungi consume lignocellulosic materials as food. As these materials are mainly cellulose-based, they are high in carbon but low in nitrogen and phosphorus. (Winquist, 2014). Furthermore, fungi can reuse the nitrogen stored in their biomass (Winquist, 2014). Older hyphae are autolyzed, and the released nitrogen is transported to the growing hyphae (Carlile et al., 2001).

LMEs production occurs during secondary metabolism and is triggered by nutrient deficiency, particularly nitrogen deficiency. However, under nitrogen sufficiency conditions, some taxa have been shown to produce LiP, MnP, and Laccase.

LiP and MnP production are generally optimal at high oxygen tensions but is inhibited by agitation of fungi grown in submerged liquid culture (in contrast, Laccase production is generally enhanced by agitation) (Pointing, 2001). Suitable growth conditions are important for WRF to produce maximal LMEs.

High activities of MnP were produced by *Phanerochaete chrysosporium* while cultivated with high glucose in a nitrogen limited-medium (Zhou et al., 2007). In contrast, Tekere et al. (2001) found that high manganese peroxidase and laccase activities were highest for *Trametes versicolor* and *Lentinus velutinus* when both carbon and nitrogen in the medium were present at high levels. While *Trametes cingulata*, *Trametes elegans* and *Trametes pocas* produced the highest MnP activities in a medium containing high carbon and low nitrogen conditions. While isolate DSPM95, *Lentinus velutinus* and *Irpex* spp. had the highest manganese peroxidase activity under conditions of high nitrogen – low carbon. The type of carbon and nitrogen sources also play an important role for LMEs production. Glucose, mannose, maltose, fructose, and lactose are the commonly used carbon sources while yeast extract, peptone, urea, $(\text{NH}_4)_2\text{SO}_4$, and NaNO_3 are the commonly used nitrogen sources (Shraddha et al., 2011). It has been proposed that not only do different fungi require different nitrogen and carbon sources to express their enzymatic potential, but the best nutritional source for one class of enzymes does not always have the same effect on another (Martani et al., 2017).

In addition to the nutritional composition of the medium, culture conditions such as temperature, pH, and agitation rate have a significant impact on enzyme production. (Dhakar & Pandey, 2013) discovered that *Trametes hirsuta* was cultivated at different temperatures (15, 25, 35 and 45°C). The maximum laccase production was recorded at 35°C with a minimum at 25°C. While the production of laccase was recorded between pH 3.5 and 11.5, the maximum laccase production was favored at pH between 5.5 and 7.5. Meanwhile, *Phlebia floridensis* LMEs profile showed that

laccase and MnP activities were best expressed at a pH of 4.5, while LiP was optimally active at a lower pH (2.5) (Arora & Gill, 2005).

Agitation (stirring) is another physical parameter affecting LMEs production. High laccase and MnP activities were achieved by *Trametes versicolor* and *Abortiporus biennis* at 130 rpm, whereas *Pleurotus ostreatus* and *Ganoderma carnosum* reached the highest enzyme levels at 165 rpm (Erden et al., 2009). While all LMEs activities were decreased for all fungi when 90 rpm agitation was implied (Erden et al., 2009). On the contrary, laccase and MnP accumulation in *Ganoderma lucidum* cultures were not influenced by the agitation rate, whereas LiP production was slightly enhanced at 100 rpm (Hariharan & Nambisan, 2012).

In nature, degradation products of lignin and metals naturally present in the soil act as inducers for WRF to produce LMEs. However, when using non-natural substrates in the laboratory, formulated growth media must be supplemented with inducers. Compounds commonly used to boost LMEs production fall into two categories: (i) metals such as copper, manganese, cadmium, magnesium, and chromium, and (ii) phenolic and aromatic compounds such as 2,5-xylidine, guaiacol, veratryl alcohol, and catechol (Martani et al., 2017).

The optimization of physicochemical conditions generally entails varying the levels of one independent variable while holding other variables constant. This one-factor-at-a-time approach is tedious and time-consuming, while the interaction effects of the parameters are frequently overlooked (Bhattacharya et al., 2011). This obvious limitation could be tackled by the use of a more recent technique that allows multiple variables to be optimized in a small number of experiments. The use of statistical techniques such as response surface methodology (RSM) for the optimization of manufacturing conditions could be a viable option. During laccase production from *Trichoderma harzianum* using wheat bran as a carbon source, statistical optimization by Plackett-Burman and RSM using central composite design (CCD) was performed.

Production under optimized conditions resulted in an 8.09-fold increase (Bagewadi et al., 2017).

2.6. LMEs characterization

The selection of the best method for purifying biomolecules is critical in assessing the economic performance of the entire upstream and downstream processes. In enzyme production processes, biosynthesis of the desired product is typically followed by several concentration and separation stages or downstream processing (DSP), which are known to be costly and time consuming (Antecká et al., 2019). DSP of LMEs has been widely studied over recent decades. In general, each preparation method consists of three major steps: (i) the removal of cell debris, (ii) the concentration of culture broth, and (iii) the removal of undesirable low and high molecular weight compounds. The culture broth can be separated from the cell debris by passing the fluid through filter paper, glass fiber filters, microfiltration (MF), or centrifugation (Bryjak & Rekuć, 2010). While protein can be concentrated using several methods, such as salting out (ammonium sulfate) and ultrafiltration (UF) and acetone (Bryjak & Rekuć, 2010; Yin et al., 2017). Chromatography, which involves different mechanisms of ion exchange, affinity and hydrophobic interactions may assist the further removal of undesired small molecules (Antecká et al., 2019). Study regarding characterization of the physico-chemical properties of fungal LMEs after the purification process was summarized in Table 2.6.

Table 2.6. Some physico-chemical characteristic of optimum condition of purified fungal LMEs

Fungal	Type of LMEs	MW (kDa)	Temp. (°C)	pH	Km (mM)	Reference
<i>Cerrena</i> sp.	Laccase	58.6	60	5.0	0.93	Yang et al. (2014)
<i>Phanerochaete chrysosporium</i>	LiP	38.5	45	3.5	0.47	Tuisel et al. (1990)
<i>Trametes polyzona</i>	MnP	44	37	4.5	0.05	Lueangjaroenkit et al. (2019)
	Laccase	71	50	4.5	0.29	
<i>Trametes hirsuta</i>	Laccase	66	30	5.0	0.02	Navada and Kulal (2021)
<i>Ganoderma lucidum</i>	Laccase	38.3	55	5.0	0.47	Manavalan et al. (2013)
<i>Trametes</i> sp.	MnP	49	70	5.0	-	Zhang et al. (2016)
<i>Trametes pubescens</i>	Laccase	68	50	5.0	0.85	Si et al. (2013)
<i>Phanerochaete sordida</i>	LiP	50	-	3.0	0.29	Sugiura et al. (2003)
<i>Irpex lacteus</i>	MnP	37.2	50-60	5.5	0.08	Baborová et al. (2006)
<i>Echinodontium taxodii</i>	MnP	53.4	55	3.5	0.0035	Kong et al. (2016)

2.7. Overview of polycyclic aromatic hydrocarbons (PAHs)

Polycyclic aromatic hydrocarbons (PAHs) are colorless, white, or pale yellow solid organic compounds. They are a ubiquitous group of several hundred chemically related compounds that are environmentally persistent and have varying toxicity (Abdel-Shafy & Mansour, 2016). The term "PAH" refers to compounds that only contain carbon and hydrogen atoms. PAHs are chemically composed of two or more benzene rings bonded in linear, cluster, or angular configurations (Abdel-Shafy & Mansour, 2016). The number of aromatic rings present, as well as the nature of the linkage between these rings influence the chemical properties and environmental fate of PAHs. PAHs are classified into two types: low molecular weight PAHs (compounds with up to three aromatic rings) and medium molecular weight PAHs (compounds with 4 rings) and high molecular weight PAHs (containing five or more aromatic rings) (Figure 2.7.1) (Doyle et

al., 2008; Gao et al., 2019). On the basis of abundance and toxicity, 16 PAHs are already enlisted as priority environmental pollutants by the United States Environmental Protection Agency (US EPA) (Ghosal et al., 2016). PAHs have high melting and boiling points, low vapor pressure, and very low aqueous solubility. The latter two characteristics tend to decrease as molecular weight increases, whereas resistance to oxidation and reduction also increases (Abdel-Shafy & Mansour, 2016). PAH aqueous solubility decreases with each additional ring. Meanwhile, because PAHs are highly lipophilic, they are very soluble in organic solvents. PAHs also have a variety of functions, including light sensitivity, heat resistance, conductivity, the ability to emit, corrosion resistance, and physiological action (Abdel-Shafy & Mansour, 2016; Ghosal et al., 2016). Physico-chemical properties of 16 PAHs were summarized in Table 2.7.

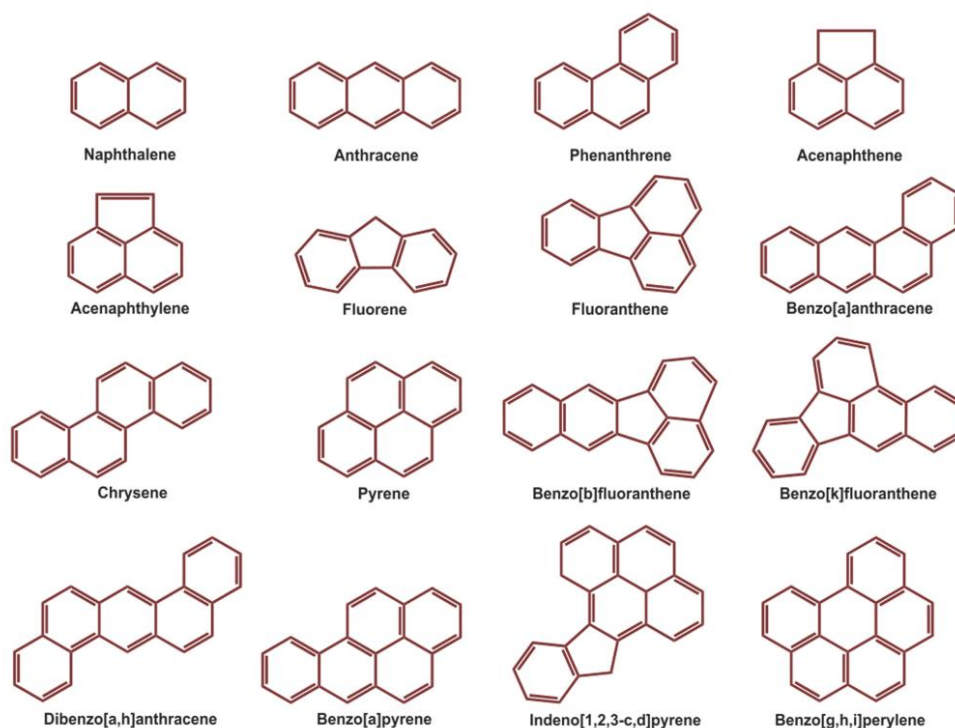


Figure 2.7.1. Structures of 16 PAHs (Ghosal et al., 2016)

The major source of PAHs is the incomplete combustion of organic materials such as coal, oil and wood. Crude oil spills from pipelines and supertankers deposit large amounts of PAHs on the soil and in the ocean (Cerniglia & Sutherland, 2010). In nature, they are formed during forest fires, volcanic eruptions, or by plant and bacterial reactions (Ghosal et al., 2016). Furthermore, *Muscodor vitigenus* an endophytic fungus has been studied for its ability to produce naphthalene (Daisy et al., 2002).

Table 2.7. Physical-chemical properties and some relevant information of 16 PAHs enlisted as priority pollutants by US EPA (Ghosal et al., 2016)

Name	Molecular formula	Molecular weight (g/mol)	Physico-chemical properties			
			Boiling point (°C)	Melting point (°C)	Vapor pressure (mmHg at 25°C)	Solubility (mg/l)
Naphthalene (Nap)	C ₁₀ H ₈	128	218	80.2	8.5 × 10 ⁻²	31
Acenaphthylene (Acy)	C ₁₂ H ₈	152	280	91.8	6.68 × 10 ⁻³	1.93
Acenaphthene (Ace)	C ₁₂ H ₁₀	154	279	93.4	2.5 × 10 ⁻³	3.93
Anthracene (Ant)	C ₁₄ H ₁₀	178	342	216.4	6.53 × 10 ⁻⁶	0.076
Phenanthrene (Phe)	C ₁₄ H ₁₀	178	340	100.5	1.2 × 10 ⁻⁴	1.20
Fluorene (Flu)	C ₁₃ H ₁₀	166	295	116-7	6.0 × 10 ⁻⁴	1.68-198
Fluoranthene (Fla)	C ₁₆ H ₁₀	202	375	108.8	9.22 × 10 ⁻⁶	0.20-0.26
Pyrene (Pyr)	C ₁₆ H ₁₀	202	150.4	393	4.5 × 10 ⁻⁶	0.132
Benzo(a)-anthracene (BaA)	C ₁₈ H ₁₂	228	438	158	4.11 × 10 ⁻³	0.010
Chrysene (Chr)	C ₁₈ H ₁₂	228	448	254	6.23 × 10 ⁻⁹	1.5 × 10 ⁻³
Benzo[a]-pyrene (BaP)	C ₂₀ H ₁₂	252	495	179	5.49 × 10 ⁻⁹	3.8 × 10 ⁻³
Benzo[b]fluoranthene (BbF)	C ₂₀ H ₁₂	252	481	168.3	5.0 × 10 ⁻⁷	0.0012
Benzo[k]fluoranthene (BkF)	C ₂₀ H ₁₂	252	480	215.7	9.7 × 10 ⁻¹⁰	7.6 × 10 ⁻⁴
Benzo(ghi)-perylene (BghiP)	C ₂₂ H ₁₂	276	500	277	1.0 × 10 ⁻¹⁰	2.6 × 10 ⁻⁵
Dibenz[a,h]anthracene (DBA)	C ₂₂ H ₁₄	278	524	262	9.55 × 10 ⁻¹⁰	5.0 × 10 ⁻⁴
Indeno [1,2,3-cd]pyrene (InP)	C ₂₂ H ₁₂	276	536	161-3	1.25 × 10 ⁻³	0.062

PAHs are abundant as contaminants in the air, soil, aquatic environments, sediments, surface water, and ground water (Ghosal et al., 2016). PAH in the environment varies according to its fate, e.g. in air, PAH can take photooxidation, while photo-oxidation and chemical oxidation may occur in soil as well as water, while some PAHs like naphthalene and alkyl-naphthalene are partly lost through volatilization (Cerniglia, 1992). The low-molecular weight (LMW) PAHs (containing two or three aromatic rings) are extremely toxic while the high-molecular-weight (HMW) PAHs (containing five or more rings) are largely considered as genotoxic (Cerniglia, 1992; Ghosal et al., 2016). Furthermore, some PAH transformation products are more toxic than parent PAHs and can lead to critical cellular effects (Schnitz et al., 1993). PAHs, some highly reactive (such as "bay-region" diol epoxides) and known as carcinogenic agents, are oxidized in humans in cytochrome P450 (mono-oxygenase group of enzymes). They are able to bind to DNA and transform normal cells into malignant cells (Ghosal et al., 2016; Schnitz et al., 1993).

LMW-PAHs are slightly more volatile and soluble in water than HMW-PAHs, making them more susceptible to biodegradation (Cerniglia & Sutherland, 2010). LMW PAHs such as naphthalene, anthracene, and phenanthrene are ubiquitous in the environment and have been designated as prototypic PAHs, serving as signature compounds to detect PAH contamination. The chemical structures of fluoranthene and pyrene are found in many carcinogenic PAHs (such as benzo[a]pyrene and benzo[b]fluoranthene), and phenanthrene is the smallest PAH to have both the bay and K regions (Figure 2.7.2). As a result, they are frequently used as a model substrate for research (Agrawal et al., 2021; Ghosal et al., 2016).

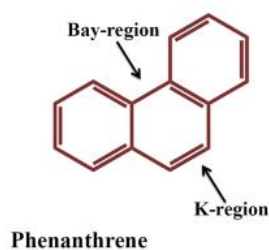


Figure 2.7.2. Structure of phenanthrene containing bay and K region

One of the deciding factors in the selection of degradation methods is the structure of PAHs (Patel et al., 2020). Although the angular arrangement is the most thermodynamically stable configuration of PAHs, their bay regions are susceptible to enzymatic degradation, therefore angular structures degrade faster than linear and clustered structures (Patel et al., 2020). Whereas linear and clustered PAHs degrade quickly through photooxidation and chemical oxidation (Abdel-Shafy & Mansour, 2016).

Studies were performed in which a single, binary, and ternary mixture was measured by the metabolization of phenanthrene, fluoranthene and benzo[a]pyrene. The PAH metabolism was found differ from the metabolism in both binary and ternary mixtures in the single PAH experiment. The metabolism of mixtures showed enzyme competition, changing the metabolism patterns of individual PAHs significantly. The PAH structure also affected the mixture metabolism and possible toxicity effects in the metabolism of the mixture's. With the faster change during single PAH metabolism, PAH concentration changes over time, followed by ternary and binary mixture metabolism (Abdel-Shafy & Mansour, 2016).

Volatilization, photo-oxidation, chemical oxidation, bioaccumulation, adsorption to soil particles, leaching, and microbial degradation are all possible fates for PAHs in the environment (Cerniglia, 1992). Metabolism and photo-oxidation influence the toxicity of PAHs to aquatic organisms. In general, they become more toxic in the presence of ultraviolet light. PAHs are moderate to highly toxic to aquatic life and birds in the short term. Except in highly contaminated soil, PAHs in soil are unlikely to be toxic to terrestrial invertebrates. Tumors, reproduction, development, and immunity are some of the negative effects on these organisms (Abdel-Shafy & Mansour, 2016). Individual PAHs, however, have different health effects. In fact, the International Agency for Research on Cancer classifies some PAHs as carcinogenic to humans as known, possibly, or probably, naphthalene, pyrene, chrysene, benz[a]anthracene, benzo[a]pyrene are among them (Figure 2.7.3). Some PAHs are well

known carcinogens, mutagens, and teratogens, posing a serious threat to human health and well-being (Abdel-Shafy & Mansour, 2016).

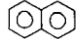
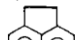
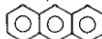
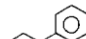
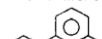
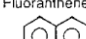
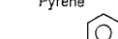
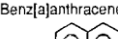
PAH	MW	Sol (mg/L)	Genotoxicity
 Naphthalene	128.2	31.700	-----
 Acenaphthene	154.2	3.900	+ Ames
 Anthracene	178.2	0.070	-----
 Phenanthrene	178.2	1.300	-----
 Fluoranthene	202.3	0.260	Weak Carcinogen
 Pyrene	202.3	0.140	+ Ames + UDS + SCE
 Benz[a]anthracene	228.3	0.002	+ Ames + CA + SCE + Carcinogen
 Benzo[a]pyrene	252.3	0.003	+ Ames + CA + UDS + DA + SCE + Carcinogen

Figure 2.7.3 Chemical structures, physical and toxicological characteristics of PAHs. The symbols are: (DA) DNA adducts, (SCE) sister chromatid exchange, (CA) chromosomal aberrations, (Ames) *Salmonella typhimurium* reversion assay, (UDS) unscheduled DNA synthesis, (-) not genotoxic (Cerniglia, 1992).

2.8. Degradation of PAHs by white-rot fungi

The biodegradation of PAHs by WRF has been reviewed extensively in the last several years. Some of the WRF have the ability to cleave the aromatic rings and mineralize PAHs (Cerniglia, 1997). Species such as *Phanerochaete*, *Pleurotus* and *Trametes* are widely used to degrade individual PAHs by their extracellular ligninolytic enzymes, including LiP, MnP and laccase. These enzymes usually break down wood

components, although they can oxidize PAHs into transient PAHs, which are easily autoxidized into quinones (Figure 2.8) (Cerniglia & Sutherland, 2010). WRF does not utilize PAHs as the sole carbon and energy. Therefore the medium must be supplemented with an additional carbon source (Cerniglia, 1997). Fungal metabolism of PAHs is highly regio- and stereoselective (Cerniglia, 1997). More of WRF studied for PAHs degradation was summarized in Table 2.8.

Table 2.8. Some of PAHs degradation by different species of WRF

Compound	White rot fungi Species	Reference
Phenanthrene	<i>Bjerkandera</i> sp.; <i>Ganoderma lucidum</i> ; <i>Pycnoporus coccineus</i> ; <i>Trametes polyzona</i> ; <i>Pleurotus ostreatus</i> ; <i>Bjerkandera adusta</i> ; <i>Phlebia brevispora</i> ; <i>Peniophora Incarnata</i> ; <i>Phanerochaete</i> sp.; <i>Phanerochaete sordida</i> ; <i>Phanerochaete chrysosporium</i>	Terrazas-Siles et al. (2005); Ting et al. (2011); Thongkred et al. (2011); Lee et al. (2014); Lee et al. (2020); Teerapatsakul et al. (2017); Schützendübel et al. (1999)
Fluoranthene	<i>Pycnoporus coccineus</i> ; <i>Trametes polyzona</i> ; <i>Pleurotus ostreatus</i> ; <i>Bjerkandera adusta</i> ; <i>Phlebia brevispora</i> ; <i>Peniophora Incarnata</i> ; <i>Phanerochaete</i> sp.; <i>Phanerochaete sordida</i> ; <i>Phanerochaete chrysosporium</i> ; <i>Trametes polyzona</i>	Thongkred et al., (2011); Lee et al. (2014); Lee et al. (2020); Teerapatsakul et al. (2017); Schützendübel et al. (1999)
Pyrene	<i>Ganoderma lucidum</i> ; <i>Pycnoporus coccineus</i> ; <i>Trametes polyzona</i> ; <i>Coriopsis byrsina</i> ; <i>Pleurotus ostreatus</i> ; <i>Bjerkandera adusta</i> ; <i>Phlebia brevispora</i> ; <i>Peniophora Incarnata</i> ; <i>Phanerochaete</i> sp.; <i>Phanerochaete sordida</i> ; <i>Phanerochaete chrysosporium</i> ; <i>Trametes polyzona</i> ; <i>Armillaria</i> sp.	Ting et al. (2011); Thongkred et al. (2011); Agrawal and Shahi (2017); Lee et al. (2014); Lee et al. (2020); Teerapatsakul et al., (2017); Schützendübel et al., (1999); Hadibarata (2013)

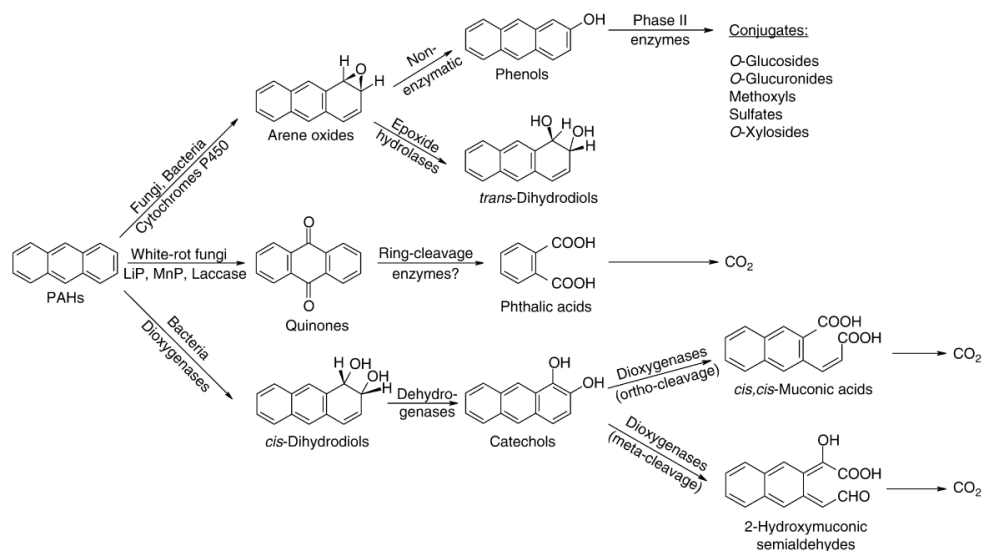


Figure 2.8. Generalized pathway for the metabolism of PAHs by fungi and bacteria (Cerniglia, 1992)

In this study, phenanthrene, fluoranthene and pyrene were used as models for PAHs' metabolism. It turns out that WRF uses several pathways to oxidize each PAH (Cerniglia & Sutherland, 2010). *P. chrysosporium* metabolizes phenanthrene to several metabolites when grown in a high-nitrogen medium under non-ligninolytic conditions, including phenanthrene trans-9S,10S-dihydrodiol, the same enantiomer as that produced by mammals (Sutherland et al., 1991). When grown in a low-nitrogen medium under ligninolytic conditions, *P. chrysosporium* converts phenanthrene to phenanthrene 9,10-quinone, followed by ring cleavage at the C-9 and C-10 positions to form 2,2'-diphenic acid and eventually CO₂ (Hammel et al., 1992). Thus, at least two PAH metabolic pathways coexist in *P. chrysosporium*, one leading to trans-dihydrodiols and the other to quinones and other oxidation products (Cerniglia & Sutherland, 2010). Two fluoranthene metabolites, naphthalene-1,8-dicarboxylic acid and phthalic acid, were found in the process of fluoranthene degradation by *Pleurotus pulmonarius* as laccase was revealed as the major enzyme that played an important role in the degradation process (Wirasnita & Hadibarata, 2016). *Pleurotus ostreatus* was also found to accumulate pyrene-4,5-dihydrodiol during pyrene degradation in Kirk's

medium. However, in the basidiomycetes-rich medium, this fungus did not accumulate pyrene-4,5-dihydrodiol, and pyrene degradation was complete, with a phenanthrene derivative and phthalic acid formed as intermediates (Pozdnyakova et al., 2010).

2.9. PAHs occurrence in coal

The raw coals are classified as lignite, bituminous coal, and anthracite coal, with lignite having the lowest coalification degree and anthracite having the highest (Gao et al., 2019). Coal's main structural unit is aromatic. There are two types of aromatic compounds in coal: macromolecular aromatic compounds that are linked together by aliphatic hydrocarbons and low molecular-weight PAHs that exist as solids and liquids in coal (Gao et al., 2019). The average number of aromatic rings per structural unit in most coal is 3–5 with some individual units containing up to 10 rings (Achten & Hofmann, 2009). PAH concentrations in coal are affected by several factors, such as carbon content, volatile matter, H/C mole ratio, and O/C mole ratio (Gao et al., 2019). Furthermore, Gao et al., (2019) reported the composition of PAHs from each rank in different coals and divided them into three groups according to their molecular weight; (LMW-PAHs: Nap, Acy, Ace, Flu, Phe, and Ant), medium-molecular-weight PAHs (MMW-PAHs: Fla, Pyr, BaA, and Chr), and high-molecular-weight PAHs (HMW-PAHs: BbF, BkF, BaP, InP, DBA, and BghiP). The result showed that the average concentrations of varied among coals (Figure 2.9). LMW-PAHs were highest, which represented 35-52% of the PAHs content of raw coals, followed by MWH-PAHs 30% in lignite then slightly decreased to 30% in bituminous and drastically decreased in anthracite (18%), while HMW-PAHs varied 25-30%. The highest PAH concentration was observed in the bituminous coal. The observed distribution characteristics are attributed to complex coal metamorphism during coal formation. Organic matter in lignite was dominated by chain hydrocarbons, with low PAH concentrations. Meanwhile, during intensified coalification, some aliphatic hydrocarbons in raw coal were dehydrogenated and cyclized to form aromatic compounds resulted PAHs in bituminous coal increased

continuously. However, PAHs concentrations in anthracite decreased because of the reduction of extractable PAHs (Gao et al., 2019).

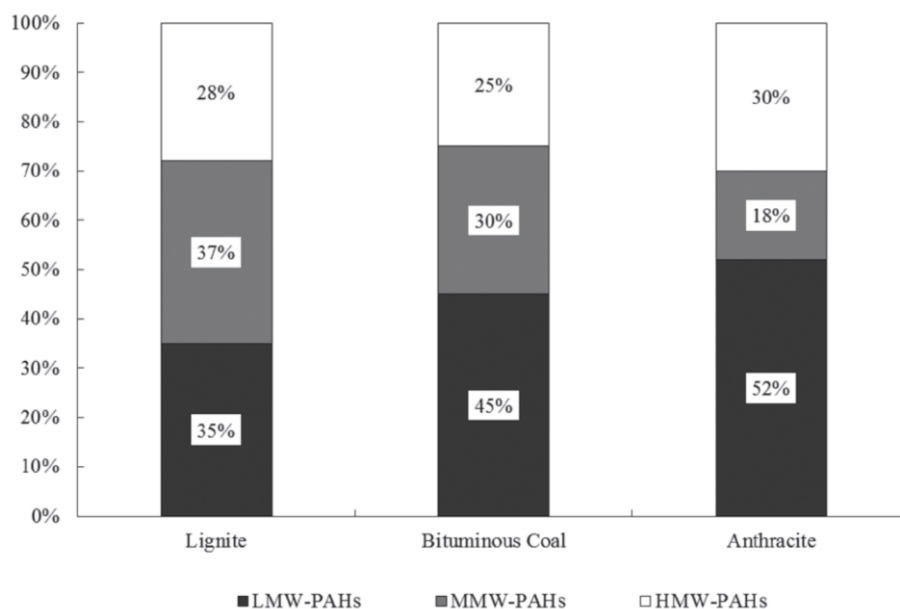


Figure 2.9. Occurrence of PAHs in raw coal (Gao et al., 2019)

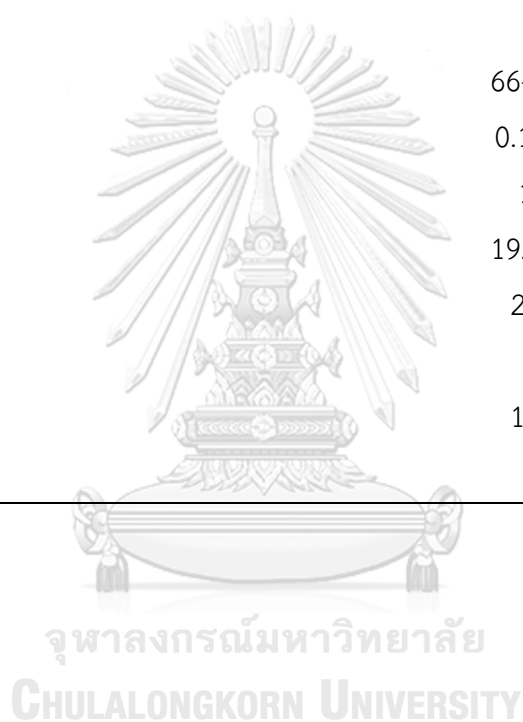
Coal slurry or sludge is a waste fluid produced by washing coal with water and chemicals prior to shipping the coal to market (Iqbal Md et al., 2015). Materials such as rocks and clays mixed within coal must be removed before it can be sold to power plants or steel mills. The raw coal is crushed and mixed with a large amount of water, magnetite, and organic chemicals in a wet washing plant, also known as a coal preparation plant. The massive amount of wastewater that remains is coal slurry (Iqbal Md et al., 2015). In industrial kilns, coal slurry was obtained from coal liquefaction residue (CLR) that had been atomized inside a gasifier with high-purity oxygen, which generated syngas and higher hydrocarbons decomposed with low methane content and no tar substance produced (Li et al., 2018). Li et al. (2018) conducted a study in China to investigate the emission characteristics and environmental risks of organic pollutants during CLR co-processing in the Texaco coal-water slurry gasifier. They reported that PAH concentration from blackwater wastewater disposal was low (37 ng/L) dominated by LMW-PAHs followed MMW-PAHs and HMW-PAHs but increased in solid waste emission. The reason for this was that PAHs have hydrophobic lipophilic

properties, making them more likely to attach to organic matter particles. This result was coherent with the study by Wu et al. (2019), that LMW-PAHs are generally present in the dissolved phase and are discharged through effluents, whereas HMW-PAHs homologues are primarily bound to solid surfaces and accumulate in sewage sludge. Furthermore, the distribution of PAHs in mine water and underground sludge in coal mining in Xuzhou, China has been studied (Chen et al., 2018). The result showed that mine water mainly contained 2-3 ring PAHs with an average concentration of 93.80% and they were higher than 4 and 5-6 ring PAHs. Whilst, in underground sludge, the concentrations of 2-3 ring, 4 ring, and 5-6 ring PAHs were 33.43%, 27.75%, and 38.82%, respectively. The source of PAHs was found to be associated with the distribution ratio of different ring PAHs in sludge. 2-3 ring PAHs in underground sludge may be caused by coal dust, and 5-6 ring PAHs may be caused by adsorption and enrichment of high-ring PAHs in mine water or the release of high-ring PAHs in coal (Chen et al., 2018).

Maiti et al. (2019) have described coal washeries have generates a huge amount of coal slurry which having large amounts of solids, chemical oxygen demand (COD) and metals. This effluent is frequently disposed of in surface water, affecting aquatic life. Table 2.9 describes the characteristics of coal water emissions.

Table 2.9. Characteristic of coal washery effluents

Parameters	Coal washery effluent
pH	2.5-8.2
Turbidity	5,387-23,360
Total suspended solids	110-30,000 mg/L
Total dissolved solids	291-729 mg/L
Alkalinity	1 mg/L
Chloride	184 mg/L
Sulphide	-
Sulphate	66-14,920 mg/L
Nitrate	0.15-0.37 mg/L
BOD	1,001 mg/L
COD	192-6,468 mg/L
Metal ions	212.14 mg/L
Phenols	-
Oil and greass	1.7-4.6 mg/L
Cyanide	0.01 mg/L



CHAPTER III

MATERIALS AND METHODS

3.1 Materials and Equipment

- Autoclave: Ta Chang Medical Instrument Factory, Taiwan
- Autopipette: Pipetman, Gilson, France
- Bright-field microscope: Model CH30, Olympus, Japan
- Centrifuge, refrigerated centrifuge: Hettich, Germany
- Centrifuge, microcentrifuge: Model Denville 260D, Denville Scientific, USA
- Electrophoresis unit: Model mini-protein cell, Bio-Rad Applied Biosystem Company, USA
- HiTrap Q Fast Flow (FF) anion exchanger column: GE Healthcare Bio-Sciences, Sweden
- Incubator Shaker: New Brunswick Scientific Co., Edison, USA
- Laminar flow: Model BV 123, ISSOC, Thailand
- Light microscope: Model BX51, Olympus, Japan
- Membrane filter: Whatman No.1, GE Healthcare Bio-Sciences, Sweden
- pH meter: Model PP-50, Sartorius, Germany
- Shaker: Model SPL15, Labcon, South Africa
- UV-Vis Spectrophotometer: Model UV-2800, Unico, USA
- Vivaflow50, MWCO 10,000. Sartorius, Germany
- Weight balance, 2 digits: Model BL610, Sartorius, Germany
- Weight balance, 4 digits: Model TC-205, Denver Instrument Company, USA

3.2 Chemicals

- ABTS (2,2'-azino-bis (3-ethylbenzthiazoline-6-sulfonic acid), SIGMA-Aldrich Inc., USA
- Acetic acid: Ajex Finechem, New Zealand
- Agarose: GenePure, USA
- Ammonium sulfate: Ajex Finechem, New Zealand
- Bovine serum albumin (BSA): Ajex Finechem, New Zealand
- Calcium chloride dihydrate: Ajex Finechem, New Zealand
- Coomassie Brilliant Blue R-250: Sigma-Aldrich Inc., USA
- Copper sulfate: Carlo Erba, Italy
- Ethylene diamine tetra-acetic acid (EDTA): Ajex Finechem, New Zealand
- Fluoranthene: Sigma-Aldrich Inc., USA
- Hydrochloric acid: Carlo Erba, Italy
- Isopropanol: Fisher Scientific, United Kingdom
- Lactophenol-cotton blue: Fluka, Switzerland
- Magnesium chloride: Ajex Finechem, New Zealand
- Manganese sulfate heptahydrate: Scharlau, Spain
- Methanol: Merck, Germany
- Methylene Blue: Merck, Germany
- Potassium chloride: Ajex Finechem, New Zealand
- Potassium hydrogen sulphate: Ajex Finechem, New Zealand
- Phenanthrene: Sigma-Aldrich Inc., USA
- Pyrene: Sigma-Aldrich Inc., USA
- Sodium carbonate: Scharlau, Spain
- Sodium chloride: Scharlau, Spain
- Sodium dodecyl sulfate: Scharlau, Spain

- Sodium hydroxide: Ajex Finechem, New Zealand
- Zinc sulfate heptahydrate: Scharlau, Spain

3.3 Collection and isolation of white rot fungi

Samarinda botanical garden (KRUS) was located at 0° 25' 10" S latitude and 117°14'4" E longitude, 20 kilometers from Samarinda city, a forest that preserved a collection of Dipterocarps. Fungal basidiocarps encountered along the trails were collected from May to July 2012. The fruiting body was cut into approximately 0.5 cm² pieces and transferred to petri dishes containing 2% potato dextrose agar (PDA) supplemented with 100 ppm of chloramphenicol. The cultures were incubated at 30°C and monitored daily until a white compact mycelium was developed. A small piece of agar containing fungal mycelia was transferred from the margin of the colony growing of each sample to petri dish containing 2% PDA to obtain purified mycelia. Pure cultures were maintained on 2% PDA slants at 4°C for further study.

3.4 Morphological observation

Using the keys described by (Gramss, 1987; Ryvarden & Johansen, 1980) white rot fungi isolates were identified based on macroscopic and microscopic morphology. By comparing the specimens to the identification keys, the macroscopic study was recorded and described (Appendix A). The fruiting bodies were dissected with a razor blade. Sections of the studies were carefully designed to be visible. The dissecting portion was rehydrated with 70% ethanol. Chemical reactions were observed in mounting media, including 5% (w/v) KOH, phenol cotton blue, phloxine, lugol, and Melzer's reagent. Using Olympus microscope, the sections were examined at magnifications ranging from 400× to 1000×.

3.5 DNA isolation, PCR amplification and nucleotide sequencing

Seven days after inoculation, the fungal isolates' mycelia were harvested from the top petri dish on 2% PDA plates. The genomic DNA was extracted using the standard phenol-chloroform method (Sambrook & Russell, 2006). Internal primers ITS4 and ITS5 were used to amplify and partially sequence the internal transcribed spacer (ITS) (White et al., 1990). Two μl of genomic DNA was used as template for PCR reaction using i-Startaq PCR premix with condition: pre-denaturation at 94°C for 2 minutes followed by 35 cycles of 94°C for 30 seconds, with annealing point at 48°C for 30 seconds and 72°C of 2.5 minutes of extension. Purified PCR product was sequenced and BLAST to the GenBank database. The PCR product was sent for sequenced at Macrogen, Korea. The new sequence was compared using nBLAST to get the similar identity with the NCBI database. DNA sequence was aligned by Clustal Omega, and phylogenetic tree was constructed using MEGA 5 (Hall, 2013).

3.6. Lignin modifying enzyme screening and determination activities

3.6.1. Qualitative screening

The lignin modifying enzyme was screened using a petri dish as described by Kiiskinen et al. (2004) and Thongkred et al. (2011). The media was prepared with 0.2% (w/v) glucose solidified with 1.8% (w/v) agar and 2% (w/v) potato dextrose broth. The disc of actively growing mycelium (8 mm) from the edge of active mycelium was inoculated onto an agar plate. Guaiacol (0.01%) and 2,2'-azino-bis (3-ethylbenzthiazoline-6-sulfonic acid (ABTS; 5 mM) were added individually into the medium before solidifying and incubated for 7 days at 30°C in triplicate. The colorless guaiacol was changed and ranged from yellow to dark brown, while ABTS was oxidized to a green color as a positive response to the assessment.

3.6.2. Quantitative assay

Seven days of fungal culture were prepared for enzyme production in 100 ml of basal medium as described by Revankar and Lele (2006) (Appendix B). Ten mycelial discs (8 mm in diameter) were inoculated into each flask and the cultures were incubated at 30°C in shaking condition at 150 rpm for 15 days. Culture supernatants were taken (1 ml) to investigate the enzyme activities daily.

Laccase activity was determined according to Park and Park (2008) by using ABTS as substrate. The assay mixture contained 5 mM ABTS, 100 mM sodium acetate buffer (pH 5.0) and 100 μ l enzyme aliquots. Oxidation of ABTS was monitored at 25°C by measuring the increase in A_{420 nm} ($\epsilon = 36.0 \text{ mM}^{-1} \text{ cm}^{-1}$). One unit (U) of laccase activity was defined as the amount of enzyme that oxidize 1 μ mol of ABTS per minute (Appendix C).

Manganese (II) peroxidase (MnP) activity was assayed according to Watanabe et al. (2001). The reaction contained 0.2 mM 2,6-DMP, 0.5 mM MnSO₄, 0.1 mM H₂O₂ (freshly prepared), 25 mM sodium tartrate buffer (pH 3.0). The reactions were started by adding H₂O₂ and monitoring the oxidation of 2,6-DMP at 469 nm ($\epsilon = 27.5 \text{ mM}^{-1} \text{ cm}^{-1}$). One unit (U) of MnP activity is defined as the amount of enzyme to be required to oxidize 1 μ mol of 2,6-DMP in per minute (Appendix C).

3.6.3. Protein determination

Protein concentration was determined by the Lowry method (Waterborg & Matthews, 1984) using 0-0.25 mg/ml bovine serum albumin (BSA) as a standard (Appendix D). The reaction mixture including: (1) 0.5 crude or diluted crude enzymes; (2) 1.5 ml Lowry reagent and incubated for 10 minutes at room temperature. Then, 0.25 ml of Folin-Ciocalteu's reagent was added to the reaction and incubated for 30

minutes at room temperature. Absorbance of the reaction was measured at 750 nm and the protein concentration was calculated using BSA standard curve (Appendix D).

3.7 PAH degradation test and PAH determination

3.7.1. PAH tolerance test

PAH tolerance of the fungi was tested by a plate assay using a modified PDA containing 100 ppm of each selected PAH (Lee et al., 2014). Fluoranthene, phenanthrene and pyrene were used for this study as PAH models. The PAH solution was prepared by diluting the PAHs into acetonitrile. PAH solution stock (1000 ppm) was added to the PDA after sterilization in final concentration of (50 ppm, 100 ppm and 250 ppm). The experiment was conducted in the dark at room temperature. Following the solidification of the PDA, a single agar disc (8 mm in diameter) cut from the actively growing colony margin of the culture was inoculated into the middle of the agar plate. Culture was incubated at 30°C for 7 days. The colony's diameter was measured daily. The experiment was carried out in triplicate.

3.7.2. PAH degradation in liquid medium

Each PAH (1000 ppm in acetonitrile) was individually added to a culture grown in 100 ml of the basal medium in a 250 ml flask to a final PAH concentration of 100 ppm after sterilization. The mixture was then incubated in the dark at room temperature for 15 days with continuous shaking (150 rpm). The experiment was carried out in triplicate. After 15 days, the fungal mycelia were removed from the culture by filtration through Whatman filter paper No.1 and the residual PAHs in the filtrate was extracted and quantitatively determined using HPLC.

3.7.2. PAHs determination

PAHs were quantified by high performance liquid chromatography (HPLC) using the suitable columns and conditions described previously by Thongkred et al. (2011). The sample was sent to scientific and technological equipment center, Chulalongkorn University. The extracted compounds were analyzed using HPLC (C18 reverse-phase HPLC column (4.6×150 mm) with 7:3 (v/v) acetonitrile: water as the mobile phase at a flow rate of 1 mL/min). Phenanthrene, pyrene and fluoranthene were determined by UV detection at 250 and 236 nm, respectively. The experiment was conducted in triplicates.

3.8. Optimization of laccase production medium

To improve the laccase production of the selected fungal isolate, the production medium was optimized. Nitrogen sources (urea, $(\text{NH}_4)_2\text{SO}_4$, peptone), carbon sources (glucose, sucrose, starch, glycerol) and laccase inducers (ethanol, gallic acid, CuSO_4) were screened along with pH range (4-5) using Plackett-Burman design (Palvannan & Sathishkumar, 2010). Each factor was examined in two levels (-1 and +1) and listed in Table 3.8.1 and the experiment matrix was provided in Appendix E. The experiment was carried out in triplicate.

Table 3.8.1. The Plackett–Burman design for screening variables in laccase production.

Factors	Code	Low level (- 1)	High level (+ 1)
Glucose	X1	5	10
Sucrose	X2	5	10
Starch	X3	5	10
Glycerol	X4	5	10
Urea	X5	1	3
(NH ₄) ₂ SO ₄	X6	1	3
Peptone	X7	1	3
Ethanol	X8	1	3
Gallic acid	X9	0.5	1
CuSO ₄	X10	0.1	0.5
pH	X11	4	5

Further optimization was conducted using Response Surface Methodology (RSM). Variable factors were selected based on the results from the screening experiment (Palvannan & Sathishkumar, 2010). Central composite design was employed to fit the RSM model using 4 levels of interactions (Table 3.8.2). According to this design, 30 runs replicated three times at central points were performed. The quadratic model established for laccase production that fit to the model was following the equation:

$$\hat{Y} = \beta_0 + \sum_{i=1}^k \beta_i X_i + \sum_{i=1}^k \beta_{ii} X_i^2 + \sum_i \sum_j \beta_{ij} X_i X_j \quad (1)$$

Where \hat{Y} is the predicted response (laccase production), β_0 is a constant; β_i is linear terms coefficients; β_{ii} is quadratic term coefficients and β_{ij} is interaction coefficients. The relation between the coded forms of the input variables and the actual values of chosen variables are described as follows:

$$X_i = \frac{Z_i - Z_i^*}{\Delta Z_i} \quad (2)$$

Where X_i is the coded value of the variables, Z_i is the actual value (uncoded value) of the variables, Z_i^* is the center point and ΔZ_i the step change between the levels.

Table 3.8.2. CCD experiment range and levels of independent variables

Variables	Unit	Code	Range and levels		
			-1	0	+1
Glucose	g/l	A	20	25	30
Peptone	g/l	B	1	2	3
CuSO ₄	mM	C	0.5	0.75	1
pH	-	D	4.0	5.0	6.0

To analyze the statistical results, ANOVA, and develop the three-dimensional response surface model, Design Expert version 7.0 (StatEast Inc., USA) was utilized. The model's optimal condition was then confirmed in a second experiment and utilized as the best medium condition.

3.9. Purification and characterization of a laccase from the selected fungal isolate

3.9.1 Laccase production profile

Trametes polyzona PBURU 12 was cultivated in the optimized medium (100 ml) at room temperature for 15 days. Laccase activity was measured following the method in (3.6.2). Dry cell weight was determined daily following the method by (Stone et al., 1992). The experiment was carried out in triplicate.

3.9.2. Purification of extracellular laccase

Crude enzyme of PBURU 12 was cultivated using optimized medium for 12 days. The culture supernatant was recovered by centrifugation ($9,000 \times g$) for 10 minutes. The culture supernatant (900 ml) was 9-fold concentrated by ultrafiltration (Vivaflow 10 kDa MW membrane cut-off, Sartorius, Germany).

The crude laccase was loaded into a Hitrap Q FF (anion exchanger chromatography column; GE Healthcare, Sweden) previously equilibrated with 50 mM sodium citrate, pH 5.0. The column was washed with the same buffer until the A280 reading was less than 0.02. Bound protein was eluted with a linear salt gradient (0-1.0 M NaCl) at flow rate 2.0 ml/minute. Two ml of each fraction were collected. The eluted fraction was assayed for laccase activity (ABTS) and A280 was monitored.

The protein from purification step was analyzed using sodium dodecyl sulphate–polyacrylamide gel electrophoresis (SDS-PAGE). SDS-PAGE were performed with 10% and 5% (w/v) resolving and stacking gels, respectively as described by Chairin et al. (2014). Standard molecular weight marker, PageRuler Prestained Protein Ladder (MW 10-180 kDa) (Thermo Scientific, USA) was used. Electrophoresis was conducted at 4 °C and run at constant current of 20 mA for 1 hour. SDS-PAGE was stained using Coomassie blue R-250.

3.9.3 Characterization of the purified laccases

Optimum pH and pH stability of the purified enzyme was determined using sodium citrate and citrate-phosphate buffer with a pH ranged between 3.0-9.0. Optimum temperature and thermal stability were determined in a range between 20-80°C. The activity of the enzymes was tested in the presence of selected metal ions commonly found in coal slurry including Ca^{2+} , Mg^{2+} , Mn^{2+} , Zn^{2+} , Cu^{2+} , Co^{2+} , Fe^{3+} and Na^+ . Three potential inhibitors (sodium azide (NaN_3), SDS and EDTA at 1-10 mM) were evaluated for their effect on the laccase activity. The effect of organic solvents

(methanol, ethanol, acetone and acetonitrile) in range concentration of 10-50% were also analyze. The percentage of inhibition was calculated as described by Yang et al. (2013). All experiments were conducted in triplicate.

The kinetic constants of four laccase substrates (ABTS, guaiacol, 2,6-DMP, and syringaldazine) were measured in a 50 mM sodium citrate buffer pH 4.5 at concentrations ranging from 0 to 20 mM. Using the Lineweaver-Burk plot, the rates of substrate oxidation were plotted and calculated.

3. 10. Degradation of PAHs using crude laccase and live fungal mycelia

The degradation of PAHs (pyrene, phenanthrene, and fluoranthene) was carried out utilizing crude laccase and live fungal mycelia. For the crude enzyme experiment, 100 ppm of each PAH was added separately into the reaction mixture 20 ml containing 1 U/ml crude enzyme and 50 mM sodium citrate buffer (pH 4.5), while the entire medium, along with fungal biomass, was then used to degrade PAHs (100 ppm) by adding each individual PAH into the medium for 24 hours with continuous shaking at 150 rpm.

After that, crude laccase was used for the next experiment, and the effect of the mediator was tested by adding 1 mM ABTS. The crude laccase concentration was also determined by raising the crude laccase concentration to 10 U/ml under the same conditions without the present of mediator. The mixture was incubated at room temperature and liquid samples were collected every 12 hours for a 24 hour period. All experiment were done in triplicate.

The effect of PAHs mixture has been conducted by adding 100 μ l of each individual PAHs (100 ppm) to 20 ml sodium citrate buffer pH 4.5 with final concentration of mixture-PAHs of 300 ppm. The control was mixture-PAHs in acetonitrile without the addition of crude enzyme. Residual PAHs were extracted using

3 volumes of ethyl acetate following the method by (Bezalel, Hadar, Fu, et al., 1996). The residual PAHs were determined by HPLC as in 3.7.2.

3.11. Phytotoxicity, Genotoxicity and Mutagenicity tests of PAHs degraded products

3.11.1. Phytotoxicity test

Healthy commercial shallot (*Allium cepa* var. *aggregatum*) bulbs of equal size were used to evaluate toxicity of PAHs and its derivatives following the method of Taranath et al. (2015) with minor modifications. The shallot bulb outer scales were cleaned and the bottom plates were cut to expose the root primordia. The bulbs were placed in 50 ml test tubes containing phenanthrene, pyrene and fluoranthene solutions (100 ppm). Distilled water was used as the control. PAHs were diluted in acetonitrile. The extracted PAHs were concentrated using a rotary evaporator after being extracted with 3 ethyl acetate and diluted with acetonitrile. The experiment was conducted in the dark to prevent PAHs auto-oxidation. The solutions were freshly prepared and changed every 24 hours. After 3-day growth in the test solution, number of roots and root length were recorded.

3.11.2. Genotoxicity test

To observe genotoxicity effect of chromosome aberrations, five root tips were randomly cut from each onion bulb (5 replicates). The cut root tips were washed thoroughly by distilled water and fixed in Carnoy's fixative (1:3 glacial acetic acid: 95% ethanol) for 24 hours. The root tips then subjected to conventional squash preparation using 1 N HCl hydrolysis of cellulosic cell wall for 5 min. Staining was done in 2% (w/v) aceto-orcein in 45% (v/v) glacial 1 N HCl (1:9) (v/v) (de Rainho et al., 2013). The mitotic cells were detected under light microscope (Olympus BX51, Canada) with

magnifications of 400x and 1000x. The mitotic index was calculated using the following formula:

$$MI = \frac{\text{Number of dividing cells}}{\text{Total number of cells}} \times 100$$

3.11.3. Mutagenicity test

Mutagenicity was determined by Ames test using the *Salmonella typhimurium* strain TA98 and TA100 without the addition of activation S9 fraction (de Rainho et al., 2013). Three replications were performed on phenanthrene, pyrene, and fluoranthene at 100 ppm/plate and mixed-PAHs at 300 ppm/plate. The extracted PAHs were concentrated using a rotary evaporator after being extracted with 3 ethyl acetate and diluted with dimethyl sulfoxide (DMSO). DMSO (100 µl) was used as a negative control. Standard mutagens including 4-nitroquinoline-1-oxide (10 µg/plate), sodium azide (10 µg/plate), 2-aminoflourene (10 µg/plate) and methyl methane sulfonates (10 µl/plate) were used as positive controls. Positive response was defined by at least 2-fold increase in revertants over the negative control. Revertant colonies were scored after 48 hours incubation at 37°C. Results were expressed as the number revertant colonies per plate. The recipe for AMES medium was described in Appendix F.

3.12. Statistical analysis

All the experiments and analyses were subjected to statistical analysis using Analysis of Variance (ANOVA) and least significant difference (LSD). In tables, the data values have been presented as mean ± standard error of three replicates.

CHAPTER IV

RESULTS AND DISCUSSION

4.1 Collection and morphological identification of white rot fungi

White-rot fungi (WRF) were collected during three sampling periods from May to August 2012 at three zones of the Samarinda botanical garden also known as kebun raya Unmul Samarinda (KRUS) (Fig. 4.1.1), which are located between 0° 25 "10" N and 117° 14 "4" S. The forest was used for conservation and education for Faculty of Forestry, Mulawarman University. The average annual rainfall is 2000 mm, with rain falling slightly less frequently from June to October. The daily maximum temperature is 33.20°C, while the daily minimum temperature is 24.50°C (Hashem, 2019). Samarinda botanical garden is a natural area with lowland tropical rainforest habitat (low land tropical rain forest) located at an elevation of +50 meters above sea level (Karyati, 2016). The Samarinda Botanical Garden is a natural forest which is dominated by *Dipterocarpaceae*. After experiencing a fire in 1983, 1993, and 1998, the vegetation mostly turned into young secondary forest in the form of *Dipeterocarpaceae*, non-*Dipterocarpaceae*, and fruit trees, and it is now an old secondary forest to primary forest (Karyati, 2016; Siswanto et al., 2018). Some of the vegetation found in Samarinda botanical garden were *Eusideroxylon zwageri*, *Shorea* sp., *Dipterocarpus* sp., *Aquilaria malacensis*, *Eugenia* sp., *Durio zibhetinus*, *Arthocarpus integra*, *Cananga odorata*, *Canarium indica*, *Schima walichii* (Siswanto et al., 2018).

The Samarinda botanical garden was divided into three zones (Trimurti & Lariman, 2018)(Figure 4.1.1): Zone 1 (Conservation zone). The conservation zone of Samarinda botanical garden was divided into two areas; a primary forest reserve (117 hectares) and an indigenous species arboretum (16 hectares). Zone 2 (Collection zone)

is the collection zone, covering an area of ± 100 ha. Zone 3 (the recreation zone) is the natural recreation zone, covering an area of ± 65 ha. Each zone's description and fungi collection are given below.

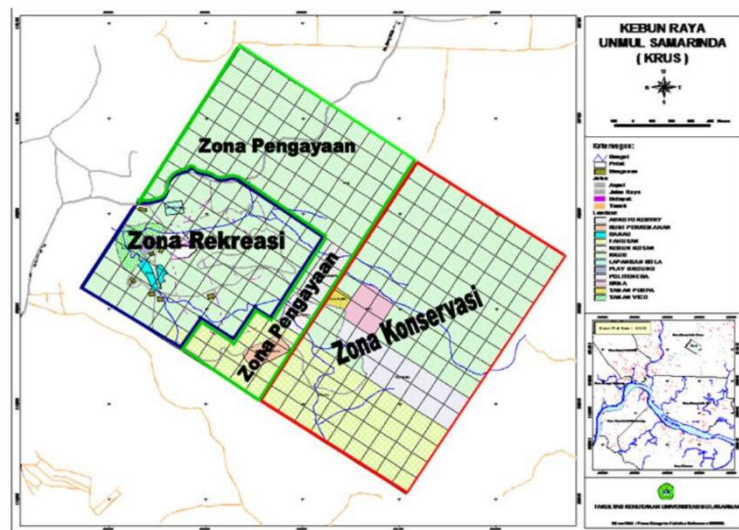


Figure 4.1.1. Map of Samarinda botanical garden (Siswanto et al., 2018)

Zone 1 (Conservation zone)

The conservation zone of Samarinda botanical garden was divided into two areas; a primary forest reserve (117 hectares) and indigenous species arboretum (16 hectares). The area was covered with native plants and trees of East Kalimantan to maintain and save the genetic resources. In this zone, *Shorea* sp., *Anisoptera* sp., *Dipterocarpus* sp. and *Dryobalanops* sp. were found with diameter up to 30 cm and height more than 30 m. While *Hopea* sp., *Vatica* sp. and *Cotylelobium* sp. were smaller trees that can be found in this area. Due to its function as a primary forest, there was an abundance of dead wood, which consisted of all the dead natural structures of trees, such as stumps, fallen trunks, standing dead trees (stags), branches, and twigs.

The fruiting bodies of polyporales fungi have been collected from this area. Twenty four species were identified from four families of *Ganodermaceae*, *Polyporaceae*, *Phanerochaetaceae* and *Meruliaceae*. The species such as *Ganoderma*

australe, *Fomitopsis* sp., *Gloeoporus dichrous*, *Polyporus ostreiformis*, *Polyporus badia*, *Corioloopsis sanguinaria*, *Trametes lactinea*, *Trametes menziesii*, *Junghuhnia* sp., *Bjerkandera* sp. were found in this zone. Furthermore, new record of *Ceriporia inflata* and *Ceriporia lacerata* from Indonesia tropical forest were also found in this zone.

The fruiting body of *Ganoderma australe*, *Microporellus obovatus* and *Rigidoporus microporus* were found on live standing trees, while other species such as *Ceriporia inflata*, *Ceriporia lacerata*, *Fomitopsis* sp., *Gloeoporus dichrous*, *Polyporus ostreiformis*, *Polyporus badia*, *Corioloopsis sanguinaria*, *Trametes lactinea*, *Trametes menziesii* were found on tree stumps, fallen trunks and standing dead trees.

Trees in tropical rainforests are hosts to a variety of stem- and root-rot pathogens, some of which are basidiomycete pathogens of the genera *Phellinus*, *Rigidoporus*, and *Ganoderma* named as heartwood rotters (Mohammed et al., 2014). These fungi are facultative saprophytes as well as pathogens and can survive for long periods on living tree, woody debris, stumps and the remains of roots (Lindblad, 2001; Mohammed et al., 2014). Heartwood rotters can infiltrate a living tree and decay the heartwood while the tree is still alive, resulting in a hollow tree (Gates, 2009).

Meanwhile, dead wood is an essential component of any forest ecosystem because it provides the energy required for tree regeneration in the form of carbon and nitrogen sources (Moose et al., 2019). Dead wood can take many forms in undisturbed and old-growth forests, ranging from entire standing or fallen trees to decomposing fragments of wood (Moose et al., 2019). When tree dies and moisture level declined, fungal invasion can occur (Gates, 2009). The fungal fruiting body can export nutrients (Ca, Fe, K, Mn, N, P, Zn) from the wood, which are then returned to the forest floor by insects and grazing animals that consume the fruit body (Gates, 2009). Therefore, the dead wood or usually named as coarse wood debris (CWD) are the best substrate for saproxylic fungi (decomposer fungi).

In this study, two new resupinate species from Indonesia, *Ceriporia inflata* and *Ceriporia lacerata*, were described for the first time. The morphological characteristics have already been described previously. These two resupinate fungi matched the holotype specimens found in China and Japan's subtropical forests. The morphological comparison of these species to the holotype was described on Table 4.1.1. and Figure 4.1.2.

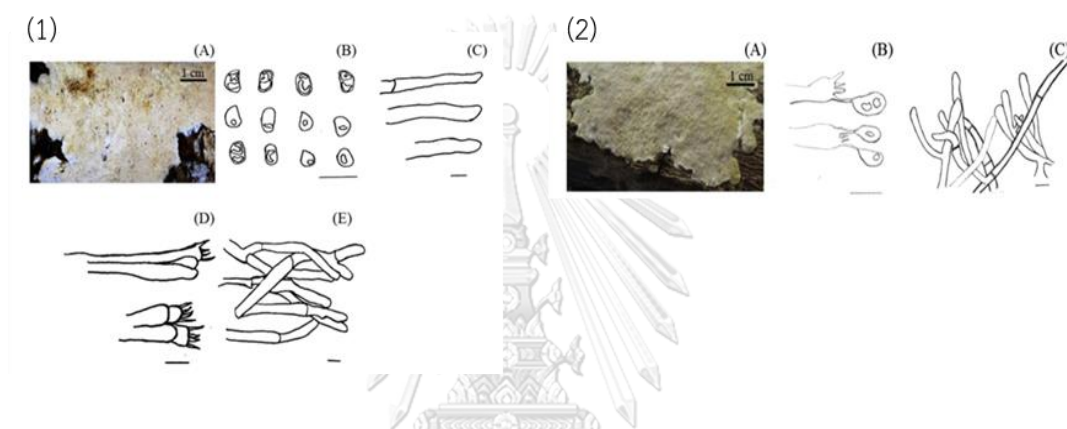


Figure 4.1.3. Morphological characteristics of *Ceriporia inflata* PBURU R1 (1); (A) Basidiocarp, (B) Basidiospore, (C) Cystidia, (D) Basidia, (E) Generative hyphae and *C. lacerata* PBURU 141 (2). (A) Basidiocarp, (B) Basidia and Basidiospore, (C) Generative hyphae.

Table 4.1.1. Morphological comparison of *Ceriporia inflata* PBURU R1 and *C. lacerata* PBURU 141 with the type specimens

Characteristic	<i>Ceriporia inflata</i> (current study)	<i>Ceriporia inflata</i> (Jia & Cui, 2013)	<i>Ceriporia lacerata</i> (current study)	<i>Ceriporia lacerata</i> Maek (Suhara et al., 2003)
Basidiocarp	Resupinate, soft corky when fresh and hard when dry	Annual, resupinate corky to brittle when dry	Resupinate, effused, confluent, soft when fresh	Resupinate, effused, confluent, soft when fresh
Pore surface	White to cream when fresh, buff to clay-buff when dry	White to cream when fresh, buff to clay-buff when dry	White, buff to ochraceous	White, buff to ochraceous
Pores (mm)	0.8-2	2-3	2.5-5	2-5
Hypha structure	Monomitic	Monomitic	Monomitic	Monomitic
Basidia (µm)	10.1-23.5 × 3.3-6.2	12.9-19 × 3.8-5.5	9-18.2 × 3.7-5.5	11-16.5 × 3.5-5.5
Basidiospore (µm)	3-5.5 × 1.2-3.4	4.93 × 2.15	3.5-5 × 1.9-3.7	3.5-5 × 2-3

Zone 2 (Collection zone)

The collection zone covering an area of ± 100 ha. In this zone, various types of plants are developed originating from East Kalimantan and those from outside East Kalimantan with collection such as from family of *Dipterocarpaceae*, non-*Dipterocarpaceae* and fruit tree. Its also the zone for precious wood and introduced species arboretum (Trimurti & Lariman, 2018). Twenty species were collected in this area. Based on the quantity of basidiocarps collected, these are the most frequently seen species were *Earliella scabrosa*, *Ganoderma applanatum*, *Ganoderma australe*, *Gloeoporus dichrous*, *Lentinus sajor-caju*, *Lentinus squarrosulus*, *Lenzites elegans*, *Microporellus obovatus*, *Microporus affinis*, *Microporus xanthopus*, *Phellinus fastuosus*, *Polyporus arcularius*, *Polyporus ostreiformis*, *Pycnoporus sanguineus*, *Rigidoporus microporus*, *Trametes hirsuta*, *Trametes lactinea*, *Trametes polyzona*, *Trametes versicolor* and *Trichaptum biforme*.

Zone 3 (Recreation zone)

The natural recreation zone covering an area of ± 65 ha. The area was prepared for development of various recreational facilities such as fish pond and floral garden (Trimurti & Lariman, 2018). Most of species that collected from this area were deemed common species since they were gathered at the majority of the research locations., such as *Lentinus sajor-caju*, *Microporus affinis*, *Microporus xanthopus*, *Schizophyllum commune*, *Polyporus arcularius* and *Pycnoporus coccineus*.

During the study period, 50 basidiocarps of white-rot fungi were morphologically identified. The basidiocarps were collected from dead trees, falling braches and living trees. The result indicated that most basidiocarps collected were in the order Polyporales, with Polyporaceae being a dominant family found in every zone. The results showed 30 isolates were placed in the families of Phanerochaeteceae, Hymenochaetaceae, Ganodermataceae, Meripilaceae, Polyporaceae and Schizophyllaceae.

Most of the basidiocarps that have been collected are common species in the area, since they can be found in every zone. From 50 isolates that have been collected, *Microporus affinis*, *Microporus xanthopus* and *Polyporus arcularius* were present in all 3 zones. While *Earliella scabrosa*, *Ganoderma australe*, *Lenzites elegans*, *Microporellus obovatus*, *Polyporus ostreiformis*, *Pycnoporus sanguineus*, *Trametes hirsuta*, *Trametes polyzona*, *Trametes versicolor*, *Trichaptum biforme* were common in zones 1 and 2. Additionally, *Schizophyllum commune* can be found in zones 2 and 3. The list and pictures of white-rot fungi collected from Samarinda botanical garden which have been taxonomically identified are described in Table 4.1.2.

Table 4.1.2. White rot isolates collected from three zones of Samarinda botanical garden

Zone 1		Zone 2		Zone 3	
Scientific name	Isolate number	Scientific name	Isolate number	Scientific name	Isolate number
<i>Bjerkandera adusta</i>	PBURU 8	<i>Ganoderma applanatum</i>	PBURU 7	<i>Lentinus sajor-caju</i>	PBURU 14
<i>Ceriporia inflata</i>	PBURU R1	<i>Ganoderma australe</i>	PBURU 5	<i>Microporus affinis</i>	PBURU 61
<i>Ceriporia lacerata</i>	PBURU 141	<i>Gloeoporus dichrous</i>	PBURU 43	<i>Microporus xanthopus</i>	PBURU 63
<i>Coriolopsis sanguinaria</i>	PBURU 11	<i>Lentinus sajor-caju</i>	PBURU 55	<i>Polyporus arcularius</i>	PBURU 69
<i>Earliella scabrosa</i>	PBURU 45	<i>Lentinus squarrosulus</i>	PBURU 48	<i>Pycnoporus coccineus</i>	PBURU 73
<i>Fomitopsis</i> sp.	PBURU 15	<i>Lenzites elegans</i>	PBURU 68	<i>Schizophyllum commune</i>	PBURU 70
<i>Ganoderma australe</i>	PBURU 30	<i>Microporellus obovatus</i>	PBURU 32		
<i>Gloeoporus dichrous</i>	PBURU 23	<i>Microporus affinis</i>	PBURU 31		
<i>Junghuhnia</i> sp.	PBURU 24	<i>Microporus xanthopus</i>	PBURU 44		
<i>Lenzites elegans</i>	PBURU 6	<i>Phellinus fastuosus</i>	PBURU 18		
<i>Lentinus squarrosulus</i>	PBURU 13	<i>Polyporus arcularius</i>	PBURU 53		
<i>Microporellus obovatus</i>	PBURU 35	<i>Polyporus ostreiformis</i>	PBURU 66		
<i>Microporus affinis</i>	PBURU 10	<i>Pycnoporus sanguineus</i>	PBURU 72		
<i>Microporus xanthopus</i>	PBURU 25	<i>Rigidoporus microporus</i>	PBURU 47		
<i>Polyporus ostreiformis</i>	PBURU 27	<i>Trametes hirsuta</i>	PBURU 41		
<i>Polyporus arcularius</i>	PBURU 17	<i>Trametes polyzona</i>	PBURU 58		
<i>Polyporus badia</i>	PBURU 47	<i>Trametes versicolor</i>	PBURU 46		
<i>Pycnoporus sanguineus</i>	PBURU 60	<i>Trichaptum biforme</i>	PBURU 74		
<i>Trametes hirsuta</i>	PBURU 3	<i>Earliella scabrosa</i>	PBURU 77		
<i>Trametes lactinea</i>	PBURU 28	<i>Trametes lactinea</i>	PBURU 62		
<i>Trametes menziesii</i>	PBURU 42				
<i>Trametes polyzona</i>	PBURU 12				
<i>Trametes versicolor</i>	PBURU 36				
<i>Trichaptum biforme</i>	PBURU 50				

Fifty white rot fungus were classified into thirty species based on their morphology. The following are the taxonomic descriptions of thirty identified species:

1. *Bjerkandera adusta* (Fr.) P. Karst.

Class Agaricomycetes; **Order** Polyporales; **Family** Meruliaceae; **Genus** .
Bjerkandera

Specimen examined: Isolate PBURU 8, Samarinda botanical garden, Indonesia.

Habitat/Substrata on falling dead deciduous wood. **Distribution** An eastern species known from a few localities in southeast Finland, more widespread in central Europe and in the Mediterranean area. Cosmopolitan species, Asia.



Figure 4.1.3. Basidiocarp of *Bjerkandera adusta* (picture credit: Ruga, R)

Basidiocarp annual, resupinate, effused-reflexed to pileate, usually with imbricate; pilei up to 2-5 cm wide, up to 5 mm thick at the base, soft and flexible when young, hard and brittle in older specimen; **Pilear** surface purple; pore surface dark purple to greyish, pores round to angular, 2-6 per mm, tubes purple to black, up to 3 mm long. **Hyphal system** monomitic; generative hyphae thin-walled with clamps, hyaline with small to large clamps, frequently branched, 1-6 μm wide. **Basidia** clavate with 4 sterigmata. **Basidiospores** oblong-ellipsoid, 4-5.5 \times 2.5-4 μm .

2. *Ceriporia inflata*/*Ceriporia jiangxiensis* (Jia and Cui)

Class Agaricomycetes; **Order** Polyporales; **Family** Phanerochaetaceae; **Genus** *Ceriporia*. **Specimen examined:** Isolate PBURU R1, Samarinda botanical garden, Indonesia. **Habitat/Substrata** on falling dead deciduous wood. **Distribution** Asia; China and Indonesia.



Figure 4.1.4. Basidiocarp of *Ceriporia inflata* (picture credit: Wulandari, R)

Basidiocarp soft corky when fresh and hard when dry. They are firmly attached to the substrate. The pore surface is hymenophore poroid, white to cream when fresh and buff to claybuff when dry. **Pores** angular to irregular, 0.8-2 per mm, dissepiments thin, lacerate. Sometimes pores extend to the very edge, flocculent. **Tubes** concolorous white the pore surface and up to 1-2 mm thick. **Hyphal system** monomitic; generative hyphae without clamps, hyaline, thin-walled, simple septa, frequently branched, interwoven with cystidia up to 2.1-3 μm . **Basidia** clavate, 10.1-23.5 \times 3.3-6.2 μm , with 4 sterigmata. **Basidiospores** allantoid to ellipsoid, 3-5.5 \times 1.2-3.4 μm .

3. *Ceriporia lacerata* (Maek, Suhara and Kondo)

Class Agaricomycetes; **Order** Polyporales; **Family** Phanerochaetaceae; **Genus** *Ceriporia*. **Specimen examined:** Isolate PBURU 141, Samarinda botanical garden, Indonesia. **Habitat/Substrata** on falling dead deciduous wood. **Distribution** Asia; China, Japan, Korea and Indonesia.



Figure 4.1.5. *Ceriporia lacerata* (picture credit: Wulandari, R)

Basidiocarp effused, confluent, soft when fresh, then fragile. They are firmly attached to the substrate. The hymenophore is poroid, white, buff to ochreous, dissepiments entire to lacerate, white to cream when fresh and buff to clay-buff when dry, firmly attached to the substrate. **Pores** angular to irregular, 2.5-5 mm. **Tubes** concolorous with the pore surface and up to 1-2 mm thick. **Hyphal system** monomitic; generative hyphae without clamps, hyaline, thin-walled, simple septa, frequently branched 3-3.7 μm . **Basidia** clavate, 9-18.2 \times 3.7-5.5 μm , with 4 sterigmata. **Basidiospores** oblong-ellipsoid to ellipsoid, 3-5.5 \times 1.9-3.7 μm .

4. *Corioloopsis sanguinaria* (Klotz.) Teng.

Class Agaricomycetes; **Order** Polyporales; **Family** Polyporaceae; **Genus** *Corioloopsis*

Specimen examined: Isolate PBURU 11, Samarinda botanical garden, Indonesia.

Habitat/Substrata on falling dead deciduous wood. **Distribution** Paleotropical species, China, Japan, Taiwan, Northern Thailand and Vietnam.



Figure 4.1.6. *Corioloopsis sanguinaria* (picture credit: Wulandari, R)

Basidiocarp annual to resupinate, pileate to effused-reflexed, solitary to imbricate, usually elongated. single pilea up to 3-6 cm wide, 5-10 cm long, 0.5-1 cm thick. **Pilear surface** ochraceous to yellowish-brown when young and become tawny in older specimen. **Pores** round, angular, 2-4 per mm. **Tubes** up to 2 mm long, concolorous with the pore surface; context fibrous, yellowish-brown to dark brown, 2-8 mm thick. **Hyphal system** trimitic; generative hyphae with clamps, hyaline, thin-walled, 1.5-2 μm wide; skeletal hyphae thick-walled, 1.5-6 μm ; binding hyphae slightly thick-walled, 1.5-4 μm . **Basidia** clavate, 15-25 \times 4-6 μm , with 4 sterigmata. **Basidiospores** oblong-ellipsoid to subellipsoid, 3-5 \times 1.5-4 μm .

5. *Earliella scabrosa* (Pers.) Gilb. & Murr.

Class Agaricomycetes; **Order** Polyporales; **Family** Polyporaceae; **Genus** *Earliella*

Specimen examined: Isolate PBURU 45, Samarinda botanical garden, Indonesia.

Habitat/Substrata on falling dead deciduous wood. **Distribution** Widespread and common in tropical and subtropical areas, especially in open and degraded forests. In East Asia known from China, Japan, Taiwan, Far East Russia, Northern Thailand, and Vietnam.



Figure 4.1.7. *Earliella scabrosa* (picture credit: Ruga, R)

Basidiocarp effused-reflexed to more rarely distinctly pileate, often widely effused along fallen logs, tough and leatherous. **Pilear** glabrous, widely concentrically zonate, White to cream at first, then covered by a reddish cuticle beginning at the base and covering almost the entire surface in older specimens. **Pores** white, round to semi-

daedaloid, 2-3 per mm. **Tubes** concolorous, up to 5 mm long. **Context** white, tough, up to 3 mm thick. **Hyphal system** trimitic; generative hyphae with clamps, thin-walled, 1-4 μm wide, skeletal hyphae dominant, thick-walled, hyaline, 2-6 μm wide; binding hyphae as skeletal hyphae. **Basidia** clavate, 15-20 μm , with 4 sterigmata. **Basidiospores** cylindrical to oblong-ellipsoid, 7-10 \times 3-4 μm .

6. *Fomitopsis* sp. (Karst)

Class Agaricomycetes; **Order** Polyporales; **Family** Fomitopsidaceae; **Genus** *Fomitopsis*. **Specimen examined:** Isolate PBURU 15, Samarinda botanical garden, Indonesia. **Habitat/Substrata** on living tree. **Distribution** Throughout forest regions of Europe and circumpolar in the boreal-temperate zone. North to Finnmark in northern Norway, Asia.



Figure 4.1.8. *Fomitopsis* sp. (picture credit: Hadi, S)

Basidiocarp perennial, sessile to effused-reflexed, tough to woody. **Pilear** ungluate; projecting up to 4 cm, 6 cm wide and 2.5 cm thick at base. Pileal surface brown to brownish-gray when fresh, glabrous, margin cream buff. **Pores** surface white to cream when fresh, becoming clay-buff to brown when dry, pore surface pores angular, 3-5 per mm, dissepiments thin to slightly thick. **Tubes** white, buff to clay-buff, paler than pore surface, fragile, up to 2 cm long. **Context** white, up to 5 mm thick, upper surface with a dark brown crust. **Hyphal system** dimitic; generative hyphae thin-walled with clamps; cystidia present or absent. **Basidia** clavate with 4 sterigmata. **Basidiospores** subglobose to cylindric, hyaline, smooth, 3.0-5.0 \times 2.0-2.5 μm .

7. *Ganoderma australe* (Fr.) Pat.

Class Agaricomycetes; **Order** Polyporales; **Family** Ganodermataceae; **Genus** *Ganoderma*. **Specimen examined:** Isolate PBURU 5, Samarinda botanical garden, Indonesia. **Habitat/Substrata** on living tree (*Shorea* sp.). **Distribution** Pantropical and common in East Africa.



Figure 4.1.9. *Ganoderma australe* (picture credit: Wulandari, R)

Basidiocarp perennial, applanate, unguulate, normally dimidiate and semicircular in outline, variable in size, from 4-10 cm long, 5-10 cm wide and up to 2 cm thick in single fruitbodies, coriaceous when young and woody hard when dry. **Pilear** dull yellowish-brown to deep umber to almost blackish in old specimens, margin light coloured in actively growing specimens, whitish to yellowish. **Pores** round to slightly angular, 2-5 per mm. **Tubes** dark brown in section with light coloured tube-walls, in older parts often stuffed with white mycelium, weakly stratified, up 3 cm thick. **Hyphal system** trimitic; generative hyphae with clamps, hyaline, thin-walled 1-3 μm wide; skeletal hyphae thick-walled 5-8 μm wide; binding hyphae thin-walled 1-2 μm and thickly branched. **Basidia** clavate, with 4 sterigmata. **Basidiospores** truncate, yellowish-brown, echinulate, 5-12 x 3-8 μm .

8. *Ganoderma applanatum* (Pers.) Pat.

Class Agaricomycetes; **Order** Polyporales; **Family** Ganodermataceae; **Genus** *Ganoderma*. **Specimen examined:** Isolate PBURU 7, Samarinda botanical garden, Indonesia. **Habitat/Substrata** on living tree (*Dipterocarpus* sp.). **Distribution** Throughout the northern hemisphere temperate zone, USA, Europe, Northern Iran, Northern Pakistan, southern slopes of the Himalayas, India and Pakistan, Asia.



Figure 4.1.10. *Ganoderma applanatum* (picture credit: Wulandari, R)

Basidiocarp perennial, sessile, dimidiate, flabelliform, 20-30 mm thick at the middle but thickening at the base, sometimes effused-reflexed. Variable in size, from 5-10 cm long, 5-15 cm wide and up to 2 cm thick in single fruitbodies, coriaceous when young and woody hard when dry. **Pilear** yellowish-brown when young, tawny-olive, powdered over by brownish spore, margin white. **Pores** round to slightly angular, 2-5 per mm. **Tubes** in one layer 3-10 mm thick in young specimens. **Hyphal system** trimitic; generative hyphae with clamps, hyaline, thin-walled 1-5 μm wide; skeletal hyphae thick-walled 5-8 μm wide; binding hyphae thin-walled 1-2 μm wide and thickly branched. **Basidia** clavate, with 4 sterigmata. **Basidiospores** ellipsoid, apex truncate, yellowish-brown, 5-10 x 4-6 μm .

9. *Gloeoporus dichrous* (Fr.) Bres.

Class Agaricomycetes; **Order** Polyporales; **Family** Meruliaceae; **Genus** *Gloeoporus*.

Specimen examined: Isolate PBURU 23, Samarinda botanical garden, Indonesia.

Habitat/Substrata on falling dead deciduous wood. **Distribution** Cosmopolitan species known through all climatical zones from equator to North Cape, but not common.



Figure 4.1.11. *Gloeoporus dichrous* (picture credit: Hadi, S)

Basidiocarp annual, resupinate to pileate, often as effused fruitbodies with reflexed pilei, imbricate. Narrow and elongated pilei from 3-5 cm long, 5-8 cm wide and up to 1 cm thick, soft when fresh, coriaceous when dry. **Pilear** white to cream, tomentose, later scruPOSE to smooth or with tufts of hispid hyphae. **Pores** pruinose and white, pores round and angular, 2-5 per mm. **Context** white, up to 5 mm thick, cottony, distinctly thicker than the tubes. **Hyphal system** monomitic with clamped generative hyphae, in the context distinct and thick-walled with large clamps, up to 5 µm wide, moderately branched. **Basidia** clavate with 4 sterigmata. **Basidiospores** allantoid to cylindrical, hyaline, thin walled, smooth and non-amyloid, 2.5-5.5 x 0.5-1.5 µm.

10. *Lentinus sajur-caju* (Fr.) Fr.

Class Agaricomycetes; **Order** Polyporales; **Family** Polyporaceae; **Genus** *Lentinus*.

Specimen examined: Isolate PBURU 14, Samarinda botanical garden, Indonesia.

Habitat/Substrata on falling dead deciduous wood. **Distribution** Tropical Africa, Asia and Australia.



Figure 4.1.12. *Lentinus sajur-caju* (picture credit: Hadi, S)

Basidiocarp dry, smooth or often with small appressed squamules in the centre, white, cream-colour. **Pilear** convex with umbilicate centre, fan-shaped, dry, smooth or often with small appressed in the centre. **Stipe** 1-5 cm x 5-20 mm, central, lateral, short, cylindrical, base abrupt, concolorous with the pileus; ring 1-10 mm wide, firm, with entire edge. **Gill** decurrent, 0.5-2 mm wide, concolorous with the pileus, darker brownish-gray towards the entire edge. **Hyphal system** dimitic; generative hyphae with clamps, hyaline, thin-walled; skeletal hyphae thick-walled 1-2 μm wide, intercalary and terminal. **Basidia** clavate with 4 sterigmata. **Basidiospores** subcylindric, 5-10 \times 1.5-3 μm .

11. *Lentinus squarrosulus* (Mont.)

Class Agaricomycetes; **Order** Polyporales; **Family** Polyporaceae; **Genus** *Lentinus*.

Specimen examined: Isolate PBURU 13, Samarinda botanical garden, Indonesia.

Habitat/Substrata on falling dead deciduous wood. **Distribution** Pantropical, in Africa noted from almost all countries south of Sahara.



Figure 4.1.13. *Lentinus squarrosulus* (picture credit: Hadi, S)

Basidiocarp smooth or often with small appressed squamules in the centre, white, cream-colour. **Pilear** 1-12 cm wide, umbilicate. **Stem** 1-6 cm x 2-6 mm, more or less excentric, subcylindric, fibrous. **Gills** deeply decurrent, thin, 35-50 primaries 1.5-8 mm wide. **Flesh** 1-2.5 mm thick in the centre of the pileus, dry, tough, flaccid. **Hyphal system** dimitic, generative hyphae 2-5 μm wide, clamped, thin-walled; skeletal hyphae wide 4-8 μm , thick-walled 1-2 μm wide, intercalary and terminal, often becoming more or less solid in the stem. **Basidia** clavate with 4 sterigmata. **Basidiospores** white, smooth, subcylindric, inamyloid, 5.0-7.0 x 1.5-3.0 μm .

12. *Lenzites elegans* (Fr.) Pat.

Class Agaricomycetes; **Order** Polyporales; **Family** Polyporaceae; **Genus** *Lenzites*.

Specimen examined: Isolate PBURU 6, Samarinda botanical garden, Indonesia.

Habitat/Substrata on falling dead deciduous wood. **Distribution** Pantropical, common species. East Africa, Asia.



Figure 4.1.14. *Lenzites elegans* (picture credit: Hadi, S)

Basidiocarp annual to perennial, sessile or with a short stipelike base, attached laterally or centrally. **Pilear** fan-shaped, upper surface white to grey or almost buff ochraceous in older specimens. **Stipe** absent or up to 0.5 cm long, 2 cm in diameter, glabrous, solid, attached to the substrate with a disc up to 2 cm wide, concolorous with pileus surface, white to pale cream. **Pores** lamellate with straight to sinuous lamellae, 3-5 per cm measured tangentially, lamellae up to 5 mm deep. **Context**

white to pale cream, up to 15 mm thick near the base, woody hard when dry. **Hyphal system** trimitic; generative hyphae with clamps, hyaline, thin-walled 2-4 μm wide, skeletal hyphae thick-walled 2-5 μm wide, binding hyphae slightly thick-walled 2-3 μm wide. **Basidia** clavate with 4 sterigmata. **Basidiospores** cylindrical to oblong ellipsoid, hyaline, smooth and thin-walled, 3-5 x 2-3 μm .

13. *Microporellus obovatus* (Jungh.) Ryv.

Class Agaricomycetes; **Order** Polyporales; **Family** Polyporaceae; **Genus** *Microporellus*. **Specimen** examined: Isolate PBURU 35, Samarinda botanical garden, Indonesia. **Habitat/Substrata** on falling dead deciduous wood. **Distribution** Pantropical, in Africa noted from almost all countries south of Sahara.



Figure 4.1.15. *Microporellus obovatus* (picture credit: Wulandari, R)

Basidiocarp annual, solitary or in small groups or clusters, usually laterally stipitate usually paper-thin along the margin, up to 5 mm thick close to the stipe, rather brittle and hard when dry. **Pilear** white to cream, ochraceous, greyish to umber, often also radially striped, when older becoming glabrous. **Stipe** 0-2 cm long, 1-5 mm wide, cream then glabrous, usually concolorous with the pileus. **Pores** white, cream to pale straw-coloured, pores angular 5-8 per mm, tubes up to 2 mm deep. **Context** white, up to 2 mm thick. **Hyphal system** dimitic, generative hyphae with 2-5 μm wide, thin to distinctly thick-walled, skeletal hyphae thick-walled 2-8 μm wide. **Basidia** clavate with 4 sterigmata. **Basidiospores** globose to subovate 1.5-5 x 3-5.0 μm , thin-walled, smooth and nonamyloid.

14. *Microporus affinis* (Blume & Nees ex Fr.)

Class Agaricomycetes; **Order** Polyporales; **Family** Polyporaceae; **Genus** *Microporus*. **Specimen examined:** Isolate PBURU 10, Samarinda botanical garden, Indonesia. **Habitat/Substrata** on falling dead deciduous wood. **Distribution** Common species through the tropics in the old world from Western Africa to the Pacific Area.



Figure 4.1.16. *Microporus affinis* (picture credit: Hadi, S)

Basidiocarp annual, solitary or in groups, laterally stipitate or with a distinct stipe, semicircular dimidiate. **Pilear** glabrous or tomentose, zoned, either as narrow bands or as slightly raised narrow zones, colour velvety brown to almost black. **Stipe** lateral, up to 2 cm. **Pores** white to light cream, margin 1-5 mm wide and pure white, pores round, 5-8 per mm diameter, tubes light cream, up to 1 mm deep. **Context** white, up to 5 mm thick near the base in old specimens covered with a distinct dark cortex. **Hyphal system** trimitic, generative hyphae hyaline, thin-walled with clamps, 1.5-3 μm in wide, skeletal hyphae thick-walled 3.5-6 μm in wide, thick-walled, binding hyphae 3.5-6 μm . **Basidia** clavate with 4 sterigmata. **Basidiospores** cylindrical to oblong ellipsoid, hyaline and thin-walled, nonamyloid, 3-4 x 1.5-2 μm .

15. *Microporus xanthopus* (Fr.) Kunt.

Class Agaricomycetes; **Order** Polyporales; **Family** Polyporaceae; **Genus** *Microporus*. **Specimen examined:** Isolate PBURU 25, Samarinda botanical garden, Indonesia. **Habitat/Substrata** on falling tree branches, dead desiduous wood. **Distribution** Very common throughout the tropics in the Old World, from Western Africa to the Pacific Area.



Figure 4.1.17. *Microporus xanthopus* (picture credit: Hadi, S)

Basidiocarp annual, solitary or in groups, centrally or laterally stipitate, sometimes two or more fruitbodies grow together. **Pilear** up to 5 cm in diameter and thin, glabrous and shiny when fresh but becoming dull-brown when dry, yellowish-brown to light colours, margin thin and wavy. **Stipe** round, glabrous, light yellowish to light brown cuticle, up to 4 cm high and 2-5 mm in diameter. **Pores** cream to pale buff, white towards the margin, pores are virtually imperceptible to the naked eye, tubes up to 0.1 mm deep. **Context** pure white, thin and covered with a distinct cuticle. **Hyphal system** trimitic; generative hyphae with clamps, hyaline, thin-walled 2-4.5 μm wide; skeletal hyphae hyaline, thick-walled, up to 4 μm wide; binding hyphae thick-walled, up to 1-5 μm wide. **Basidia** clavate with 4 sterigmata. **Basidiospores** cylindrical, often slightly bent, smooth, hyaline 4-7 \times 1-2.5 μm .

16. *Phellinus fastuosus* (Lév.) Ryv.

Class Agaricomycetes; **Order** Hymenochaetales; **Family** Hymenochaetaceae; **Genus** *Phellinus*. **Specimen examined:** Isolate PBURU 18, Fig.4.1.3 (15), Samarinda botanical garden, Indonesia. **Habitat/Substrata** on living tree. **Distribution** Widespread and common in the tropical zone.



Figure 4.1.18. *Phellinus fastuosus* (picture credit: Wulandari, R)

Basidiocarp perennial, solitary or imbricate, pileate, broadly attached, dimidiate, flat to convex, up to 20 cm broad, 30 cm wide and 3 cm thick, woody when dry. **Pilear** velvety tomentose to almost black and with a distinct black crust up to 1 mm thick, margin usually rather thick, obtuse with yellowish-brown. **Pores** surface yellowish-brown to rusty-brown, dark brownish-gray in older specimens, pores round and regular, 7-12 per mm, dissepiments entire and thick. **Tubes** fulvous as the pore surface, strongly stratified, each strata usually 1-3 mm thick. **Context** yellowish-brown to more dark cinnamon up to 12 mm thick. **Hypthal system** dimitic; generative hyphae simple-septate, hyaline, slightly thick-walled, 2-3 μm wide, skeletal hyphae yellow 2-5 μm wide, thick-walled with a distinct lumen. **Basidia** clavate with 4 sterigmata. **Basidiospores** ellipsoid to subglobose, thick-walled, smooth, 3.5-6 x 4-6 μm .

17. *Polyporus arcularius* (Fr.) Bres.

Class Agaricomycetes; **Order** Polyporales; **Family** Polyporaceae; **Genus** *Polyporus*. **Specimen examined:** Isolate PBURU 17, Fig.4.1.3 (16), Samarinda botanical garden, Indonesia. **Habitat/Substrata** on falling dead deciduous wood. **Distribution** The

species is found throughout the tropics, subtropics and the warmer parts of the temperate zone, in Africa collected from Sierra Leone to Kenya and Tanzania, and south to South Africa.



Figure 4.1.19. *Polyporus arcularius* (picture credit: Hadi, S)

Basidiocarp annual, solitary or in groups of 2-3, centrally stipitate with round pileus up to 3 cm in diameter and 1-1,5 mm thick, brittle and fragile when dry. **Pileus** circular, umbilicate or dull infundibuliform, ochraceous to dark umber, often darker towards the margin. **Stipe** ochraceous to dark brown, centrally attached, up to 5 cm long and 2-4 mm in diameter, glabrous to tomentose, often slightly longitudinally wrinkled in dry condition. **Pores** ochraceous, reddish-brown to brown often paler than the pileus, pores angular and radially elongated, 1-3 per mm. **Context** white to pale-yellow, up to 0.5 mm thick. **Hyphal system** dimittic, generative hyphae very thin walled, 2-5 μm wide, binding hyphae, thick-walled, up to 5 μm wide. **Basidia** clavate with 4 sterigmata. **Basidiospores** cylindrical, smooth, hyaline and thin-walled, 5-10 x 2-5 μm .

18. *Polyporus badius*

Class Agaricomycetes; **Order** Polyporales; **Family** Polyporaceae; **Genus** *Polyporus*.

Specimen examined: Isolate PBURU 47, Samarinda botanical garden, Indonesia.

Habitat/Substrata on falling dead deciduous wood. **Distribution** Widespread to tropics and subtropical regions.



Figure 4.1.20. *Polyporus badius* (picture credit: Hadi, S)

Basidiocarp perennial, ungulate. **Pilear** Upper brownish black. **Pores surface** dark brown, pores 5-8 per mm, mostly angular. **Tubes** layers up to 5 mm thick each, individual layers not distinct, pale brown. **Context** yellowish brown, hard. **Hyphal system** dimitic; generative hyphae simple-septate, hyaline to pale yellow, slightly thick-walled, 1.5-5 μm in wide, skeletal hyphae yellow, thick-walled up to 5 μm wide with a distinct lumen. **Basidia** clavate with 4 sterigmata. **Basidiospores** broadly ovoid to subglobose 5-7.5 x 3.5-6 μm .

19. *Polyporus ostreiformis* (Berk)

Class Agaricomycetes; **Order** Polyporales; **Family** Polyporaceae; **Genus** *Polyporus*

Specimen examined: Isolate PBURU 66, Samarinda botanical garden, Indonesia.

Habitat/Substrata on falling dead deciduous wood. **Distribution** Common species through the tropics in the old world from Western Africa to the Pacific Area.



Figure 4.1.21. *Polyporus ostreiformis* (picture credit: Wulandari, R)

Basidiocarp sessile, effuse-reflexed, creamy white. **Pilear** up 3 cm in radius, up to 5 cm wide, dimidiate, imbricate, tomentose, margin obtuse. **Tubes** 5 mm long; pores 2-

5 per mm. **Context** Thin at the base of the pileus, fibrous then corky tough. **Hyphal system** trimitic, generative hyphae hyaline, slightly thick-walled with clamps, 1-3 μm wide, skeletal hyphae thick-walled 2.5-6 μm wide. **Basidia** clavate with 4 sterigmata. **Basidiospores** short cylindrical to oblong ellipsoid, hyaline and thin-walled, 2-3 x 1.5-3 μm .

20. *Pycnoporus coccineus* (Fr.) Bond & Sing

Class Agaricomycetes; **Order** Polyporales; **Family** Polyporaceae; **Genus** *Pycnoporus*. **Specimen examined:** Isolate PBURU 73, Samarinda botanical garden, Indonesia. **Habitat/Substrata** on falling dead deciduous wood. **Distribution** Throughout forest regions of Europe and circumpolar in the boreal-temperate zone. North to Finnmark in northern Norway, Asia.



Figure 4.1.22. *Pycnoporus coccineus* (picture credit: Wulandari, R)

Basidiocarp annual, sessile to effused-reflexed, single or in imbricate cluster up to 8 x 5.5 x 0.4 cm. **Pilear** dimidiate, broadly attached, deep orange to orange-red. **Pores** 4 to 6 per mm, the dissepiments relatively thick near the margin, becoming thinner with age. **Tubes** 1-3 per mm, with thick, entire dissepiments that become thin with age. **Context** suberose, showing distinct alternating bands of white and moderate orange, when broken or teased out appearing floccose or cottony, turning black immediately with KOH. **Hyphal system** trimitic, generative hyphae thin-walled, with clamps, 3-8 μm wide, skeletal hyphae thick-walled 3-9 μm wide, binding hyphae thick-walled, non

septate 2-4 μm wide. **Basidia** clavate with 4 sterigmata. **Basidiospores** cylindrical, hyaline, smooth or slightly curved, 3-4.5 x 2-2.5 μm .

21. *Pycnoporus sanguineus* (Fr.) Murr.

Class Agaricomycetes; **Order** Polyporales; **Family** Polyporaceae; **Genus** *Pycnoporus*. **Specimen examined:** Isolate PBURU 60, Samarinda botanical garden, Indonesia. **Habitat/Substrata** on falling dead deciduous wood. **Distribution** Pantropical, common species. East Africa, Asia.



Figure 4.1.23. *Pycnoporus sanguineus* (picture credit: Hadi, S)

Basidiocarp annual, sessile to effused-reflexed, single or imbricate cluster. **Pileus** 5-10 cm in diameter and 1-5 mm thick, with lighter and darker zones, first orange then red to cinnabar, later often intensively red-orange, margin acute, entire or somewhat incised, often lighter than the rest of the pileus. **Pores** red-orange to cinnabar. Pores circular, 5-6 per mm, with thick dissepiment. **Context** tough-fibrous, orange buff and azonate up to 3 mm thick appearing cottony floccose. **Hyphal system** trimitic, generative hyphae hyaline, thin-walled with clamps, 2-5 μm wide, skeletal hyphae thick-walled 2-7 μm wide, binding hyphae thick-walled, non septate 2-4 μm wide. **Basidia** clavate with 4 sterigmata. **Basidiospores** cylindrical, smooth, hyaline and non-amyloid, 4-6 x 2-2.5 μm .

22. *Rigidoporus microporus* (Sw.) Ovr.

Class Agaricomycetes; **Order** Polyporales; **Family** Meripilaceae; **Genus** *Rigidoporus*.

Specimen examined: Isolate PBURU 47, Samarinda botanical garden, Indonesia.

Habitat/Substrata on falling dead deciduous wood. **Distribution** Widespread to tropics and subtropical regions.



Figure 4.1.24. *Rigidoporus microporus* (picture credit: Ruga, R)

Basidiocarp annual, perennial, sometimes resupinate but mostly pileate, sessile and broadly attached, up to 20 cm long and 10 cm from margin attached. **Pilear** often imbricate. **Pores** 80-100 μm wide, or 130-150 μm , dissepiments 30-100 μm thick, waxy with a white. **Tubes** often with 2-3 indistinct layers. **Hyphal system** dimitic, generative hyphae with simple septa thin- to slightly thick walled, 3-5 μm wide, skeletal hyphae up to 8 μm wide. **Cystidia** present **Basidia** clavate with 4 sterigmata. **Basidiospores**, smooth, subglobose, thin-walled 3-5 x 2.5-4 μm .

CHULALONGKORN UNIVERSITY

23. *Schizophyllum commune* (Fr.)

Class Agaricomycetes; **Order** Polyporales; **Family** Schizophyllaceae; **Genus**

Schizophyllum. **Specimen examined:** Isolate PBURU 70, Samarinda botanical garden, Indonesia. **Habitat/Substrata** on falling dead deciduous wood.

Distribution Widespread to tropics and subtropical regions.



Figure 4.1.25. *Schizophyllum commune* (picture credit: Hadi, S)

Basidiocarp shell-shaped when attached above or below; upper surface covered with small hairs, dry, white to grayish, beneath surface comprised of gill-like folds that are split along the center; upper surface coated with small hairs, dry, white to grayish; **Pilear** with a pellicle of loosely interwoven hyphae covering it and a content of tightly aggregated hyphae with small lumens. **Gills** are bifurcate and covered with abhymenial hairs at the extremities, with the hymenial layer mainly rolled inside in dry conditions. **Hyphal system** trimitic, thin- to slightly thick-walled, 1.5-2 μm wide, skeletal hyphae slightly yellow, thick-walled with a defined lumen, binding hyphae thick-walled, non septate 2-4 μm wide. **Cystidia** present **Basidia** clavate with 4 sterigmata. **Basidiospores** hyaline, smooth, ellipsoid, or cylindrical 3-4 x 1.5-3 μm .

24. *Trametes lactinea* (Berk.) Pat.

Class Agaricomycetes; **Order** Polyporales; **Family** Polyporaceae; **Genus** *Trametes*.

Specimen examined: Isolate PBURU 28, Samarinda botanical garden, Indonesia.

Habitat/Substrata on falling dead deciduous wood. **Distribution** Palaeotropical; fairly common in Malesia.



Figure 4.1.26. *Trametes lactinea* (picture credit: Hadi, S)

Basidiocarp annual or reviving a second season, pileate narrowly attached or effused-reflexed, solitary, imbricate, laterally fused or forming rosettes, when solitary up to 5 cm wide and 10 cm broad, 0.5 cm thick, consistency tough and coriaceous when fresh, more hard on drying. **Pilear** 5 cm in radius, sessile, azonate or faintly zoned, white, sometimes with faint brownish zones, drying pale brownish buff. **Pores** 3-5 mm wide, dissepiments 1-3 mm thick, subcircular, in some collections shortly radially elongate to sublamelliform, white. **Context** 1.5-5 mm wide, thick, subcircular, in some collections shortly radially elongate to sublamelliform, white. **Hyphal system** trimitic, trimitic, thin- to slightly thick-walled with clamps 1.5-2 μm wide, skeletal hyphae, thick-walled 3-5 μm wide, binding hyphae thick-walled, non septate 1-2.5 μm wide, unbranched. **Basidia** clavate with 4 sterigmata. **Basidiospores** white, smooth, ellipsoid to subcylindric, thin-walled, inamyloid, 4-6 x 2.5-3 μm .

25. *Trametes hirsuta* (Fr.) Pilat

Class Agaricomycetes; **Order** Polyporales; **Family** Polyporaceae; **Genus** *Trametes*

Specimen examined: Isolate PBURU 3, Samarinda botanical garden, Indonesia.

Habitat/Substrata on falling dead deciduous wood. **Distribution** Throughout forest regions of Europe and circumpolar in the boreal-temperate zone. North to Finnmark in northern Norway, Asia.



Figure 4.1.27. *Trametes hirsuta* (picture credit: Hadi, S)

Basidiocarp annual, effused-reflexed or rarely resupinate, coriaceous when young. Pilear dimidiate, applanate to thick, upper surface hirsute, gray, zonate or concentrically sulcate; border yellowish-brown and tomentose. Surface pores white to tan or cinereous, pores 1-4 per mm, with thick, complete dissepiments that thin with age, context duplex, top layer gray, soft-fibrous, up to 3 mm thick, at least at the base divided by a thin black line from the bottom portion, the later ivory white, corky, up to 10 mm thick. Tubes 1-4 per mm in diameter, with thick, complete dissepiments that thin with age. **Context** duplex, the upper layer gray, soft-fibrous, up to 2 mm thick, at least at the base separated by a thin black line from the lower part, the latter ivory white, corky, up to 15 mm thick. **Hyphal system** trimitic, generative hyphae thin-walled, with clamps, 2.5-6 μm wide, skeletal hyphae thick-walled, hyaline 3-7 μm wide, binding hyphae, thick walled, nonseptate, 2-4 μm wide. **Basidia** clavate with 4 sterigmata. **Basidiospores** cylindrical; hyaline, smooth, negative in Melzer's reagent, 6-9 x 2-2.5 μm .

26. *Trametes menziesii* (Berk.) Ryv.

Class Agaricomycetes; **Order** Polyporales; **Family** Polyporaceae; **Genus** *Trametes*

Specimen examined: Isolate PBURU 42, Samarinda botanical garden, Indonesia.

Habitat/Substrata on falling dead deciduous wood. **Distribution** Paleotropical species, widespread in Africa, but apparently not as common as in South-East Asia. In Africa seen from Ghana, Sierra Leone, Nigeria, The Cameroons, Zaire, Burundi, Ethiopia, Kenya, Tanzania and Zaire. In Asia from Pakistan to the Pacific Islands and south to Australia.



Figure 4.1.28. *Trametes menziesii* (picture credit: Hadi, S)

Basidiocarp annual-perennial, very variable in size, pileate and applanate with a narrow contracted base to almost semi-stipitate, up to 10 cm wide and long, 1-10 mm thick, fairly flexible and tough in fresh, hard when old in thicker specimens. **Pilear** velvety becoming glabrous, first white to ochraceous, 1-3 mm wide. **Pores** white becoming creamish when dry, round to angular and from 2-5 per mm. **Tubes** more or less concolorous with the pore surface, up to 2 mm deep. **Context** pure white and fairly dense when fresh, becoming ochraceous to very pale cinnamon-fulvous in old specimens, **Stipe** often distinct with a 2-10 mm long sterile area between the pore layer and the substrate, colour white to deep grey. **Hyphal system** trimitic; generative hyphae with clamps, thin-walled, 2-3 μm wide; skeletal hyphae dominant, thick-walled to solid, hyaline, 3-7 μm wide; binding hyphae branched with tapering side-branches. **Basidia** clavate, 15-22 μm , with 4 sterigmata. **Basidiospores** cylindrical to oblong-ellipsoid, 7-10.5 \times 3-4 μm .

27. *Trametes polyzona* (syn. *Coriolopsis polyzona*) (Pers.) Ryv.

Class Agaricomycetes; **Order** Polyporales; **Family** Polyporaceae; **Genus** *Trametes*.

Specimen examined: Isolate PBURU 12, Samarinda botanical garden, Indonesia.

Habitat/Substrata on falling dead deciduous wood. **Distribution** Pantropical, in Africa noted from almost all countries south of Sahara.



Figure 4.1.29. *Trametes polyzona* (picture credit: Wulandari, R)

Basidiocarp annual to perennial, pileate, sessile, dimidiate, elongated lobed fruitbodies, single pilei up to 10 cm wide and 15 cm long, flexible to corky. **Pilear** yellowish-ochraceous when young, later darker, fulvous, ochraceous-brown. **Pores** cream to beige when young, darkens to yellowish-brown or fulvous, pores angular to round, on average 2-3 per mm **Context** duplex, lower part fibrous and subshiny in section, ochraceous to yellowish-brown. **Hyphal system** trimitic, generative hyphae with clamps, thin-walled and hyaline, branched, 1-3 μm wide. Skeletal hyphae, thick-walled, hyaline to yellow, 3-5 μm wide. Binding hyphae, hyaline to slightly yellowish, with short branches, 3-5 μm wide. **Basidia** clavate with 4 sterigmata. **Basidiospores** oblong to slightly ellipsoid, smooth and thin-walled, 3-7 x 2-3 μm , non-amyloid.

28. *Trametes versicolor* (Berk.) Ryv. มหาวิทยาลัย

Class Agaricomycetes; **Order** Polyporales; **Family** Polyporaceae; **Genus** *Trametes*

Specimen examined: Isolate PBURU 36, Samarinda botanical garden, Indonesia.

Habitat/Substrata on falling dead deciduous wood. **Distribution** Pantropical, in Africa noted from almost all countries south of Sahara.



Figure 4.1.30. *Trametes versicolor* (picture credit: Wulandari, R)

Basidiocarp annual, pileate, narrowly attached or effused-reflexed, single, imbricate, laterally fused. Pilear dimidiate, flabelliform or circular with a central attachment, convex, upper surface initially completely velutinate to tomentose, frequently silky, strongly concentrically zoned and sulcate in thin bands, occasionally radially striate or wavy. Pores white to cream, drying to deep cream or pale fulvous, pores 3-5 per mm, dissepiments whole and thin, tubes single-layered, concolorous with the pore surface, up to 2 mm long **Context** white to cream 0.5-3 mm thick. **Hyphal system** trimitic, generative hyphae clamped, usually hyaline and thin-walled 2-4 μm wide. Skeletal hyphae thick-walled hyaline to yellow, 3-8 μm wide. Binding hyphae hyaline to pale yellow, thick-walled 2-5 μm wide. **Basidia** clavate with 4 sterigmata. **Basidiospores** cylindrical, slightly curved to allantoid, hyaline, smooth and thin-walled, 4.5-6.5 x 1.5-2.5 μm , non-amyloid.

29. *Trichaptum biforme* (Fr. in Klotzsch) Ryvarden

Class Agaricomycetes; **Order** Polyporales; **Family** Polyporaceae; **Genus** *Trichaptum*

Specimen examined: Isolate PBURU 50, Samarinda botanical garden, Indonesia.

Habitat/Substrata on falling dead deciduous wood. **Distribution** An eastern species known from a few localities in southeast Finland, more widespread in central Europe and in the Mediterranean area. Cosmopolitan species, Asia.



Figure 4.1.31. *Trichaptum biforme* (picture credit: Hadi, S)

Basidiocarp annual, sessile; pilei solitary or imbricate, dimidiate to flabelliform or petaloid, up to 6 cm wide and 3 mm thick. **Pilear** solitary or imbricate, dimidiate to flabelliform or petaloid, up to 6 cm wide and 3 mm thick; pileus surface gray to buff, hirsute to glabrous with age, zonate. **Tubes** violaceous or concolorous with context, up to 2 mm thick. **Context** pale buff, azonate, tough-fibrous, up to 1.5 mm thick; tube layer violaceous or concolorous with context, up to 2 mm thick. **Hyphal system** dimitic, generative hyphae thin-walled, with clamps, occasionally branched, 2.5-6 μm wide, skeletal hyphae thick-walled, nonseptate, rarely branched, 4-6 μm wide. **Cystidia** present. **Basidia** clavate with 4 sterigmata. **Basidiospores** cylindrical, slightly curved, hyaline, smooth, non-namyloid 5-7 x 2-3 μm .

30. *Junghuhnia* sp. (Fr. in Klotzsch) Ryvarden

Class Agaricomycetes; **Order** Polyporales; **Family** Steccherinaceae; **Genus** .
Junghuhnia. **Specimen examined:** Isolate PBURU 24, Samarinda botanical garden, Indonesia. **Habitat/Substrata** on falling dead deciduous wood. **Distribution** An eastern species known from a few localities in southeast Finland, more widespread in central Europe and in the Mediterranean area. Cosmopolitan species, Asia.



Figure 4.1.32. *Junghuhnia* sp. (picture credit: Wulandari, R)

Basidiocarp resupinate, effuse, appressed closely to the substrate 5-7 mm thick, bright orange when fresh and ochraceous when dry. **Pores** round or angular, 5-7 per mm. **Hyphal system** dimitic; contextual generative hyphae thin-walled, with clamps, occasionally branched, 2.5-7 μm in diam; contextual skeletal hyphae thick-walled,

nonseptate, rarely branched, 3-6 μm in diam; tramal hyphae similar. **Cystidia** present. **Basidia** clavate with 4 sterigmata. **Basidiospores** ellipsoid to oval, smooth, hyaline, 3.0-3.5 x 1.0-3.5 μm .

White-rot fungi (WRF) are an outstanding wood decomposer group (Kirk et al. 1998). WRF is a diverse eco-physiological group which includes basidiomycetes and litter-decomposing fungi capable of degrading lignin and able to secrete more extracellular LMEs that enable them to degrade a wide range of xenobiotics (Cabana et al. 2007). The most advanced group of WRF belongs to the phylum Basidiomycota, which contains approximately 30,000 described species, or only 37% of the true fungi (Carlile et al., 2001). In this study, 50 specimens, mostly belonging to the phylum Basidiomycota, were obtained from a survey in Samarinda botanical garden, East Kalimantan, Indonesia. Most fungal specimens are known as wood saprotrophs and happen to be generalist species which can be easily found in tropical rain forests. Fungal diversity in East Kalimantan is expected to be relatively high due to the species richness of woody plants, the most important biomass used by fungi. Many studies on the use of white rot fungi have been conducted throughout Indonesia, including East Kalimantan. *Armillaria* sp., *Pleurotus eryngii* and *Polyporus* sp. isolated from Samarinda Botanical Garden in East Kalimantan have been studied intensively for their roles in biodegradation of PAHs (Hadibarata & Kristanti, 2013; Hadibarata, 2013; Hadibarata, et al., 2012). Meanwhile, *Phanerochaete* sp., *Pycnoporus* sp., *Schizophyllum* sp. and *Trametes* sp. from Java and Sumatra islands were studied for their lignin modifying enzymes (LMEs) production for lignin degradation in pretreatment of biomass (Hermiati et al., 2013).

4.2. Screening of white rot fungi for PAH degradation

Screening procedures for selecting WRF to degrade PAHs were studied regarding four following steps which sequentially conducted; Guaiacol assay (step 1), ABTS assay (step 2), PAHs tolerance test (step 3) and PAHs degradation (step 4). The result of each screening procedures is described in the following sections.

4.2.1. Guaiacol Assay

In the first screening attempt, 50 fungi that could be isolated were aseptically inoculated onto 2% potato dextrose agar (PDA) plates supplemented with 0.01% guaiacol and incubated at 30 °C for seven days. The inoculated plates that changed color and turned brown were a visual indication of guaiacol oxidation. The WRF isolates were selected for the intensity of their oxidative activity towards guaiacol. Furthermore, the isolates were ranked based on color intensities. It was classified according to the strength of color of the brownish-colored zone as follows: dark brown (DB), brown (B), light brown (LB), yellowish (Y), (Figure 4.2.1). Table 4.2.1 lists the 50 isolates that were screened using the guaiacol on plate assay for each zone of collection sites. Most of the isolates were able to oxidize guaiacol by changing the color of the agar. 15 isolates showed a dark brown and brown color change in the agar, 25 showed a light brown color change, and 10 isolates showed a yellowish color change in response to guaiacol. It was also discovered that the same strain had different color responses to guaiacol, indicating strain-specific behavior. Fifteen fungi were chosen for further testing because they exhibited dark brown and brown color reactions.

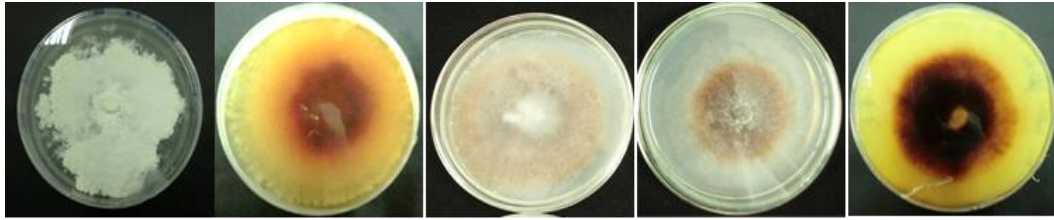


Figure 4.2.1. Phenoloxidase agar assay using 0.01% guaiacol sequentially; Control agar; yellowish (Y); light brown (LB); brown (B); dark brown (DB).

Guaiacol (2-methoxyphenol) is a phenolic natural product that was first isolated from lignin oxidation and is frequently employed in screening regimes for the identification of fungi with phenol oxidase activity because it turns yellowish brown or reddish brown when oxidized (Batista-Garcia et al., 2017). In this study, guaiacol has been successfully used for the preliminary screening of LMEs. It was indicated by the ability of 50 isolates to change the color of agar from clear to brown, with 15 isolates showing a strong positive response. This result was in line with a study conducted by Afrida et al. (2009). They obtained 258 positive responses to guaiacol from 600 WRF isolates collected throughout Indonesia. The majority of the identified isolates are polyporales.

The variety of color changes in each isolate demonstrated the oxidation variation of white rot fungi toward guaiacol. *Ganoderma australe*, *Pycnoporus sanguineus*, *Trametes hirsuta*, *Trametes polyzona*, and *Trametes versicolor*, all found in zones 1 and 2, have different color reactions to guaiacol. *Microporus affinis*, found in zones 1, 2, and 3, exhibits the same behavior, but with different colors for each zone. While *Gleoporus dichrous*, *Lenzites elegans*, *Lentinus squarrosulus*, *Microporellus obovatus*, *Microporus xantophus*, *Polyporus ostreiformis*, *Polyporus arcularius*, and *Trametes lactinea* demonstrated consistency of color reaction to guaiacol. This result was in accordance with Machuca et al. (2011), they discovered a higher degree of strain-specific variability in the enzymatic activity of *Ganoderma australe* and *Stereum hirsutum* isolates that gave varying reactions to guaiacol.

Table 4.2.1. White rot isolates and their reaction to guaiacol oxidation

Zone 1		Zone 2		Zone 3	
Isolate number	Guaiacol reaction	Isolate number	Guaiacol reaction	Isolate number	Guaiacol reaction
PBURU 8	Y	PBURU 7	LB	PBURU 54	LB
PBURU R1	DB	PBURU 5	DB	PBURU 61	Y
PBURU 141	DB	PBURU 43	LB	PBURU 63	LB
PBURU 11	DB	PBURU 55	LB	PBURU 69	LB
PBURU 45	LB	PBURU 48	LB	PBURU 73	DB
PBURU 15	Y	PBURU 68	Y	PBURU 70	B
PBURU 21	LB	PBURU 32	LB		
PBURU 23	LB	PBURU 31	LB		
PBURU 24	Y	PBURU 44	LB		
PBURU 6	Y	PBURU 18	DB		
PBURU 13	LB	PBURU 53	LB		
PBURU 35	LB	PBURU 66	LB		
PBURU 10	B	PBURU 72	B		
PBURU 25	LB	PBURU 11	Y		
PBURU 27	LB	PBURU 41	LB		
PBURU 17	LB	PBURU 58	LB		
PBURU 47	Y	PBURU 46	DB		
PBURU 60	DB	PBURU 74	LB		
PBURU 3	DB	PBURU 77	LB		
PBURU 28	LB	PBURU 62	LB		
PBURU 42	B				
PBURU 12	DB				
PBURU 36	B				
PBURU 50	LB				

The strength of color of the brownish colored zone as follows: dark brown (DB), brown (B), light brown (LB), Yellowish (Y)

4.2.2. ABTS assay

Fifteen isolates from preliminary screening using guaiacol were tested for secondary screening of ABTS-oxidizing enzyme activity on an agar plate supplemented with 5 mM 2,2'-azino-bis(3-ethylbenzothiazoline-6-sulphonic acid) (ABTS). After 7 days of incubation, the colony diameter and the width of the green zone surrounding the colony were measured (Table 4.2.2.1). The positive response to ABTS-oxidizing enzyme activity was visualized by the change of color from colorless to green or dark green on agar due to the oxidation of ABTS into ABTS-azine (Figure 4.2.2). ABTS is easily oxidized by different peroxidases and laccase to the cation radical $ABTSC^{\bullet}$, while cation radical can be oxidized further to form $ABTS^{2+}$ (Christopher et al., 2014). The selection of potential isolate for ABTS-oxidizing enzyme was determined by the ratio (diameter of green halo/diameter of colony) that greater than 1.5 (Dhouib et al., 2005).

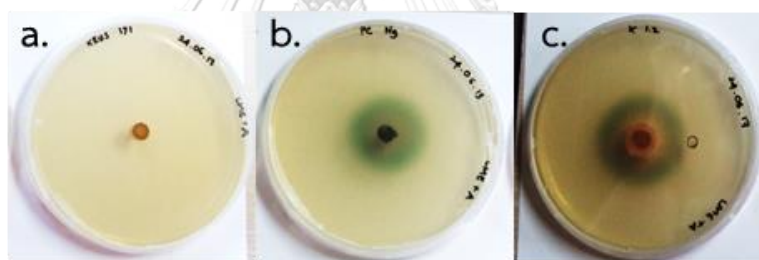


Figure 4.2.2. LME agar assay supplemented with 5 mM ABTS after 3 days of cultivation. A. No reaction to ABTS; B. Color zone with limited growth; C. Color zone with growth

The results revealed that 14 of the 15 isolates secreted green color along with growth, with a ratio ranging from 1.05-2.09. While growth was inhibited and no green zone appeared for isolate PBURU 141. Furthermore, four isolates (PBURU 11, PBURU 60, PBURU 12 and PBURU 5) were found to have a higher more than 1.5 ratio when compared to other isolates, indicating that they are capable of producing more ABTS-oxidizing enzyme than other isolates. The isolates were identified as *Ganoderma australe*, *Pycnoporus sanguineus*, *Trametes polyzona*, and *Coriolopsis sanguanaria*.

Previously, all of those genus were known to produce ABTS-oxidizing enzyme. *Ganoderma* can oxidize ABTS, whereas *Coriolopsis*, *Pycnoporus*, and *Trametes* have a stronger response to ABTS-oxidizing enzyme secretion (Dhouib et al., 2005; Thongkred et al., 2011; Wang et al., 2018). Therefore, the 4 isolates were selected for the next experiment.

Table 4.2.2.1. Secondary screening of white rot fungi on LME agar supplemented with 1 mM ABTS.

Isolate	Mycelial growth			Selection
	Fungal colony diameter (cm)	Colour zone diameter (cm)	Ratio of green zone diameter to colony diameter	
1. PBURU 3	4.0 ± 0.0	5.3 ± 0.3	1.33	
2. PBURU 5	4.0 ± 0.0	6.3 ± 0.3	1.58	*
3. PBURU 10	2.0 ± 0.0	2.5 ± 0.0	1.25	
4. PBURU 11	3.6 ± 0.1	6.0 ± 0.0	1.67	*
5. PBURU 12	3.3 ± 0.3	6.9 ± 0.1	2.09	*
6. PBURU 18	4.3 ± 0.3	4.5 ± 0.0	1.05	
7. PBURU 36	4.3 ± 0.3	4.9 ± 0.1	1.14	
8. PBURU 42	2.0 ± 0.0	2.5 ± 0.0	1.25	
9. PBURU 46	2.5 ± 0.0	3.0 ± 0.0	1.2	
10. PBURU 60	3.2 ± 0.1	6.5 ± 0.0	2.03	*
11. PBURU 70	3.2 ± 0.1	3.9 ± 0.1	1.22	
12. PBURU 72	3.0 ± 0.0	3.5 ± 0.0	1.17	
13. PBURU 73	2.2 ± 0.1	2.9 ± 0.1	1.31	
14. PBURU 141	NG	NR	-	
15. PBURU R1	3.0 ± 0.0	4.0 ± 0.0	1.33	

Remarks: NG= No growth; NR= No reaction

4.2.3. PAH tolerance

The tolerance level of fungal isolates to 3- and 4- ring PAHs (fluoranthene, phenanthrene and pyrene) in varied concentrations was investigated. The end result is depicted in Figure 4.2.3. Four isolates were able to grow in the presence of PAHs in various concentrations (50-250 ppm) compared to the control (PDA) with the solvent (acetonitrile) after 7 days of incubation at 30°C in the dark incubator. The following are the specifics:

The relative growth of four isolates was found to be higher when fluoranthene was added to the medium at concentrations ranging from 50 to 100 ppm in the range of 80 to 98%. However, growth has been reduced by more than 5-fold as fluoranthene concentration has increased (250 ppm). At 50 and 100 ppm concentrations, PBURU 12 grew at the same rate to PBURU 5, PBURU 11, and PBURU 60. At 250 ppm fluoranthene concentration, all four isolates' growth was nearly completely depleted to less than 20%. The ANOVA test revealed that there was no significant difference in growth between isolates and concentrations when incubated at 50 and 100 ppm, but there was at 250 ppm. The post-hoc analysis using the least significant difference (LSD) method revealed that there was no significant difference between the four isolates when the fluoranthene concentration was between 50 and 100 ppm. Concurrently, when cultivated at 250 ppm, isolate PBURU 12 was significantly different from isolates 5 and 11, but not from isolate 60. In terms of concentration, 250 ppm was discovered to be significantly different from 50 and 100 ppm.

Growth was inhibited by the addition of phenanthrene to the media. PBURU 12 exhibited the greatest growth at 50 ppm at 80% relative growth, while the other three isolates grew at less than 60%. When the concentration of phenanthrene was increased to 100 ppm, the growth of all four isolates was inhibited. PBURU 12 had the highest growth rate of 45%. While phenanthrene was increased to 250 ppm, the growth rate was significantly reduced to less than 15% for all strains. The results of the ANOVA analysis show that there are significant differences in growth between isolate groups.

The LSD analysis revealed that PBURU 12 was significantly different from PBURU 5, 11, and 60 at 50 ppm phenanthrene concentration. When the concentrations were increased to 100 ppm, PBURU 60 and 12 showed a significant difference from the other isolates, whereas all strains showed no difference when the concentrations were increased to 250 ppm. The LSD analysis also revealed a statistically significant difference in three concentrations (50, 100 and 250 ppm).

The addition of pyrene into the media demonstrated varied growth in the 4 isolates. The addition of 50 ppm of pyrene into the media exhibited relative growth of up to 85%, with the highest growth shown by PBURU 11 at 92%. The growth of PBURU 60, 12 and 11 has decreased up to 1-fold and 3-fold toward the concentration of 100-250 ppm, with the highest growth being shown by PBURU 11 for every concentration. Only PBURU 5 expressed a significant lower growth compared to others. The ANOVA test showed there was a significant difference in growth among isolates 11, 12 and 60 when incubated at 100 and 250 ppm, except for PBURU 5. The LSD analysis revealed when pyrene concentration was at 50 ppm, there was no significant difference between PBURU 11, 12 and 60 except for PBURU 11 that significantly different from PBURU 5. Concurrently, Isolate PBURU 11, 12 and 60 were significantly different from PBURU 5 when cultivated at 250 ppm, respectively. Furthermore, the LSD analysis showed a significant difference between three concentrations (50, 100 and 250 ppm).

The result from the tolerant test demonstrated that all 4 isolates were able to grow more than 90% in the presence of 50 ppm fluoranthene and pyrene, while only PBURU 12 that was able to grow up until 80% in phenanthrene media. When the concentration was increased to 100 ppm, there was less growth inhibition happened to both fluoranthene and pyrene to 4 isolates, since they were still able to grow more than 80%, while there was a strictly decrease of growth happened due to the addition of phenanthrene. Thongkred et al. (2011) discovered that the growth of *Pycnoporus coccineus* Thongkred 013 BCU was depleted to only 22%, 20%, and 24.6% during a tolerance test with media containing 100 ppm (individual phenanthrene, fluoranthene,

and pyrene), respectively. Meanwhile, *Trametes polyzona* RYNF13 was found to be tolerant to phenanthrene and pyrene when 4 mg/ml of each individual PAH in diethyl ether was sprayed on wood meal-based agar (WMBA) (Teerapatsakul et al., 2017). Furthermore, *Phanerochaete* sp. T20 was able to survive on fluoranthene, phenanthrene and pyrene at some extent, up to 500 mg/l for at least 30 days (Juckpech et al., 2012).

The increasing of concentration to 250 ppm in this study was causing deterioration of growth to 4 isolates indicates the concentration was toxic for fungi to withstand the growth. Higher concentrations of PAHs increasing their toxicity which leading to an inhibition of fungal growth (Teerapatsakul et al., 2017). Therefore, a concentration of 100 ppm was chosen for the next study to give the proper growth for fungal isolate.

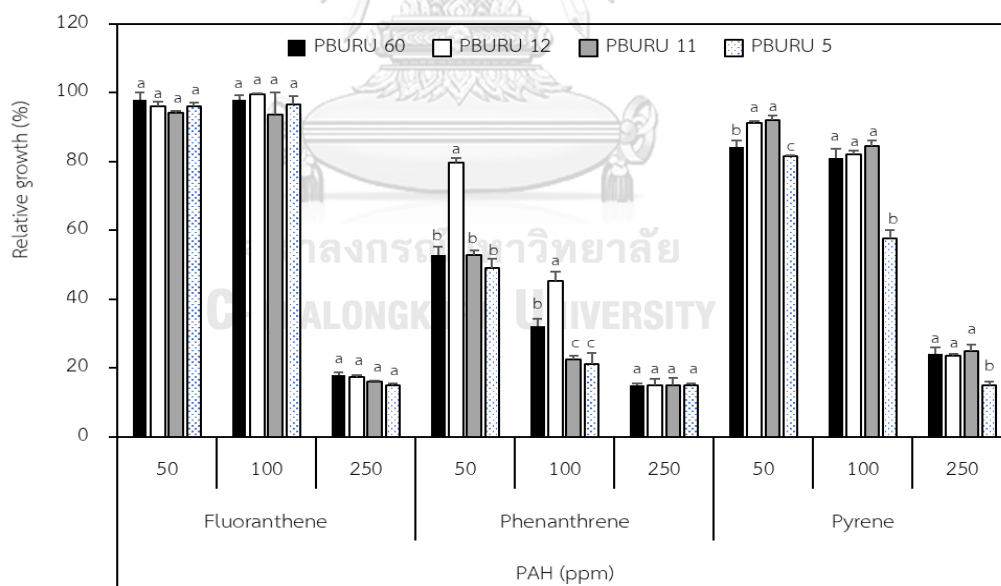


Figure 4.2.3. Relative growth (%) of selected WRF isolates on fluoranthene, phenanthrene and pyrene in different concentrations.

4.2.4. PAHs degradation in liquid medium by white-rot fungi

The degradation (%) of 4 white-rot isolates to degrade PAHs (phenanthrene, fluoranthene and pyrene) in liquid medium (basal medium) using 100 ppm of concentration (Fig. 4.2.4) and its lignin-modifying enzymes (LMEs) profile were studied (Table 4.2.4). All 4 isolates selected from the screening process demonstrated a significant improvement in PAH degradation following their cultivation on a PAH-added medium. The average degradation varied from 80-88% for phenanthrene, 80-90% for fluoranthene and 70-85% for pyrene. The LMEs profile showed that all 4 isolates secreted two extracellular enzymes (laccase and manganese peroxidase) with laccase as the major enzyme produced. The results showed all isolates were able to degrade PAHs, but the degradation rate varied depending on the PAH type and fungal isolate.

Phenanthrene degradation by 4 isolates exhibited over 80% after 15 days of cultivation. PBURU 12 showed the highest degradation activity at 88% and found to be significant compared to PBURU 11 and 60, while it was not significant for PBURU 5. There was slightly increase in the activity of LMEs enzymes when phenanthrene was added to the medium compared to the control. Fluoranthene degradation by 4 isolates resulted in a high degradation of over 80-90% after 15 days of cultivation. Again, PBURU 12 showed the highest degradation activity by 90%, but it was not significantly different compared to PBURU 60, 5 and 11. Laccase activities of PBURU 12 and 60 were found to be three times higher than the control, whereas PBURU 5 and 11 laccase activities were found to be slightly higher than control. The activity of manganese peroxidase for 4 isolates remained low compared to laccase. The pyrene degradation exhibited a degradation of over 60-80% after 15 days of cultivation. PBURU 60 and 12 were able to degrade pyrene up to 79 and 85%, while PBURU 5 and 11 degraded pyrene to 69 and 71%. The LMEs profile showed there was slightly increase in 4 isolates when pyrene was added to the medium.

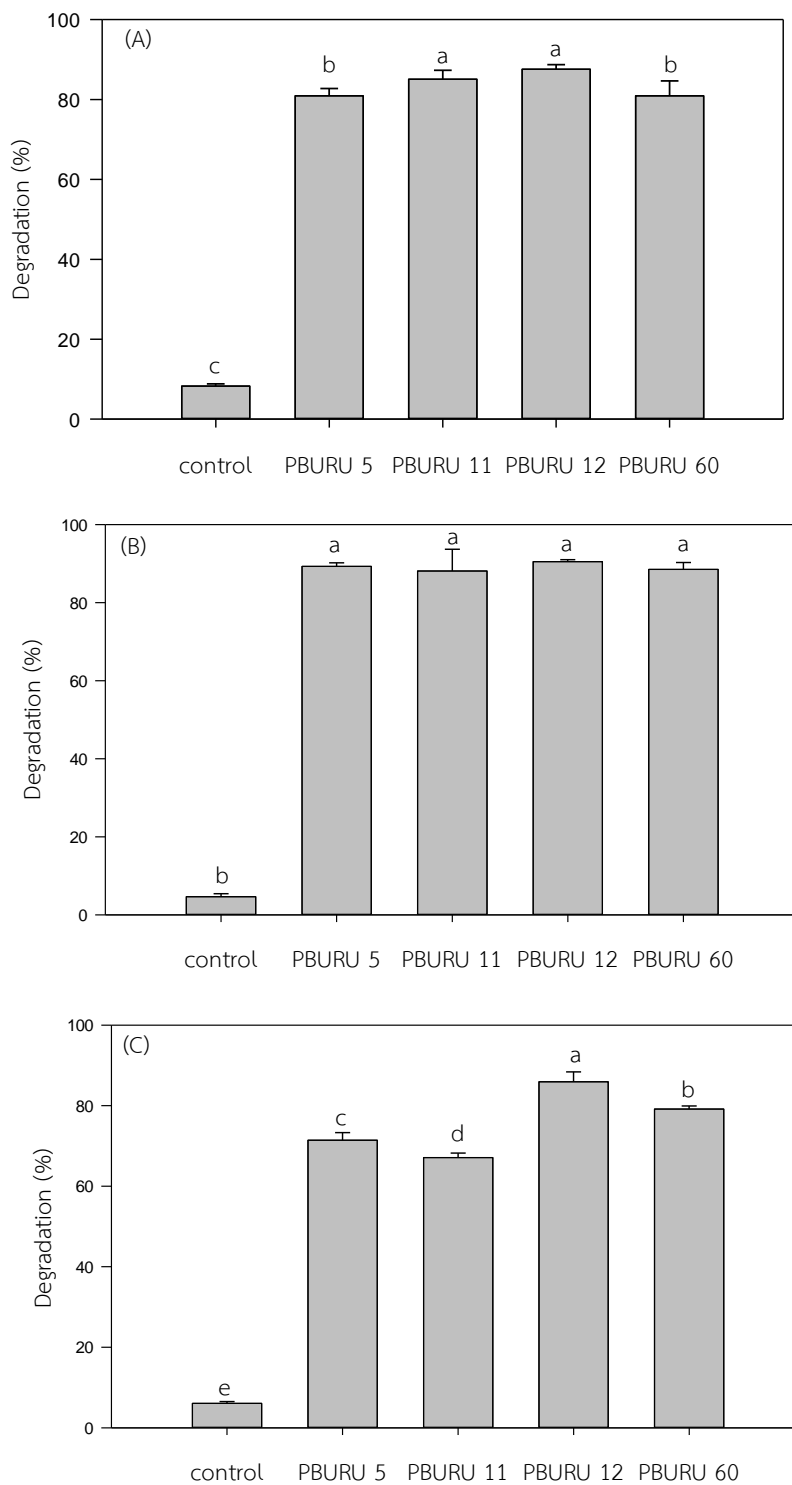


Figure 4.2.4. Degradation (%) of 100 ppm PAHs by selected isolates cultivated using basal medium at 30°C, shaking 150 rpm for 15 days. (A) Phenanthrene-100 ppm; (B) Fluoranthene-100 ppm; (C) Pyrene-100 ppm.

The ability of 4 isolates to degrade individual PAHs (phenanthrene, fluoranthene and pyrene) was compared to the results from other studies. *Trametes polyzona* RYNF13 was able to completely degrade 100 ppm phenanthrene, whereas only 50% pyrene was degraded at 30°C within 18 days. The fungus also produces all three enzymes (Laccase, MnP and LiP) during phenanthrene and pyrene degradation using mineral salt glucose medium (MSG). All three enzymes were induced by PAHs, showing increasing activity compared to the control, with MnP as the major enzyme (Teerapatsakul et al., 2017). Phenanthrene and pyrene degradation by *Ganoderma lucidum* was also studied (Agrawal et al., 2018). The result showed *G. lucidum* was able to almost degrade 20 ppm phenanthrene and pyrene (99.65% and 9.58%) after 30 days of incubation using a mineral salt medium. The PAH was found induced the three major LME enzymes (Laccase, Lip, and MnP). *Pycnoporus sanguineus* H1 was found to be capable of degrading 1 ppm pyrene up to 30%, which was followed by an increase in laccase activity (Zhang et al., 2015). Fluoranthene degradation was studied using *Pleurotus pulmonarius* F043. The result showed a complete degradation of fluoranthene (10 ppm) for 30 days using a modified mineral salt medium with laccase and MnP were found in the medium (Wirasnita & Hadibarata, 2016). Although the results above showed that PAH can induce the production of LMEs, it may also have no effect or inhibit the production of LMEs. Pozdnyakova et al. (2011) discovered that when grown in Kirk's medium, the production of laccase by *Pleurotus ostreatus* D1 was insignificantly increased in the presence of pyrene. Meanwhile, another study reported that *P. Ostreatus* laccase production increased in the presence of phenanthrene but decreased in the presence of pyrene and fluoranthene (Bezalel, Hadar, & Cerniglia, 1996). This could explain the four isolates' varying activity in the production of LMEs.

The result of PAHs degradation by 4 isolates was varied in degradation. However, PBURU 60 and 12 showed they able to degrade phenanthrene, fluoranthene and pyrene with higher rates compared to PBURU 5 and 11. Nevertheless, PBURU 12

showed the highest degradation and growth tolerance toward PAHs made PBURU 12 a good candidate and have been selected for further experiment.

Table 4.2.4. Lignin-modifying enzymes (LMEs) profiles of 4 isolates.

	Control	Phenanthrene	Fluoranthene	Pyrene
PBURU 60				
Laccase	1.16 ± 0.03	1.89 ± 0.51	3.73 ± 1.12	1.22 ± 0.03
MnP	0.14 ± 0.01	0.17 ± 0.01	0.03 ± 0.01	0.15 ± 0.01
PBURU 12				
Laccase	1.13 ± 0.03	1.33 ± 0.17	3.41 ± 1.91	1.64 ± 0.21
MnP	0.07 ± 0.01	0.05 ± 0.01	0.02 ± 0.01	0.02 ± 0.01
PBURU 11				
Laccase	1.04 ± 0.03	1.97 ± 0.06	1.52 ± 0.02	1.20 ± 0.02
MnP	0.22 ± 0.01	0.33 ± 0.05	0.20 ± 0.01	0.20 ± 0.01
PBURU 5				
Laccase	0.94 ± 0.15	1.03 ± 0.02	1.79 ± 0.02	1.02 ± 0.05
MnP	0.22 ± 0.01	0.13 ± 0.01	0.16 ± 0.06	0.14 ± 0.01

* Control was cultivation medium without the addition of PAHs (solvent only).

The activity was express as U/ml.

4.3. Characterization of selected isolate

4.3.1. Molecular identification of isolate PBURU 12

The molecular identification of isolate PBURU 12 by ITS rDNA sequencing show 99% similarity to the genus *Trametes* and identified as *Trametes polyzona* (Pers.) Justo, comb.nov. (Syn: *Coriolopsis polyzona*). The nomenclature of *Coriolopsis polyzona* in *Trametes* was revised, the name *Coriolopsis* (only *Coriolopsis polyzona*) becomes a synonym of *Trametes* (Justo & Hibbett, 2011). The sequence has been deposited at the NCBI database with accession number KY234233. The ITS sequence BLAST result return to maximum similarity index of 99% to strains *Trametes polyzona* IPBCC.18.1413 (LC412113) from Indonesia and *Coriolopsis polyzona* Dai9495 (FJ627247) from China. The phylogenetic tree described relationship among *Trametes* genus to PBURU 12. *Phellinus igniarius* voucher BRNM 714866 (GQ383710) was used as an outgroup for ITS rDNA analyses. The phylogenetic tree of *Trametes polyzona* PBURU 12 was constructed using MEGA-X, the neighbor-joining method (p-distance) with 1000 bootstrap replications. The ITS rDNA final dataset of 35 sequences comprised 690 characters. In phylogenetic analyses, PBURU 12 is highly supported and placed in the same clade as other *Trametes polyzona*, which were correspondence with the morphological results (Figure 4.3.1). Appendix G and H contains the sequence of PBURU 12 and complete gene bank accession numbers for all taxa used in this study.

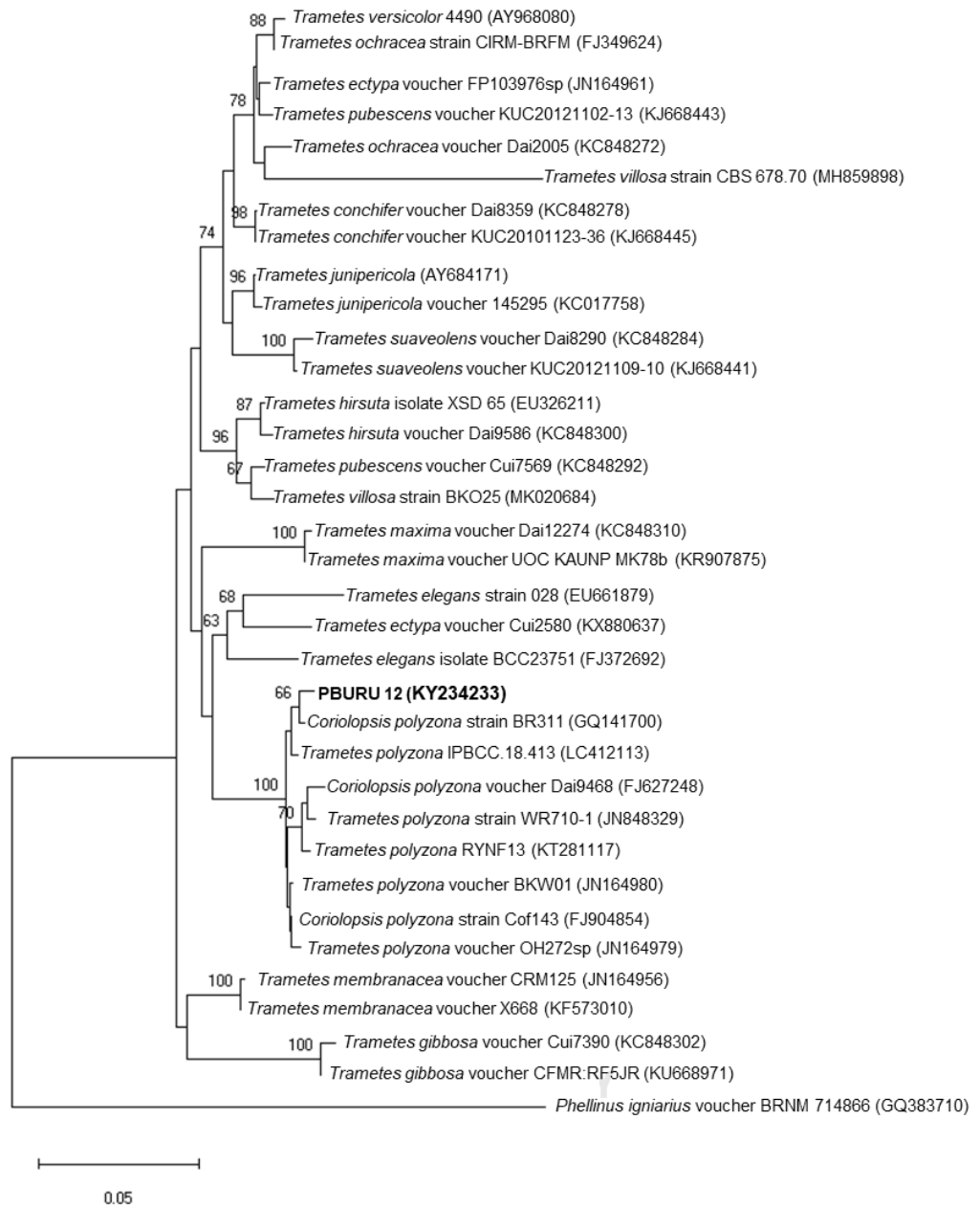


Figure 4.3.1. Phylogenetic tree of genus *Trametes* related to PBURU 12. Bar 0.05 = base substitution. Bootstrap values are shown next to the branches.

4.3.2. Optimization and production of laccase from PBURU 12

4.3.2.1. Screening of the medium composition for laccase production using the Plackett-Burman design

Plackett-Burman (PB) design was used in this study to statistically select medium components which gave positive effect to laccase production by PBURU 12 (Jegatheesan & Eyini, 2015). Statistical methods for medium optimization have been proved to be powerful and useful tools in industrial biotechnological processes. PB design is a promising experimental design for identifying the significant factors influencing productivity. Based on Plackett-Burman factorial design, each selected cultural factor was examined in two level for its influence on laccase production by *T. polyzona* PBURU 12: -1 for low level and +1 for high level.

To screen the optimum medium composition for laccase production by PBURU 12, 11 components were tested using the Plackett-Burman design. The independent variables examined in the Plackett-Burman design and their settings are shown in table 4.3.2.1. All experiments were carried out in triplicate and the average of the laccase activity from PBURU 12 was taken as the response in Design Expert 7 software. The Plackett-Burman design (PBD) show various in laccase activity started from 0.5 U/ml to 2.87 U/ml, which manifested the present of main medium components that could enhance laccase activity. The main effects of parameters on laccase production were estimated by subtracting the mean responses of parameters at their lower levels (-1) from their corresponding higher levels (+1) and dividing by the total number of experimental runs.

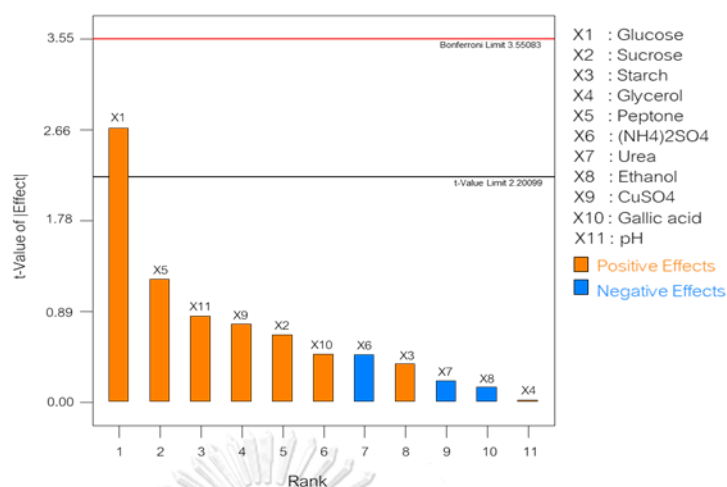


Figure 4.3.2.1. Pareto chart of factors effects on laccase production by PBURU 12

Out of the eleven variables screened using PBD, seven of them identified to be positive for laccase activity. Glucose, sucrose, starch, peptone, glycerol, CuSO₄, gallic acid and pH gave positive response to laccase activity while NH₄(SO)₄, ethanol and urea exerting negative influence on laccase production (Figure 4.3.2.1). Analysis of variance (ANOVA) of PBD for laccase production by PBURU 12 showed the model *F*-value of 21.48 and Values of "Prob > *F*" less than 0.05 indicate model terms were significant (Table 4.3.2.2). Statistical analysis from ANOVA suggested that among the positive effects on laccase production by PBURU 12, glucose, peptone, CuSO₄ and pH were the factors which showed the highest positive influence above 95% (*p*-value). Therefore, these factors were chosen for further analysis using Response Surface Methodology (RSM).

Table 4.3.2.1. The Plackett-Burman experimental design observed and predicted values effected laccase production by PBURU 12.

Run	Coded values of variables											Observed response (U/ml)	Predicted response (U/ml)
	X ₁	X ₂	X ₃	X ₄	X ₅	X ₆	X ₇	X ₈	X ₉	X ₁₀	X ₁₁		
1	10.00 (+1)	5.00 (-1)	5.00 (-1)	5.00 (-1)	3.00 (+1)	1.00 (-1)	3.00 (+1)	3.00 (+1)	0.10 (-1)	0.10 (+1)	5.00 (+1)	2.38	2.28
2	5.00 (-1)	5.00 (-1)	5.00 (-1)	10.00 (+1)	1.00 (-1)	3.00 (+1)	3.00 (+1)	1.00 (-1)	0.50 (+1)	0.10 (+1)	5.00 (+1)	0.81	1.39
3	10.00 (+1)	5.00 (-1)	10.00 (+1)	10.00 (+1)	1.00 (-1)	3.00 (+1)	3.00 (+1)	3.00 (+1)	0.10 (-1)	0.05 (-1)	4.00 (-1)	1.19	1.38
4	10.00 (+1)	10.00 (+1)	10.00 (+1)	5.00 (-1)	1.00 (-1)	1.00 (-1)	3.00 (+1)	1.00 (-1)	0.50 (+1)	0.10 (+1)	4.00 (-1)	2.34	1.18
5	5.00 (-1)	5.00 (-1)	10.00 (+1)	5.00 (-1)	3.00 (+1)	3.00 (+1)	1.00 (-1)	3.00 (+1)	0.50 (+1)	0.10 (+1)	4.00 (-1)	1.17	1.27
6	10.00 (+1)	10.00 (+1)	5.00 (-1)	10.00 (+1)	3.00 (+1)	3.00 (+1)	1.00 (-1)	1.00 (-1)	0.10 (-1)	0.10 (+1)	4.00 (-1)	2.26	0.93
7	5.00 (-1)	10.00 (+1)	10.00 (+1)	5.00 (-1)	3.00 (+1)	3.00 (+1)	3.00 (+1)	1.00 (-1)	0.10 (+1)	0.05 (-1)	5.00 (+1)	1.26	2.36
8	5.00 (-1)	10.00 (+1)	10.00 (+1)	10.00 (+1)	1.00 (-1)	1.00 (-1)	1.00 (-1)	3.00 (+1)	0.10 (-1)	0.10 (+1)	5.00 (+1)	1.18	2.25
9	5.00 (-1)	10.00 (+1)	5.00 (-1)	10.00 (+1)	3.00 (+1)	1.00 (-1)	3.00 (+1)	3.00 (+1)	0.50 (+1)	0.05 (-1)	4.00 (-1)	1.21	2.25
10	5.00 (-1)	5.00 (-1)	5.00 (-1)	5.00 (-1)	1.00 (-1)	1.00 (-1)	1.00 (-1)	1.00 (-1)	0.10 (-1)	0.05 (-1)	4.00 (-1)	0.15	1.05
11	10.00 (+1)	10.00 (+1)	5.00 (-1)	5.00 (-1)	1.00 (-1)	3.00 (+1)	1.00 (-1)	3.00 (+1)	0.50 (+1)	0.05 (-1)	5.00 (+1)	2.15	2.67
12	10.00 (+1)	5.00 (-1)	10.00 (+1)	10.00 (+1)	3.00 (+1)	1.00 (-1)	1.00 (-1)	1.00 (-1)	0.50 (+1)	0.05 (-1)	5.00 (+1)	2.87	0.035

Table 4.3.2.2. Analysis of variance (ANOVA) of PBD for laccase production by PBURU 12

Source	Sum of squares	Df	Mean square	F-value	P-value (Prob > F)
Model	6.84	7	0.98	21.48	0.0051*
A-Glucose	4.58	1	4.58	100.51	0.0006*
B-Sucrose	0.28	1	0.28	6.13	0.0685
C-Starch	0.092	1	0.092	2.02	0.2285
E-Peptone	0.92	1	0.92	20.30	0.0108*
J-CuSO ₄	0.38	1	0.38	8.30	0.0449*
K-Gallic acid	0.14	1	0.14	3.14	0.1510
L-pH	0.45	1	0.45	9.94	0.0344*
Residual	0.18	4	0.046		
Cor Total	7.03	11			

Model summary: $R^2 = 97.41\%$; Adj $R^2 = 92.87\%$; Coefficient of variance = 13.50%; Significant at $P < 0.05$

The result of the Plackett-Burman indicated the preferences of PBURU 12 toward medium compositions. White rot fungi are known to be able to use a variety of types of carbon sources. In this study, glucose was found to be the best carbon source compared to sucrose, starch and glycerol. This finding was in line with the result of Lee et al. (2006) where they found laccase activity from *Trametes versicolor* was increased with glucose as a carbon source compared to sucrose and fructose. Moreover, *Pleurotus eryngii* 616 and *Pleurotus ostreatus* 493 and 494 cultures found that laccase activity was higher in glucose than in maltose (Mikiashvili et al., 2006). This result was the opposite of the finding from (Eugenio et al., 2009), They found that fructose and sucrose increased the laccase activity of *Pycnoporus sanguineus*. Therefore, it was suggested that the suitable carbon source depends on the particular fungus in each case (Eugenio et al., 2009).

Ligninolytic systems of white-rot fungi were mainly activated during the secondary metabolic phase and were often triggered by nitrogen concentration (Buswell et al., 1995). Moreover, Buswell et al. (1995) found that laccases were produced at high nitrogen concentrations. Laccase was also produced earlier when the fungus was cultivated in a substrate with a high nitrogen concentration and these changes did not reflect differences in biomass. Most studies reported the used of yeast extract, peptone, urea, $(\text{NH}_4)_2\text{SO}_4$ as nitrogen sources for laccase production (Mikiashvili et al., 2006; Vaithanomsat et al., 2010; Zhu et al., 2016). Laccase production from *Lentinus strigosus* was increased when peptone was used as carbon (Vaithanomsat et al., 2010), whereas inorganic nitrogen sources such as urea and $(\text{NH}_4)_2\text{SO}_4$ could not compete with organic nitrogen sources (yeast extract, peptone) for *Coriolus versicolor* laccase production (Revankar & Lele, 2006). This may explain why urea and $(\text{NH}_4)_2\text{SO}_4$ resulted a negative effect toward laccase production.

Copper has been chosen as the best inducer compared to gallic acid and ethanol in this study. The finding was in line with another study that reported copper to be a strong laccase inducer in several species, for example, *Trametes trogii*, *Lentinus strigosus*, *Pleurotus ostreatus* (Levin et al., 2002; Vaithanomsat et al., 2010; Zhu et al., 2016). The addition of copper strongly stimulated ligninolytic enzyme production of *Trametes trogii*, and higher decolorization of polymeric dyes-poly R-478 was observed (Levin et al., 2002).

The pH of the culture medium is critical and plays a significant role in the growth and laccase production of the organism. The optimum value of pH for laccase production varies according to the substrate (Shraddha et al., 2011). Most report indicated initial pH level was set from 4.0 to 6.0 (Viswanath et al., 2014). While many white rot fungi can such as *Coriolopsis brysina*, *Pycnoporus coccineus*, *Ganoderma lucidum*, *Pleurotus florida*, *Trametes polyzona* produce laccase when pH 5.0-5.5 (Agrawal & Shahi, 2017; Agrawal et al., 2018; Eugenio et al., 2009; Teerapatsakul et al., 2017; Ting et al., 2011)

4.3.2.2. Medium optimization for laccase production using Response Surface Methodology (RSM)

Four medium components, glucose (A), peptone (B), CuSO₄ (C) and pH (D) were selected from preliminary screening using Plackett-Burman design were further analyzed using RSM. The RSM experiment was carried out using central composite design (CCD) to reach optimal condition for laccase production by PBURU 12. The observed and predicted responses from 30 experiment runs of which contained different combination of 4 components at three different level of concentration were shown in Table 4.3.2.3. The maximum laccase activity was found to be 4.85 ± 0.06 U/ml (trial 22) and the minimum was found to be 0.3 ± 0.01 U/ml (trial 17). The CCD experiment outcomes of the correlation of laccase production with the factors A, B, C, and D are revealed in expression of coded variables and fitted with the second-order polynomial equation as follow:

$$Y = 3.86 + 0.32 * A + 0.36 * B + 0.094 * C + 0.24 * D - 0.14 * A * B - 0.24 * D + 0.028 * A * D + 0.20 * B * C + 0.021 * B * D + 0.014 * C * D - 0.93 * A^2 - 0.42 * B^2 + 0.14 * C^2 - 1.11 * D^2$$

Where Y is the forecasted response (laccase activity), A, B, C and D were the coded values for glucose, peptone, CuSO₄ and pH, respectively.

Table 4.3.2.3. Central composite design matrix and their observed responses for laccase production by PBURU 12

Standard No.	A Glucose (g/l)	B Peptone (g/l)	C CuSO ₄ (mM)	D pH	Actual laccase activity (U/ml)	Predicted laccase activity (U/ml)
1	20.00	1.00	0.50	4.00	0.95	0.41
2	30.00	1.00	0.50	4.00	1.74	1.74
3	20.00	3.00	0.50	4.00	0.63	0.96
4	30.00	3.00	0.50	4.00	1.75	1.74
5	20.00	1.00	1.00	4.00	0.41	0.65
6	30.00	1.00	1.00	4.00	1.15	1.02
7	20.00	3.00	1.00	4.00	1.86	2.00
8	30.00	3.00	1.00	4.00	1.60	1.83
9	20.00	1.00	0.50	6.00	0.81	0.77
10	30.00	1.00	0.50	6.00	2.51	2.21
11	20.00	3.00	0.50	6.00	1.45	1.40
12	30.00	3.00	0.50	6.00	2.35	2.30
13	20.00	1.00	1.00	6.00	1.23	1.06
14	30.00	1.00	1.00	6.00	1.70	1.55
15	20.00	3.00	1.00	6.00	2.31	2.49
16	30.00	3.00	1.00	6.00	2.07	2.44
17	16.41	2.00	0.75	5.00	0.62	0.57
18	33.59	2.00	0.75	5.00	1.65	1.67
19	25.00	0.28	0.75	5.00	1.36	2.00
20	25.00	3.72	0.75	5.00	3.89	3.23
21	25.00	2.00	0.32	5.00	3.73	4.11
22	25.00	2.00	1.18	5.00	4.85	4.44
23	25.00	2.00	0.75	3.28	0.30	0.15
24	25.00	2.00	0.75	6.72	0.87	0.99
25	25.00	2.00	0.75	5.00	4.21	3.86
26	25.00	2.00	0.75	5.00	3.52	3.86
27	25.00	2.00	0.75	5.00	3.60	3.86
28	25.00	2.00	0.75	5.00	3.81	3.86
29	25.00	2.00	0.75	5.00	3.98	3.86
30	25.00	2.00	0.75	5.00	4.02	3.86

Table 4.3.2.4. Analysis of variance (ANOVA) of the Central Composite Design experimental model developed for laccase production by PBURU 12

Source	Sum of squares	Df	Mean square	F-value	P-value (Prob > F)
Model	48.53	14	3.47	21.59	< 0.0001
A-Glucose	2.22	1	2.22	13.82	< 0.0021
B-Peptone	2.82	1	2.82	17.54	< 0.0008
C-CuSO ₄	0.19	1	0.19	1.21	0.2886
D-pH	1.29	1	1.29	8.04	< 0.0125
AB	0.29	1	0.29	1.84	0.1955
AC	0.91	1	0.91	5.65	< 0.0312
AD	0.013	1	0.013	0.080	0.7817
BC	0.63	1	0.63	3.95	0.0653
BD	6.824E-003	1	6.824E-003	0.042	0.8395
CD	2.992E-003	1	2.992E-003	0.019	0.8932
A ²	15.01	1	15.01	93.47	< 0.0001
B ²	3.12	1	3.12	19.44	< 0.0005
C ²	0.34	1	0.34	2.13	0.1654
D ²	21.68	1	21.68	134.97	< 0.0001
Residual	2.41	15	0.16		
Lack of Fit	2.06	10	0.21	2.98	0.1200
Pure Error	0.35	5	0.069		
Cor Total	50.94	29			

$R^2 = 0.9527$; Adj $R^2 = 0.9086$; Coefficient of variance = 18.52%; Significant at $P < 0.05$

The results of analysis of variance (ANOVA) for above equation were shown in table 4.3.2.4. Prob > F values were fewer than 0.05 signify the significance of model stipulation, where A, B, D, AC, A², B² and D² were significant term for the model. On the contrary, the values of the model terms were grater then 0.1000 indicated the insignificance of the model terms. R -squared (R^2) was found to be 0.9527 which suggested that the model could explain up to 95% of the variability and only 5% of the total variance could not be explained by the model. The adjusted R -squared (adj

$R^2 = 0.9086$) and predicted R -squared (pre $R^2 = 0.7677$) also suggested that the model was significant and explained further that the enzyme activity was attributed to the independent variables. The P -value of 0.1200 for the lack of fit means the insignificance of the lack of fit comparative to the pure error which was a positive indication as the model should fit. From the Prob $> F$ value, the chance of value of 18.52% for the lack of fit F -value to large was possible to noise. Adeq precision ratio value of 15.120 point to and adequate signal where ratio superior than 4 was advantageous.

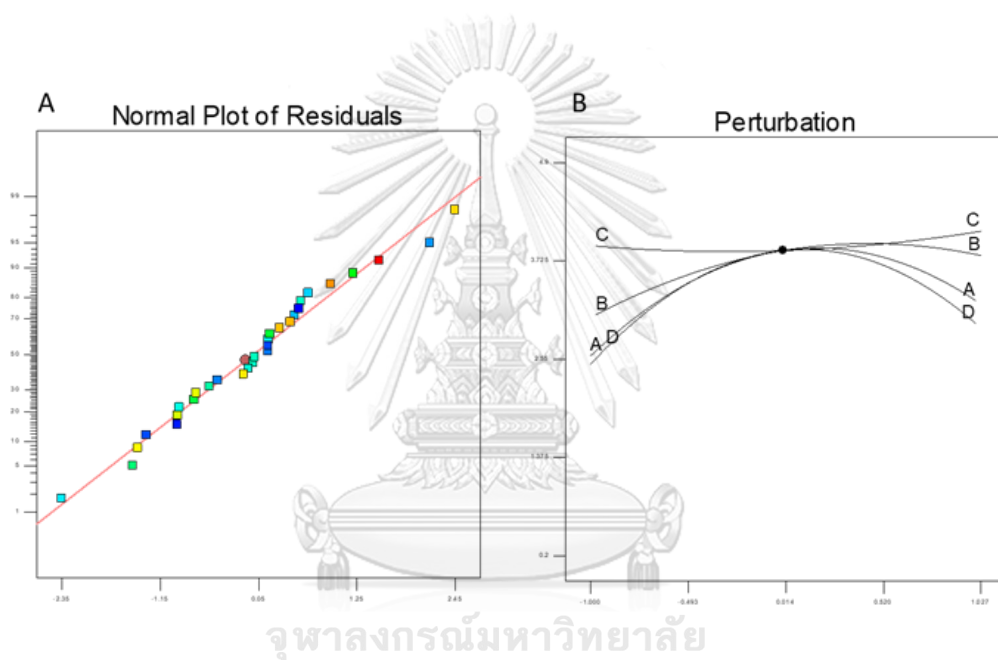


Figure 4.3.2.5. Normal probability plot residual of laccase activity (A) and perturbation graph (B) for 4 factors affecting laccase activity.

The relationship between the actual and predicted laccase activity (response) is shown in figure 4.3.2.5 (A). The cluster of the measurements near the diagonal line in the parity plot indicated a good fit and of the model and demonstrated a decent correlation between the actual and predicted values. The perturbation graph showed the response changes following the change of factor from the chosen reference point, with other factors were held constant at the reference value. Figure 4.3.2.5 (B) showed that laccase activity was affected by peptone followed by glucose, pH and CuSO_4

concentration. Increasing glucose, peptone concentration and pH resulted in increase on laccase activity while increasing the CuSO_4 concentration resulted slightly increase on laccase activity.

The interaction between variables on laccase production was shown through three-dimensional plot in figure 4.3.2.6. A plot was constructed by plotting the central values of the variables that influence the laccase production.

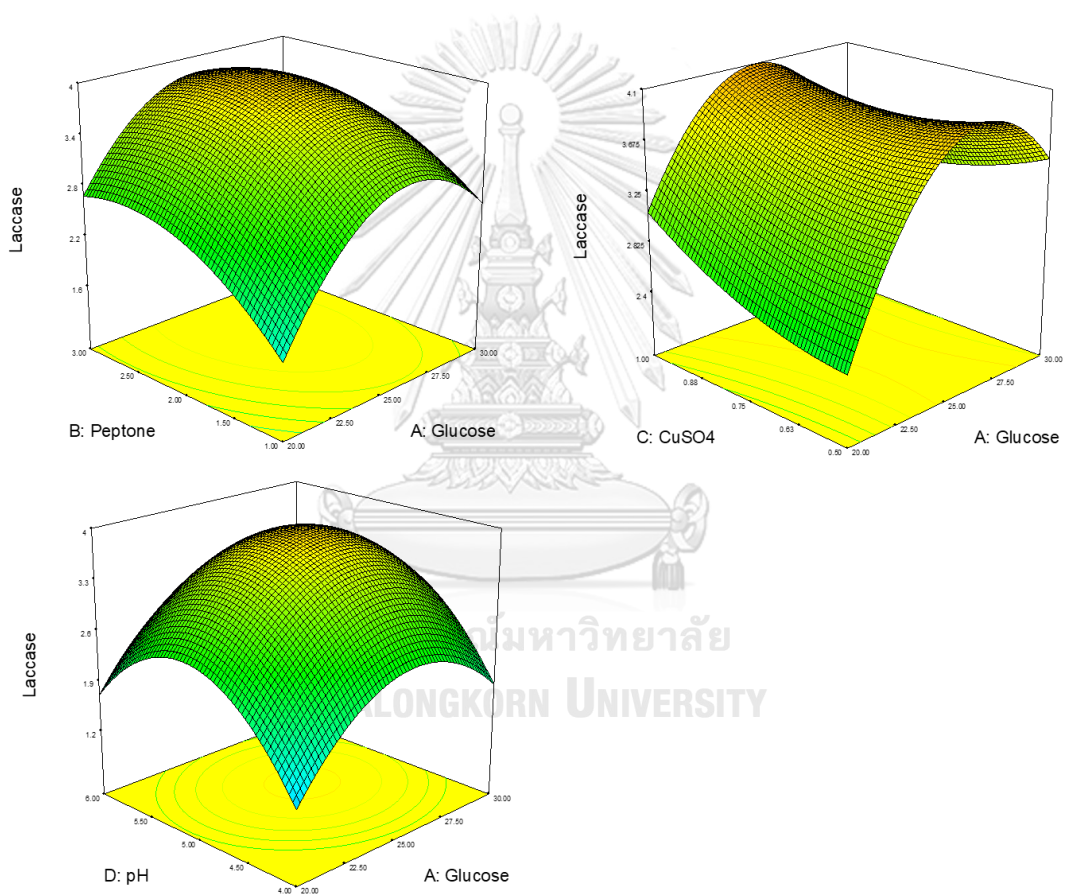


Figure 4.3.2.6. Three-dimensional response surface plots of the effect combinations on laccase production by *T. polyzona* PBURU 12

Three-dimensional response plots were drawn according to second-order equation to illustrate the interaction among the variables and to determine the optimum concentration of each factor to obtain maximum laccase production. Figure 4.3.2.6 presented the effect among two variables, while the other variables held at the central (0) level. The laccase production was increased along with the increasing of along with the increasing of glucose and peptone. The laccase production efficiencies obtained from the experiments were significantly influenced by glucose, peptone and pH but not CuSO_4 . The maximum laccase activity was 4.85 U/ml, which would correspond to the concentrations of 25 g of glucose, 2 g of peptone, 1.18 mM CuSO_4 and pH 5.0, respectively (run no. 22).

Central composite design (CCD) has been shown to be effective for laccase optimization. According to the findings of this study, laccase production increased as a result of the interactions between all of the variables. CCD was used to optimize the *Pleurotus Florida* laccase. The results show that glucose, asparagine, CuSO_4 , and incubation time are the best variables for maximum laccase production (Palvannan & Sathishkumar, 2010). Another study used *Polyporus arcularius* to produce laccase, and the CCD successfully increased laccase activity threefold over the basal medium (Jegatheesan & Eyini, 2015).

The model forecasted the laccase activity production of 3.57 U/ml when the conditions of glucose, peptone, CuSO_4 and pH were 26.43 g/l, 2 g/l, 0.51 mM and pH 5.0. Laccase activity obtained from basal salt medium was 1.13 U/ml, but the optimized medium induced nearly three-fold increase in laccase activity (3.57 U/ml) in the medium containing these four components at optimized condition, but still lower than the optimized medium from CCD experiment (4.85 U/ml). The validity of the result predicted by the model was confirmed by repeated experiments under optimal conditions. The result showed that the maximum laccase activity production was 3.08 U/ml which was 1.18-fold lower to the predicted value (3.57 U/ml).

The growth and laccase production profiles of *T. polyzona* PBURU 12 in the basal and optimized medium were showed in Figure 4.3.2.7. Laccase production reached the highest activity in the value of 3.08 ± 0.28 U/ml after 12 days of cultivation the optimized medium, while a maximum activity found in basal medium was 1.13 ± 0.05 U/ml. The peak of laccase production for both media were found at 12 days of cultivation time. The fungal biomass from optimized medium was weight at 0.6 ± 0.04 g/l increased 1.5-fold compared to the biomass from basal medium (0.4 ± 0.05 g/l).

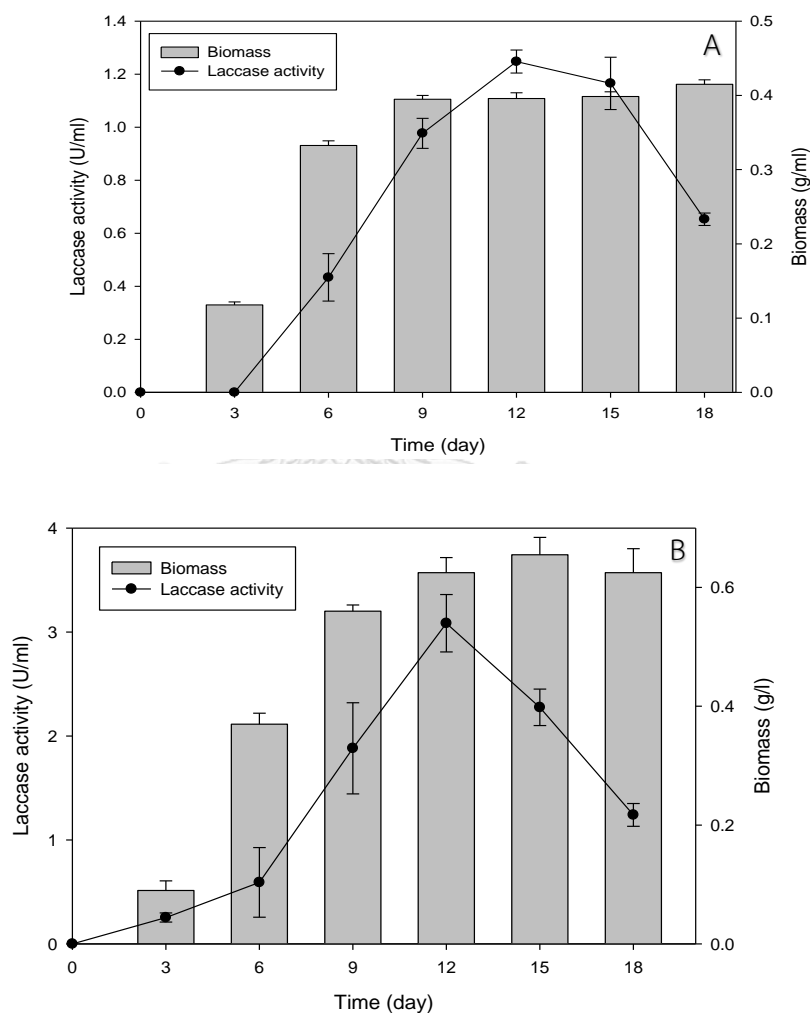


Figure 4.3.2.7. Time course and growth of laccase production by PBURU 12 at room temperature, Shaked at 150 rpm in (A) the basal and (B) optimized medium. Results showed as a mean with standard deviation from three replications.

4.3.3. Purification of laccase from PBURU 12

The summary of purification procedure was shown in table 4.3.3.1. Crude laccase was prepared at approximately 1000 ml from the optimized production medium as described previously. After 12 days of cultivation, the biomass was separated from the supernatant. The biomass was removed using filter paper and vacuum pump. The filtered supernatant then centrifuged at 9000 g at 4°C to remove remaining debris. The total volume after separation was 900 ml with laccase activity from the crude enzyme was found out to be 3394 U/ml and total protein of 2029.45 mg/ml, respectively. The concentration of crude laccase was conducted with ultrafiltration by 10 kDa cutoff membrane. The step included 900 ml of crude laccase extract were pushed to pass through membrane using pressure from the pump and concentrated to 9-fold. The obtained retentate with the volume of 100 ml had the total laccase activity of 1360 U/ml, and recovery yield of 40%. Laccase was purified from retentate by anion-exchange chromatography column (HiTrap Q FF, GE Healthcare). The chromatographic eluent profile was illustrated in figure 4.3.3.2. The unbound protein was eluted from the column using citrate buffer 50 mM (pH 5.0). The bound protein washed with a linear salt gradient (0-1.0 M NaCl). The eluted fractions were assayed for laccase activity and the A280 monitored. The active fractions were then pooled and dialyzed against the running buffer. The peaks of laccase activity and protein at A280 were detected when eluted with NaCl at the concentration between 0.1-0.5 M. This step resulted a total activity of 174.18 U/ml and specific activity of 24.95 U/mg. Laccase was purified to 14.92-fold with approximately 5.13% of recovery yield. The retentate enzyme from anion-exchange chromatography (20 ml; total protein of 6.98 mg/ml).

Table 4.3.3.1. Summary of purification step laccase from PBURU 12

Purification step	Volume (ml)	Total activity (U/ml)	Total Protein (mg/ml)	Specific activity (U/mg)	Purification (fold)	Recovery Yield (%)
Crude extract	900	3394	2029.45	1.67	1	100
Ultrafiltration	100	1360	151.22	8.99	5.38	40.07
HiTrap Q FF	20	174.18	6.98	24.95	14.92	5.13

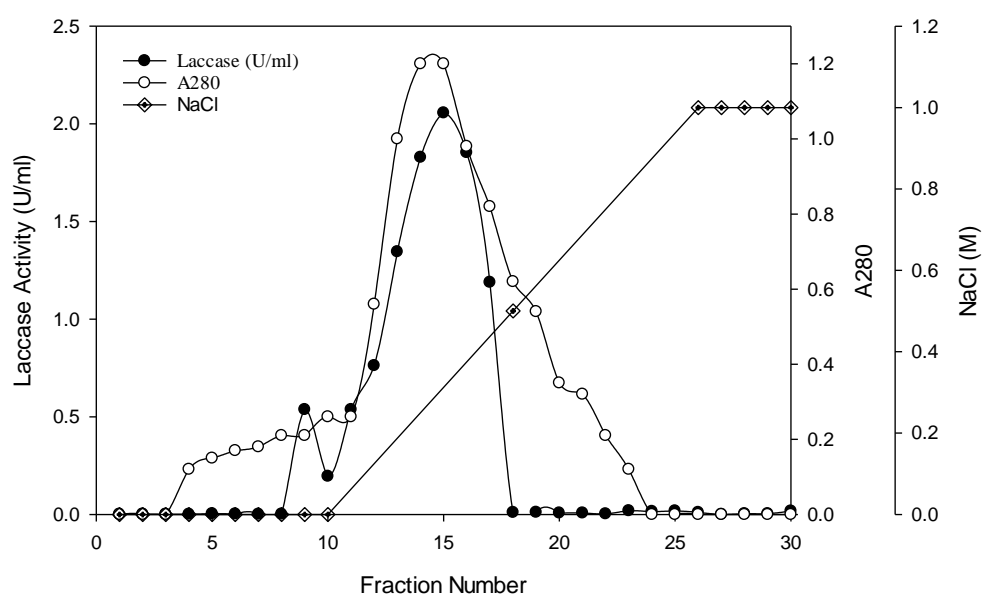


Figure 4.3.3.2. Chromatographic profile of laccase activity and absorbance at 280 nm after fractionation using HiTrap Q Sepharose Fast Flow (FF) anion-exchange column.

The result from SDS-PAGE analysis was described in figure 4.3.3.3 displayed a single band with approximately molecular weight of 70 kDa.

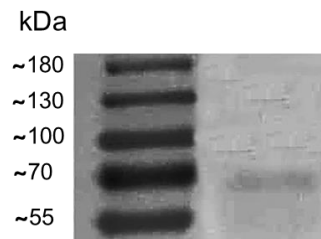


Figure 4.3.3.3. The SDS-PAGE analysis of purified laccase of *T. polyzona* PBURU 12: Lane 1; molecular weight protein marker; 2; purified laccase (10 μ g of protein)

The current study's findings were similar to those of Chairin et al. (2014) and Lueangjaroenkit et al. (2019). In SDS-PAGE, the molecular weight of 70 kDa obtained in this study corresponds to that of laccase from *Trametes polyzona*. Another *T. polyzona* strain, surprisingly, was reported to have a molecular weight of 66 kDa (Ezike et al., 2020). In another study, Li et al. (2016) discovered that the molecular weight laccase from *Trametes* sp was 70 kDa. A typical laccase gene codes for a protein of 500–600 amino acids, and laccase molecular weights are typically in the 60–90 kDa range when determined by SDS-PAGE (Viswanath et al. 2014).

4.3.4. Characterization of the purified laccases

4.3.4.1. pH optimum and stability of the purified laccase of *T. polyzona* PBURU

12

A 60-minute incubation revealed that purified laccase was active across a broad pH range (3.0-7.0). The activity was highest at pH 4.5 and gradually decreased as pH increased, with no activity detected at pH 8.0. After 60 minutes of incubation, more than 80% activity was observed between pH 4.0-5.0. Enzyme activity was reduced to less than 60% from pH 5.5 to 7.0. Laccase was stable from pH 5.0 to 7.0, retaining more than 90% of its activity after 60 minutes of incubation. After 24 hours of incubation at 27°C, laccase activity became inactive at pH 3, but maintained more than 60% of its activity at pH 5.0-7.0.

The laccase from *T. polyzona* PBURU 12 had a pH optimum of 4.5, which was similar to the laccases from *T. polyzona* WRF03 and KU-RNW027 (Ezike et al. 2020; Lueangjaroenkit et al. 2019). Chairin et al. 2014 reported a pH optimum of 2.2 for laccase from *Trametes polyzona* WR710-1, whereas Asgher et al. (2017) found an optimum pH of 5.0 when ABTS was used as substrate for *Trametes versicolor* IBL-04. The laccase activity of PBURU 12 decreased as the pH increased (neutral/alkaline). This could be due to the binding of a hydroxide anion (a laccase inhibitor) to the T2/T3 coppers of laccase, disrupting the internal electron transfer from T1 to T2/T3 centers and thus inhibiting the enzyme activity (Xu, 1997). The effect of pH on laccase stability was considered when determining the ideal conditions for enzyme purification, application, and storage. Laccase from *T. polyzona* PBURU 12 was more than 98% stable at pH (5.0-7.0), but less stable at acidic pH. (below 5.0). Similarly, Ezike et al. 2020 reported *T. polyzona* WRF03 stability at (5.5 to 6.5), whereas Chairin et al. 2014 reported laccase stability from *T. polyzona* WR710-1 between pH 6.0 and 7.0. According to Lueangjaroenkit et al. 2019, laccase activity was 100 percent stable at pH 7.0-10.0 and slightly decreased below 7.0.

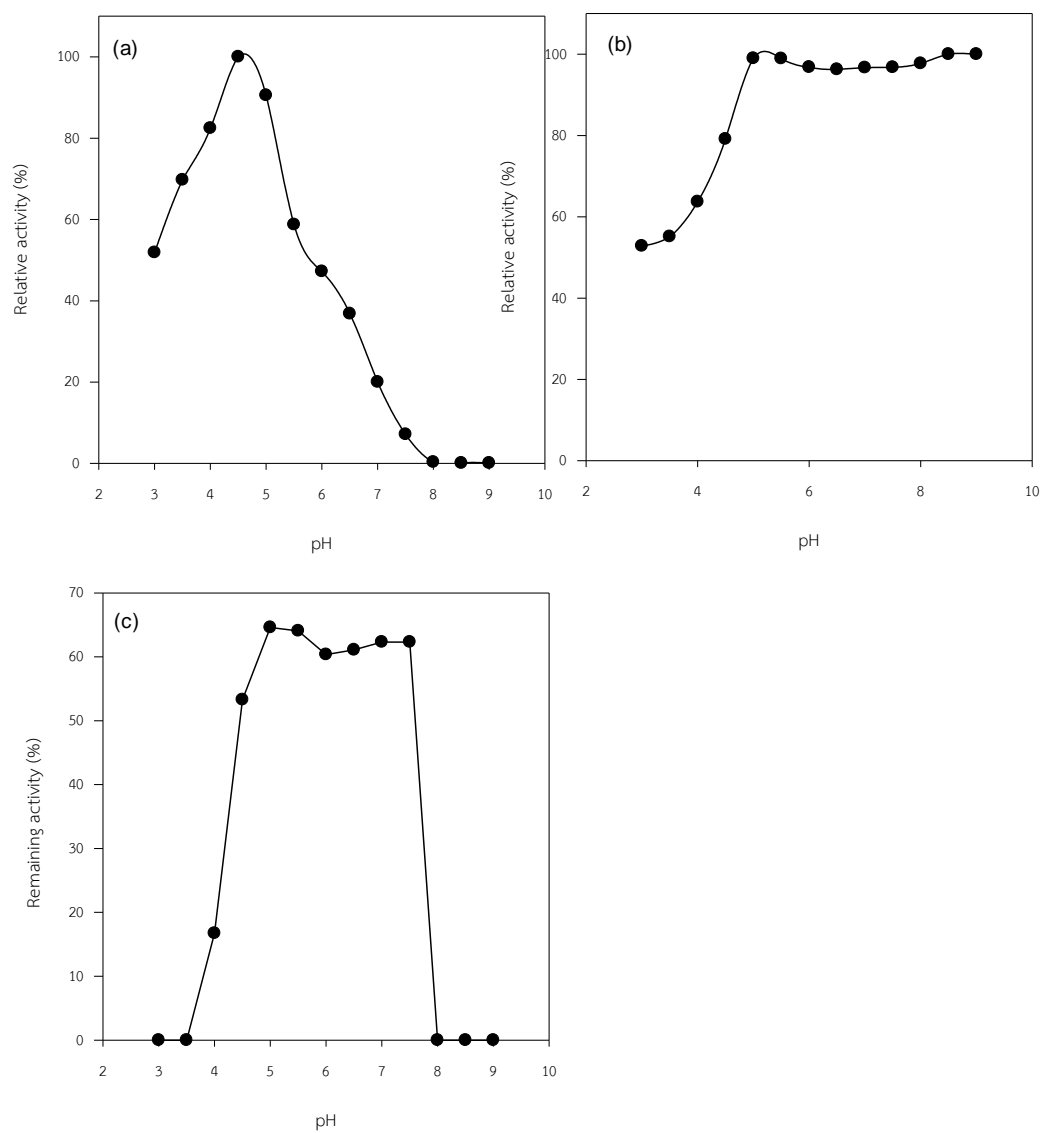


Figure 4.3.4.1. Effect of pH on laccase activity (a); stability of laccase after incubation for 60 minutes (b) and remaining activity of laccase after incubation for 24 hours (c).

4.3.4.2. Thermostability of purified laccase of *T. polyzona* PBURU 12

The effect of temperature on purified laccases using ABTS as substrate was studied and shown in figure 4.3.4.2. The laccases were active in vary range of temperature (20-70°C), whereas laccases were entirely inactive at 80°C. The enzyme achieved the highest activity at 40°C. The stability test showed laccase relatively stable at 20-40°C after incubation for 60 minutes. However, at 50°C, laccase was decreased after incubation at 60 minutes. Additionally, laccase was rapidly declined below 30% at 60-70°C and completely inactive at 80°C, respectively.

The activity of laccase was decreased more than 20% after being kept at 20°C for 24 hours, while 60% remained at 30°C. Furthermore, the laccase was nearly loss all the activity at 40°C and completely inactive at from 50-80°C.

PBURU 12 laccase had a lower optimum temperature of 40°C than *T. polyzona* KU-RNW027 laccase, which had a temperature of 50°C and *T. polyzona* WRF03 laccase, which had a temperature of 55°C. This finding was similar to the study by Mukhopadhyay and Banerjee (2015), were they found that the optimum temperature of laccase from *Lentinus squarrosulus* was 40 °C. Furthermore, laccase from *T. polyzona* PBURU 12 was more stable at temperatures ranging from 20 to 40°C over the course of the heat treatment. *T. polyzona* PBURU 12 laccase shared the same stability temperature as Ezike et al. 2020 but lower than Lueangjaroenkit et al. 2019 and Chairin et al. 2014) which reported stability up to 50°C for 60 minutes. Laccase temperature stabilities vary greatly depending on the source organism. Laccases are generally stable at 30-50°C and rapidly lose activity at temperatures above 60°C (Viswanath et al., 2014). The ability of *T. polyzona* PBURU 12 laccase that able to act in broad temperature range of 20-70°C and stability at 20-40°C makes it a valuable biocatalyst for many biotechnological applications such as bioremediation of recalcitrant.

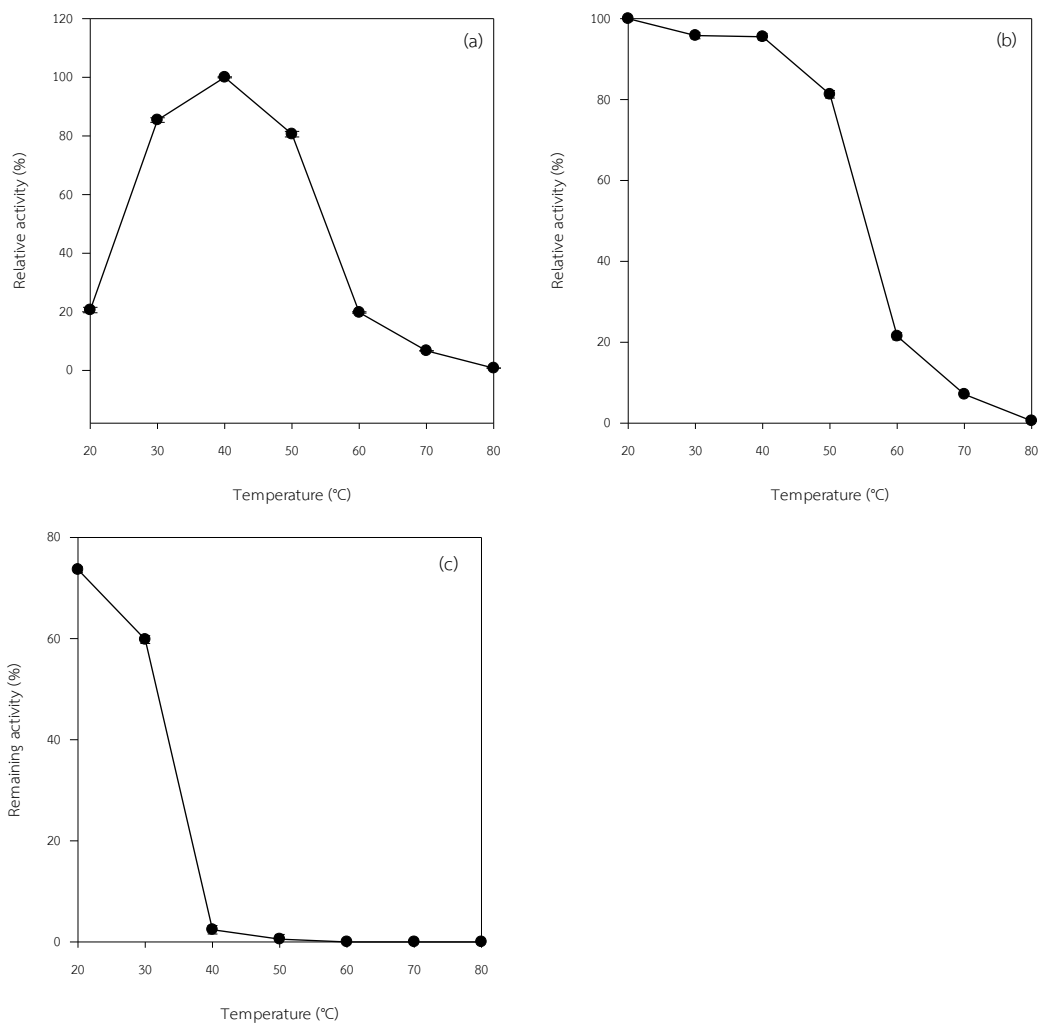


Figure 4.3.4.2. Effect of temperature on laccase activity (a); stability of laccase after incubation for 60 minutes (b) and remaining activity of laccase after incubation for 24 hours (c).

4.3.4.3. Effect of metal ions and inhibitors on PBURU 12 purified laccase

The effect of metal ions and inhibitors toward the activity of purified laccase were tested and shown in table 4.3.4.3. Laccase was active by almost all the metal and salt ions such as CuSO_4 , MnSO_4 , MgSO_4 , FeSO_4 , CoCl_2 , ZnCl_2 , CaCl , NaCl . An increase in metal and salt ions concentration (1–10 mM) gradually inhibited the enzyme activity except for Zn^{2+} and Cu^{2+} , in contrary, the addition of Cu^{2+} showed stimulatory effect on laccase activity by 10%. Among the metal ions tested, Fe^{2+} was found to be a potent inhibitor of laccase activity, causing more than 96.56% inhibition at 1 mM and 98.55% at 10 mM. The addition of monovalent ions such as Na^+ and Ca^+ toward laccase activity was examined. The relative activity (%) of laccase declined with the addition of Na^+ and Ca^+ from 100 to 96.98 and 78.44, respectively. Furthermore, increasing ions concentration to 5 and 10 mM also resulting in a slight decreased in laccase activity. The inhibitor study revealed that NaN_3 inhibited laccase activity up to 90.40% at 1 mM while complete inhibition occurred when NaN_3 was increased up to 5-10 mM. Whilst the occurrence of chelating agent and detergent such as EDTA and SDS showed when the small amount of EDTA and SDS (1mM) were introduced into the reaction, laccase activity was not affected and remained similar to control (100%). Consequently, the increasing concentrations of EDTA and SDS to 5 and 10 mM gradually inhibit laccase activity. The presence of various organic solvents on laccase activity has been investigated. The laccase showed decreasing on activity when 10% of methanol, ethanol, acetone and acetonitrile were added into the reaction, while more than 80% of activity was inhibited when the concentrations were increased up to 50%.

Metal ions have both an inhibitory and a stimulatory effect on laccase activity (Ezike et al. 2020). This is critical because metal ions are common environmental pollutants that can interfere with both the production and stability of extracellular enzymes (Park & Park, 2014). The results showed that all metal ions studied reduced laccase activity, with the exception of Zn^{2+} and Cu^{2+} , which had a slight stimulatory effect on laccase activity. A similar finding was made in other fungi. Laccases from

Paraconiothyrium variabile and *Trametes pubescens* were found to have similar properties (Forootanfar et al., 2011; Si et al., 2013). While *Trametes polyzona* WR710-1 and WRF03 were found to be slightly inhibited by Cu^{2+} (Chairin et al., 2014; Ezike et al., 2020), KU-RNW027 showed no inhibition (Lueangjaroenkit et al., 2019). Cupric ions have varying (positive, negative, or neutral) effects on laccase activities because white rot fungal laccases are multicopper-containing oxidases (Wang et al., 2017). The Cu^{2+} activation of laccase may be due to copper ions filling type-2 at copper binding sites. (Sadhasivam et al., 2008). While NaN_3 at 1 mM completely inhibited laccase activity by preventing electron transfer (Zhou et al., 2014).

Table 4.3.4.3.1. Effect of metal ions, inhibitors and chelating agents on PBURU 12 purified laccase

Substances	Relative activity (%)		
	Concentration (mM)		
	1	5	10
Control	100	100	100
Cu^{2+}	100	100	110
Mn^{2+}	100	92.40	83.16
Mg^{2+}	100	89.62	80.65
Fe^{2+}	3.44	3.09	1.55
Co^{2+}	77.24	69.51	62.56
Zn^{2+}	100	100	100
Ca^{2+}	96.98	87.29	78.56
Na^+	78.44	70.60	63.54
NaN_3	9.60	0	0
EDTA	100	80.95	47.62
SDS	100	81.08	78.71

Organic solvents are important non-aqueous media commonly used for biocatalysis (Ezike et al. 2020). Hence, determination of laccase stability in various organic solvents will provide useful information for the choice of suitable reaction

media for its application in biocatalysis and biotransformation. Laccase from *T. polyzona* PBURU 12 showed a relatively gradual decrease in relative activity (%) from 10-50 increase in the concentration of various organic solvent (Table 4.3.4.3.2). Lueangjaroenkit et al. (2020) obtained similar result trend for laccase from *T. polyzona* KU-RNW027 except in the presence of 10– 30% butanol. The while (Ezike et al. 2020) reported that *T. polyzona* WRF03 was more stable in acetone (50%), methanol (45.65%) and propanol (41.57%) than in acetonitrile (31.18%) and ethanol (14.55%) when exposed to these solvents for 60 minutes. Although the enzyme is relatively stable at different organic solvents, its activity was lower when compared to the aqueous solution.

Table 4.3.4.3.2. Effect of solvents on PBURU 12 purified laccase

Substance	Concentration (%)		
	10	25	50
Methanol	72.50	58.93	16.11
Ethanol	77.34	39.28	11.05
Acetone	87.26	32.72	7.27
Acetonitrile	87.07	38.58	31.35

4.3.4.4. The effect of substrate specificity and kinetic parameters

The substrate specificity of purified laccase was evaluated using different phenolic compounds (2,6-DMP, guaiacol and syringaldazine) and a non-phenolic compound (ABTS). Purified laccase was able to oxidize phenolic and non-phenolic compounds with substantially different kinetics constants. The result in table 4.3.4.4 and figure 4.3.4.4 demonstrated that purified laccase showed a different kinetic action depending on the type of substrates and various concentrations (1-20 mM). The lowest K_m value was found at 4.45 when ABTS was used as a substrate following syringaldazine, 2.6 DMP and guaiacol (5.23, 8.19 and 9.73 mM⁻¹). Catalytic rate constant (K_{cat}) or turnover number of purified laccases were found to be varied among substrates. The highest K_{cat} was ABTS (51.71 S⁻¹) following with guaiacol (49.21 S⁻¹), 2,6 DMP (43.90 S⁻¹) and syringaldazine (31.30 S⁻¹).

Fungal laccases are known generally to possess a greater affinity for ABTS than for other substrates (Ezike et al., 2021). The kinetic parameters (V_{max} and K_m) influence the substrate specificity value which means that the lower the K_m value or higher K_m (rapid turnover), the more the affinity of that substrate to the enzyme and the higher the substrate specificity (Ezike et al., 2021). The laccase from *T. polyzona* PBURU 12 was possessed the same affinity towards ABTS. Hence, in the previous study, the K_m value showed that *T. polyzona* WRF03 and WR710-1 has a higher affinity towards ABTS than other substrates tested (Chairin et al., 2014; Ezike et al., 2021).

Table 4.3.4.4. Substrate specificity and kinetic constants from PBURU 12

Substrate	ϵ (cm ⁻¹ mM ⁻¹)	V_{max} (mM min ⁻¹)	K_m (mM)	k_{cat} (S ⁻¹)	k_{cat}/K_m (S ⁻¹ mM ⁻¹)
ABTS	36.0	5.23	4.45	51.71	11.62
Guaiacol	12.0	4.97	8.19	49.21	6.01
2,6-DMP	49.6	4.44	9.73	43.90	4.51
Syringaldazine	65.0	3.17	5.23	31.30	5.98

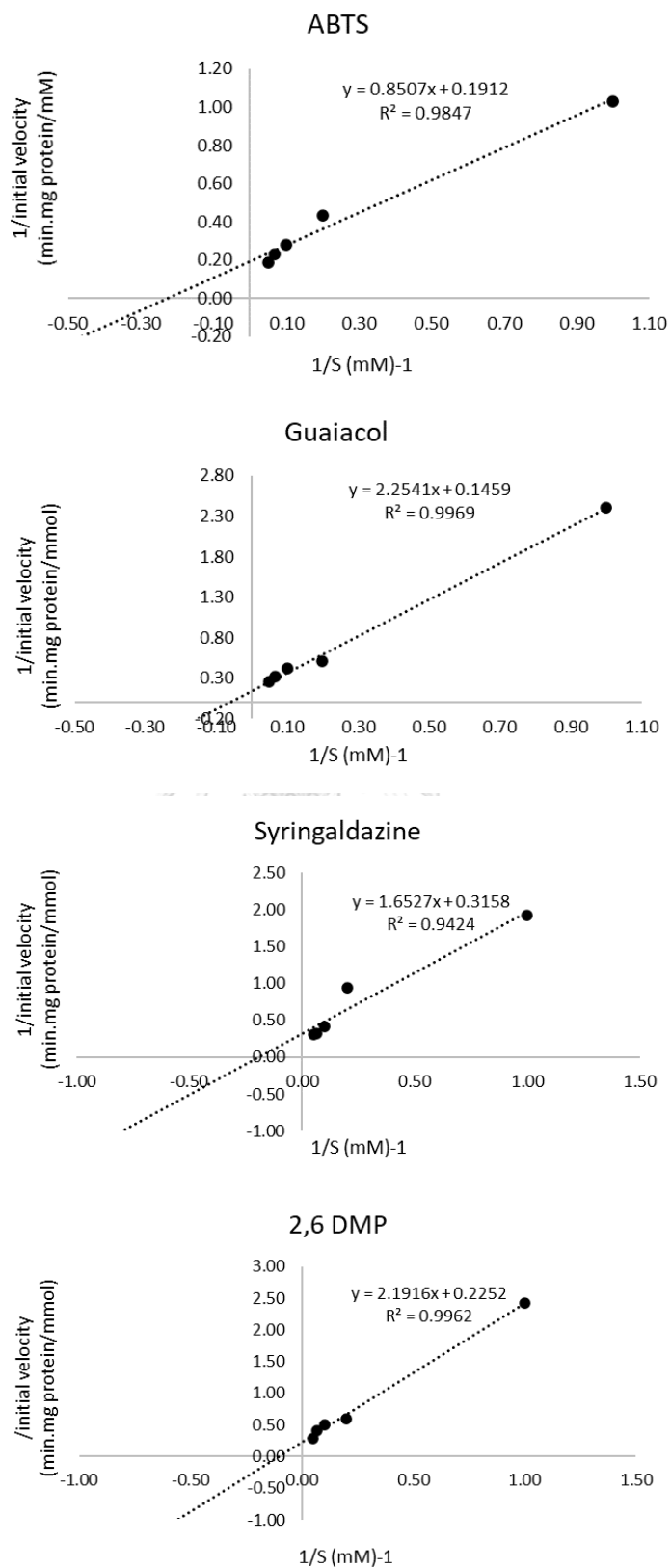


Figure. 4.3.4.4. Lineweaver-Burk plot of the purified laccase from PBURU 12 using different substrates.

4.4. Degradation of PAHs using live mycelia and crude laccase of PBURU 12

The degradation of PAHs was further studied using live mycelia of PBURU 12 with an optimized laccase medium for 7 days. The result demonstrated laccase activity was ranged at 0.95-1.19 U/ml after 7 days of cultivation. The whole medium along with fungal biomass was then used to degrade PAHs (100 ppm) by adding each separate PAHs into the medium for 24 hours with continuous shaking at 150 rpm. Another experiment was carried out using crude laccase (1 U/ml) to degrade PAHs within 24 hours. The result expressed from both experiments stated that more than 50% of PAHs were able to degrade within 24 hours using either live mycelium or crude laccase (Table 4.4.1). More than half (55.16 ± 1.87 ; 56.39 ± 3.72 and 51.49 ± 5.31 ; $53.95 \pm 1.06\%$) of phenanthrene and fluoranthene were degraded by a liquid culture of PBURU 12 both when using live mycelia and crude enzyme prior to 24 hours period. Whereas more than 70% of pyrene was degraded (75.95 ± 2.98 ; $79.19 \pm 1.02\%$, respectively) in the same period. Furthermore, a statistical analysis was performed using t-Test to compare live mycelia and crude enzyme treatments. The highest PAHs degradation was found when the crude laccase was used. Under these conditions almost 1.02-fold higher level of degradation of phenanthrene was observed, while 1.04-fold higher for fluoranthene and pyrene. Nevertheless, t-Test result stated there was no significant difference between live mycelia and crude laccase. Regardless, the crude laccase from PBURU 12 appeared to be more efficient in the degradation of PAHs tested. Therefore, the next experiment was conducted using crude laccase.

Table 4.4.1. Degradation (%) of phenanthrene, fluoranthene and pyrene (100 ppm) after 24 hours of incubation with PBURU 12.

PBURU 12	Phenanthrene (%)	Fluoranthene (%)	Pyrene (%)
Live mycelia	55.16 ± 1.87 ^{ns}	51.49 ± 5.31 ^{ns}	75.95 ± 2.98 ^{ns}
Crude enzyme (1 U/ml)	56.39 ± 3.72 ^{ns}	53.95 ± 1.06 ^{ns}	79.19 ± 1.02 ^{ns}

t-Test was performed in column with Significant at $P < 0.05$; ns: not significant.

The crude laccase from PBURU for PAHs degradation was further studied in following treatment: a. 1 U/ml crude laccase was used for PAHs degradation; b. the addition of 1 mM ABTS to 1 U/ml of crude laccase for PAHs degradation; c. 10 U/ml crude laccase was used for PAHs degradation. Further studied were carried out by comparing the incubation time between 1 and 24 hours (Figure 4.4.1). The outcome demonstrated that within 1 hour of incubation time, 1 U/ml crude laccase (treatment a) was able to degrade 17.95 ± 6.58; 21.83 ± 1.50; 19.21 ± 1.02 % of phenanthrene, fluoranthene and pyrene, respectively. The addition 1 mM of ABTS as laccase-mediator (treatment b) was slightly enhanced the degradation of three PAHs. The degradation of phenanthrene and fluoranthene were increased to 1.12-fold and 1.49-fold, respectively, while pyrene was increased to 1.60-fold. Degradation of three PAHs was significantly enhanced when laccase concentration was increased to 10 U/ml (treatment c). The degradation percentage increased to 2.50-fold; 2.20-fold; 3.25-fold for phenanthrene; fluoranthene; pyrene subsequently compared to when 1 U/ml was used. The one-way analysis of variance (ANOVA) was performed and supported that there was a significant difference among treatments. Furthermore, a post-hoc test was performed using Fisher's least significant difference (LSD). It was suggested when the crude enzyme from PBURU 12 was used to degrade phenanthrene and pyrene, there were no significant difference between treatment a and b, while both treatments were significantly different compared to treatment c. Fluoranthene degradation resulted a significant difference in all the treatments. The same trend was found when incubation time was extended to 24 hours. One U/ml crude laccase (treatment a) was able to

degrade 55.16 ± 1.87 ; 53.95 ± 1.06 ; $79.19 \pm 1.02\%$ of phenanthrene, fluoranthene and pyrene, respectively. After the addition of 1 mM ABTS, the degradation of phenanthrene and fluoranthene were increased to 1.18-fold and 1.24-fold, respectively. In contrast, the addition of ABTS adversely affected pyrene with an approximately reduction to 0.95-fold. A nearly completed degradation (%) was achieved after phenanthrene, fluoranthene and pyrene was treated using 10 U/ml of crude laccase resulted 98.88 ± 0.01 , 91.53 ± 0.13 and 90.37 ± 0.01 , respectively. The one-way analysis of variance (ANOVA) was performed and supported that there was a significant difference among treatments. Furthermore, a post-hoc test was performed using Fisher's least significant difference (LSD). It was suggested when the crude enzyme from PBURU 12 was used to degrade phenanthrene and fluoranthene, there was a significant difference among treatment a, b and c. Pyrene degradation resulted no significant difference between treatment a and b, while both treatments were significantly different compared to treatment c. The incubation time played an important role in PAHs degradation. It was suggested that by prolonging the incubation time prior to 24 hours improved the degradation of three PAHs. To support the finding of experiment above, statistical analysis was conducted to compare means between incubation times (1 and 24 hours) using t-Test. The outcome indicated from three individual PAHs that have been tested (phenanthrene, fluoranthene and pyrene), 24 hours of incubation time are significantly increasing the degradation compared to 1 hour of incubation time.

Thongkred et al. (2011), study about *Pycnoporus* crude laccase was able to degrade phenanthrene, fluoranthene, and pyrene more than 60% in 24 hours without the addition of a mediator, but when ABTS was added to the reaction, the degradation increased more than 1.5-fold. *Ganoderma* sp. UH-M was able to degrade 81.03% phenanthrene using crude laccase within 7 incubation days (Torres-Farrada et al., 2019). While crude laccase from *Agaricus bisporus* was able to degrade 15 PAHs with varied degradation percentage (Li et al., 2010).

The addition of ABTS to PAH degradation was found to be only slightly enhanced. This finding was similar to that of Thongkred et al. (2011) who discovered that adding ABTS to the reaction only slightly enhanced the degradation of some PAHs while decreasing the degradation of others. *Trametes versicolor* and *Ganoderma lucidum* Chaaim-001 BCU were found to be capable of degrading PAH in the absence of a redox mediator (Punnapayak et al., 2009). Another finding was revealed that without the presence of a redox mediator (ABTS), purified laccase from *Trametes versicolor* 95122 was unable to breakdown phenanthrene (Han et al., 2004).

In this study, the incubation time was discovered to be an important factor in the degradation of PAHs. It was discovered that increasing the incubation time (from 1 to 24 hours) increased PAH degradation. *Pycnoporus sanguineus* KUM 60953 and 60954 crude laccase (30 U/ml) were exposed to phenanthrene and pyrene, and it was discovered that degradation of phenanthrene and pyrene at 4 hours increased to 1.9-fold after incubation at 24 hours, indicating that incubation time has a significant effect on PAH degradation (Munusamy et al., 2008).

In this investigation, increasing enzyme concentration was found to be efficient for PAH breakdown. The degradation was found to be 2 to 3 times higher when the concentration was increased from 1 to 10 U/ml, and when combined with the incubation duration, the entire degradation was practically reached. The results were similar to those reported by (Çifçi et al., 2019) when doing dye decolorization using laccase, the increasing laccase concentration who discovered that increasing the laccase concentration from 0.05 g/l to 0.25 g/l resulted in a threefold increase in dye decolorization.

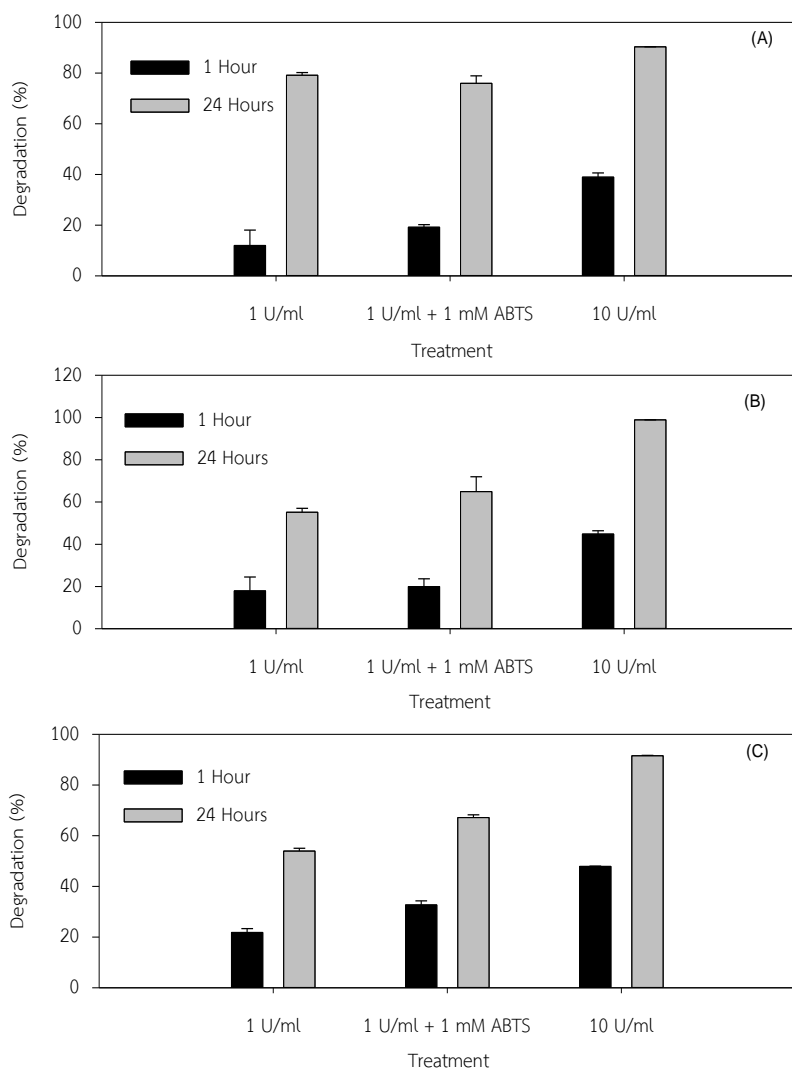


Figure 4.4.1. PAHs degradation using crude enzyme of PBURU 12 for 1 hour and 24 hours at 30°C with continuous shaking at 150 rpm in dark condition. (A) Fluoranthene-100 ppm; (B) Pyrene-100 ppm; (C) Phenanthrene-100 ppm.

To further test for the potential use of crude laccase from PBURU 12 (10 U/ml) has been evaluated for its ability to degrade an equal concentration of mixed-PAHs (phenanthrene, fluoranthene and pyrene) at 100 ppm/each in liquid medium. After 24 hours of incubation time, mixed-PAHs were extracted using 3 times ethyl-acetate and analyzed by HPLC. The result obtained from HPLC were compared with those from control (buffer and mixed-PAHs only). A decreased in the area of the substrate peaks and the appearance of new peaks were associated with degradation occurred caused by crude laccase were detected. It was indicated that the ability of crude laccase from PBURU 12 to degrade mixture of PAHs with initial concentration of 100 ppm. The reduction in the level of each PAH was calculated and the result revealed that PBURU 12 crude laccase was able to eliminate phenanthrene, fluoranthene and pyrene by 87.53 ± 1.98 , 70.56 ± 1.75 , $79.14 \pm 0.79\%$, respectively. Hence, the finding from this experiment suggested that crude laccase from PBURU 12 as the potential ability to degrade and remove a mixture of three PAHs. This study was in accordance with the finding from Juckpech et al (2012) which using *Phanerochaete* sp. T20 to degrade a mixture of four PAHs (25 mg/l each) resulting in the reduction of 97, 59, 39, and 47% of fluorene, phenanthrene, fluoranthene, and pyrene, respectively.

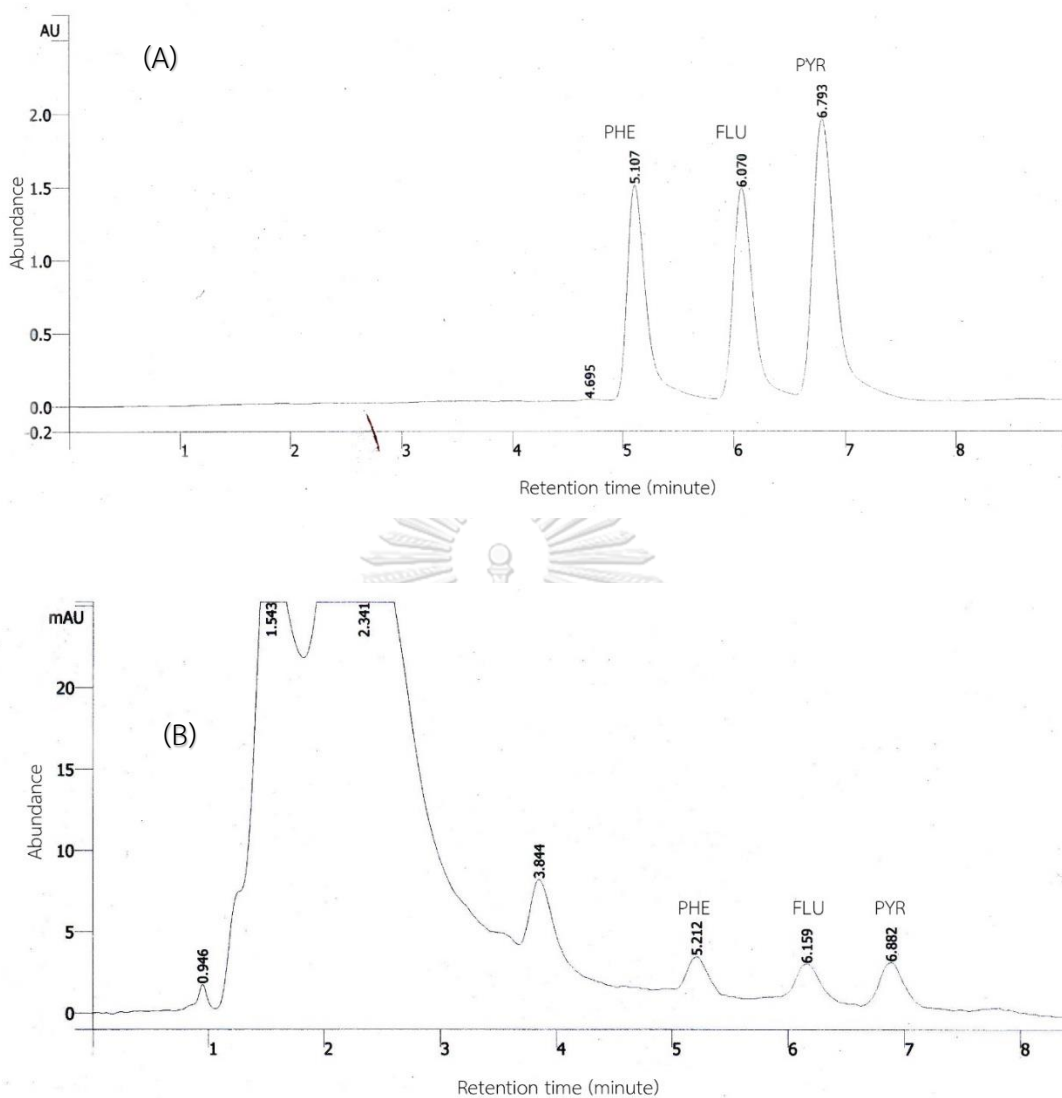


Figure 4.4.2. HPLC chromatograms of mixed-PAHs degradation by PBURU 12 crude laccase (10 U/ml). The media containing phenanthrene, fluoranthene, and pyrene at 100 ppm each. Representative HPLC chromatograms from 24 hours mixture of PAHs (A) mixed-PAHs control and (B) Treated mixed-PAHs. The retention time of phenanthrene, fluoranthene, and pyrene were \pm 5.21, 6.16, and 6.88 minutes, respectively.

4.5. Phytotoxicity and genotoxicity tests of PAHs and treated-PAHs

The phytotoxicity effect of PAHs was measured in term of root growth inhibition test using *Allium cepa*. Root growth inhibition in *Allium cepa* can be considered as toxicity indicator. The effect of different treatment of PAHs on root growth and length *Allium cepa* was showed in Figure 4.5.1. The result showed that compared to control (tap water), all treatments were inhibited by the present of PAHs and its product. The recorded mean root lengths (in mm) after 2 days treatment was 48.18 ± 14.11 (control); 3.56 ± 0.69 (PHE 100 ppm); 14.056 ± 5.15 (treated PHE); 2.86 ± 0.99 (FLU 100 ppm); 27.77 ± 6.73 (treated Flu); 4.67 ± 2.19 (PYR 100 ppm); 22.67 ± 2.52 (treated PYR); No growth (mixed PAHs 100 ppm); 1.79 ± 0.46 (treated mixed PAHs), respectively. The addition of PAHs (100 ppm) was significantly decreased the root length of *Allium cepa* by approximately, more than 12-fold compared to the control, whereas the were no growth detected from the mixed-PAHs. Morphological deformities observed in tested concentrations were short and bent. The treatment using crude laccase from PBURU 12 demonstrated the increasing of root length compared to non-treated PAHs but at the same time is still significantly decreased by 1.17-fold to 3.07-fold compared to the control.

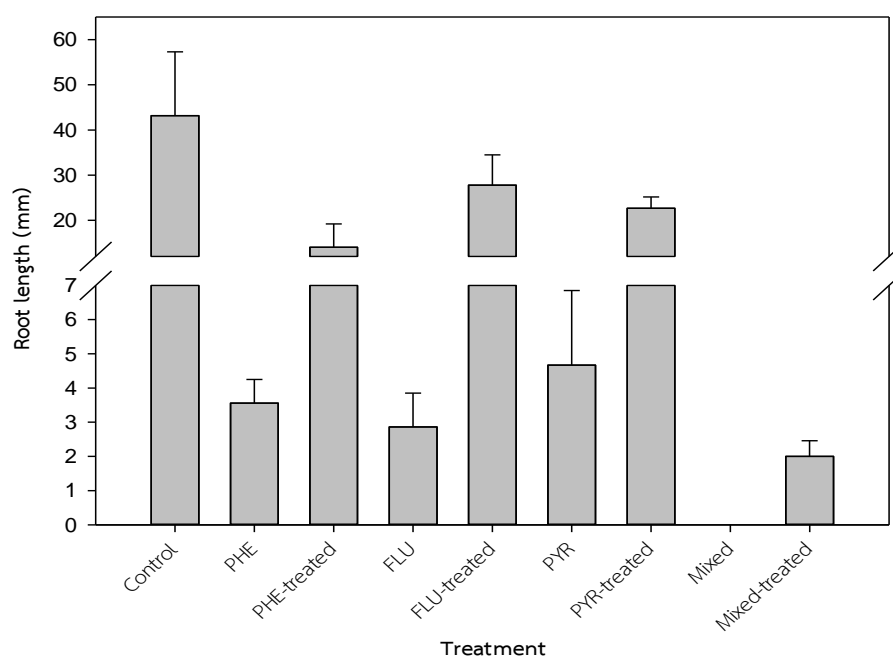


Figure 4.5.1. Root length of *Allium cepa*. Values are mean \pm SD of five samples.

Most plant species are susceptible to PAHs to some extent because PAHs can impede plant growth and development, limiting productivity and biological activity in the environment (Greenberg, 2003). PAHs are generally phytotoxic at high concentrations and it was also suggested that smaller PAHs seemed to be the most toxic (Greenberg, 2003). Previous research found that fluoranthene reduced the germination rate of *Allium cepa* and inhibited the length of both the root and shoot (Kummerová & Kmentová, 2004). While Benzo[a]pyrene caused a significant inhibition in roots, bulbs and leaves of *Allium cepa* (Geremias et al., 2011). When compared to untreated leachate, the treatment increased *Allium cepa* root length and reduced root growth inhibition (Bortolotto et al., 2009). Furthermore, Somtrakoon and Chouychai (2013) have conducted study of single and mixture PAHs (anthracene, fluoranthene, fluorene, phenanthrene) toxicity to three crops (sweet corn, waxy corn, and rice seeds). The result showed that germination of three crops seeds were delayed by

single and mixture PAHs, especially at the high concentration. While root and shoot elongation were more sensitive to PAH (Greenberg, 2003).

The toxic effects of PAHs on plants are determined by a number of variables (Somtrakoon & Chouychai, 2013). The major factors influencing PAH toxicity are their chemical structure and chemical characteristics (Somtrakoon & Chouychai, 2013). PAH phytotoxicity is determined by their solubility and may vary in bioavailability, for example, low molecular weight PAHs are mobile and readily deposited on the root surface (Greenberg, 2003). The phytotoxicity evaluation of pyrene has been conducted using *Cicer arietinum* as plant assay and the result showed that root elongation was 100% for water, while 39% for control and 87% for sample after degradation (Agrawal & Shahi, 2017). The phytotoxicity of metabolites was investigated on the *Vigna radiata*, the result showed the increased in length of *V. radiata* root compared to control (Agrawal et al., 2021). Furthermore, PAH metabolism in different plant species results in distinct metabolites and as a result, varied harmful effects (Kolb & Harms, 2000). It has been discovered that PAHs degraded in the soil may result hazardous and mutagenic intermediates such as quinones or hydroxy derivatives, which are more harmful than the parent chemicals (Agrawal et al., 2021).

Many studies have been conducted on the metabolites chemicals that result from the breakdown of PAHs. The metabolites produced by ligninolytic fungus in the breakdown of phenanthrene differed depending on the fungal species and medium. Phenanthrene degradation by *Phanerochaete chrysosporium* resulted trans-9,10-dihydrodiol, phenanthrene trans-3,4-dihydrodiol, 9-phenanthrol, 3-phenanthrol, 4-phenanthrol, and 9-phenanthryl β -D-glucopyranoside (Sutherland et al., 1991). *Pleurotus ostreatus* degraded phenanthrene to produce 9-10-phenanthrenequinone and 2,2-diphenic acid (Bezalel et al., 1996). While *Ganoderma* sp. and *Podoscypha elegans* resulted 9-10-dihydroxyphenanthrene, protocatechuic acid and phthalic acid (Agrawal et al., 2021; Torres-Farrada et al., 2019). The degradation of fluoranthene by *Pleurotus pulmonarius* produced naphthalen-1,8-dicarboxylic acid and phthalic acid,

while *Irpex lacteus* resulted 2-formyl-acepnaphthen-1-carboxylic acid methyl ester and 1,8-naphthalic anhydride (Cajthaml et al., 2002; Wirasnita & Hadibarata, 2016). The degradation of pyrene by *Corioloropsis byrsina* resulted benzoic acid 2-hydroxy pentyl ester, phenanthrene 4,5 dihydroxy pyrene, pyruvic acid, benzoic acid, benzoic acid 2-hydroxy pentyl ester, phthalic acid diisopropyl ester, 4,5 di hydroxy pyrene (Agrawal & Shahi, 2017).

Mitotic behavior (MI) of chromosomes in the root tips of *A. cepa* was used as a genotoxicity test. Table 4.5.1 showed the percentage of MI and damage index observed when *A. cepa* root tips were treated with the 100 ppm PAHs solution. The root tips exposed to 100 ppm of phenanthrene showed a significant and 1.37-fold decreased MI compared to the control. However, although the laccase-treated phenanthrene caused a less marked MI reduction than phenanthrene (1.13- vs. 1.37-fold), this was still significantly lower than in the control. The similar condition was occurred during the exposition of the root tips to 100 ppm of fluoranthene. The Mi was decreased to 1.53-fold, while laccase-treated fluoranthene was 1.11-fold decreased compared to control. The exposure of pyrene (100 ppm) to the root tip also decreased the MI down to 1.24-fold compared to the control, in contrasts, the laccase-treated pyrene resulted the nearly similar MI to the control suggested that the treatment was less toxic to *A. cepa* root tips. The lowest MI was found at treated-mixed PAHs that only resulted $7.67 \pm 1.44\%$.

Table 4.5.1. Genotoxicity of PAHs (100 ppm) and their laccase-treated degradation products against *A. cepa* root tip cells.

Treatment	No. cells	No. dividing cells	Mitotic index (%)	Chromosomal damage
Control (distilled water)	325.80 ± 77.85	55.00 ± 7.00	18.52 ± 8.89	0.00
Phenanthrene (100 ppm)	144.40 ± 26.96	19.40 ± 3.11	13.56 ± 4.02	0.06 ± 0.02
Laccase-treated phenanthrene (100 ppm)	289.40 ± 34.82	46.60 ± 3.19	16.14 ± 2.29	0.03 ± 0.01
Fluoranthene (100 ppm)	147.00 ± 38.16	17.20 ± 4.61	12.07 ± 3.68	0.05 ± 0.03
Laccase-treated fluoranthene (100 ppm)	219.20 ± 75.80	32.40 ± 9.02	16.73 ± 8.36	0.04 ± 0.02
Pyrene (100 ppm)	129.20 ± 10.26	19.40 ± 3.44	14.97 ± 1.93	0.03 ± 0.02
Laccase-treated pyrene (100 ppm)	135.40 ± 5.81	25.60 ± 4.56	18.96 ± 3.74	0.03 ± 0.02
Mixed-PAHs (100 ppm)	159.80 ± 41.52	12.00 ± 2.83	7.68 ± 1.44	0.13 ± 0.03
Laccase-treated mixed-PAHs (100 ppm)	116.40 ± 11.78	12.00 ± 2.83	10.27 ± 2.17	0.10 ± 0.03

In terms of the chromosomal damage of *A. cepa* root tips, exposure to 100 ppm phenanthrene increased the damage up to 0.06 ± 0.02 compared to the control (0.00). However, the laccase-treated phenanthrene had a two-fold and significantly lower damage than with phenanthrene. The same trend was occurred to during the exposition of the root tips to 100 ppm of fluoranthene, the laccase-treated fluoranthene had 1.25-fold and significantly lower damage than with fluoranthene. Remarkably, the exposure of pyrene to *A. cepa* root tips resulted similar to pyrene (100 ppm), laccase-treated pyrene, and laccase-treated phenanthrene. The highest chromosomal damage was found at mixed-PAHs scored (0.13 ± 0.03). The chromosomal aberration damage index is distinguished by alterations in either the chromosomal structure or the total number of chromosomes that can occur both spontaneously and as a result of physical exposure as well as chemical agents (de

Rainho et al., 2013; Leme & Marin-Morales, 2009). Formation nuclei abnormalities, such as micronuclei and binuclei, were found when the root was exposed to phenanthrene, while chromosome bridge was found in treated phenanthrene. Fluoranthene exposure to *Allium cepa* root tips resulted laggard metaphase and chromosome bridge (anaphase) while treated fluoranthene formed sticky metaphase and anaphase. The exposure of pyrene to *Allium cepa* root tip formed a sticky and thickening of metaphase and chromosome bridge at anaphase with chromosome break while treated pyrene formed chromosome bridge at anaphase with chromosome break. The mixed-PAH formed binuclei or multinuclei at interphase, sticky metaphase, chromosome bridge at anaphase and telophase with chromosome break while treated mixed-PAH formed prolonged and abnormal kinetics at prophase, chromosome bridge at anaphase with chromosome break.

Micronuclei are caused by acentric fragments or lagging chromosomes that fail to integrate into either of the mitotic cells' daughter nuclei during telophase (Türkoğlu, 2007). Stickiness of chromosomes can also develop as a result of enhanced chromosomal contraction and condensation, or as a result of depolymerization of DNA and partial dissolution of nucleoproteins that led to cell death (Rojas et al., 1993; Türkoğlu, 2007). The chromosomal bridges observed in the cells are most likely generated by chromosomal and chromatid breaking and fusion that may occur due to toxic substances such as clastogens (Yadav et al., 2019). Bridges between chromosomes can be caused by chromosomal stickiness and the consequent inability of free anaphase separation, or they can be caused by uneven translocation or inversion of chromosome segments (Türkoğlu, 2007).

PAHs at 100 ppm showed a high toxic effect toward *A. cepa* root tips compared to the control. The reduction in MI, that is the percentage of mitotic cells in certain stages of the cell cycle, may indicate the need to disrupt the mitotic cycle to repair the damage caused by the components of PAHs toxicity (de Rainho et al., 2013). Benzo[a]pyrene at 1.0–5.0 µg/ml was previously reported to cause a decreased MI and

an increased frequency of abnormal mitosis compared to the control, which was a result of the change in the metaphase/prophase (M/P) ratio, with a tendency for the M/P ratio to decrease with increasing benzo(a)pyrene concentrations and exposure times, leading to inhibition of the cell cycle in prophase (Cabaravdic 2010). Potter et al. (1999) studied the genotoxicity effect of composting of PAH contaminated soil to the *Allium cepa*, they found out that untreated soil triggering the anaphase abnormalities in the *Allium cepa* while no significant effect was observed after composting.

4.6. Mutagenicity (Ames) test of degraded PAHs

Five treatments (negative control (DMSO), positive control, PAHs addition (100 ppm), laccase-treated PAHs and mixed-PAHs) were tested for mutagenicity in the Ames test using both the TA98 and TA100 strains of *S. typhimurium*, with the results summarized in Table 4.6. In this study, the highest activity appeared with the positive controls: 4-nitroquinoline-oxide and sodium azide at 1.5- to 1.6-fold higher than the control for strain TA100, and with 2-aminofluorene and methyl methane sulfonate at 2.3- to 2.8-fold higher than the control for strain TA98. The addition of phenanthrene to media did not increase the number of revertant, and so phenanthrene was not mutagenic in this assay. Likewise, the laccase-treated phenanthrene also showed no mutagenic activity in this assay. The similar event also happened when fluoranthene (100 ppm), laccase-treated fluoranthene (100 ppm), pyrene (100 ppm) and laccase-treated pyrene (100 ppm) was added to TA98 medium. The revertant number was not increased compared to the negative control. In contrast, the addition of fluoranthene (100 ppm), laccase-treated fluoranthene (100 ppm), pyrene (100 ppm) and laccase-treated pyrene (100 ppm) into the TA100 medium increased the revertant number and it was higher than the negative control, but it was still less than twice as high as the control, which was set up as the standard for mutagenic. Furthermore, there was no

growth detected in both mixed-PAHs and treated mixed-PAHs suggested that the environment was too toxic for TA98 and TA100.

Table 4.6. Mutagenic study of phenanthrene (100 ppm) and its laccase-treated degradation products using *S. typhimurium* strains TA98 and TA100.

Chemical	Mutagenic activity (revertant/ μ g/plate)	
	TA98	TA100
<i>Negative control</i>		
DMSO (100 μ l)	36 \pm 5.29	112 \pm 7.55
<i>Positive controls</i>		
4-Nitroquinoline-oxide (10 μ g)	-	183 \pm 13.31
Sodium azide (10 μ g)	-	173 \pm 16.04
2-Aminofluorene (10 μ g)	102 \pm 4.58	-
Methyl methane sulfonates (10 μ l)	83 \pm 13.45	-
<i>Test compounds</i>		
Phenanthrene (100 ppm)	15 \pm 1.53	95 \pm 15.18
Laccase-treated phenanthrene (100 ppm)	23 \pm 18.48	63 \pm 30.92
Fluoranthene (100 ppm)	16 \pm 7.93	143 \pm 35.92
Laccase-treated fluoranthene (100 ppm)	26 \pm 5.13	114 \pm 5.51
Pyrene (100 ppm)	15 \pm 2.64	126 \pm 9.45
Laccase-treated pyrene (100 ppm)	17 \pm 6.5	173 \pm 5.57
Mixed-PAHs (300 ppm)	No growth	No growth
Laccase-treated mixed-PAHs (300 ppm)	No growth	No growth

According to (Hakura et al., 2005) phenanthrene and pyrene was not induced even with the addition of S9 rat liver. The addition of phenanthrene, fluoranthene, and pyrene to media did not increase the number of revertants. These results are consistent with the previous report that phenanthrene and pyrene showed no

mutagenic response in the Ames test with or without metabolic activation from rat or human liver S9 (cytosol containing microsome) fractions (Hakura et al., 2005). Furthermore, the laccase-treated pyrene and laccase-treated fluoranthene showed the increasing number of revertants, but it still in the range of the standard set up following the previously study by Mortelmans and Zeiger (2000) which stated that spontaneous revertant control values for TA98 without the addition of S9 mix was 20-50 and 75-200 revertants for TA100, respectively. Likewise, the laccase-treated PAHs also showed no mutagenic activity in this assay.

Indeed, all three PAHs and their degradation metabolites in this study were generally considered as non-carcinogen. Moreover, in the study by Hakura et al. (2005), when the phenanthrene and pyrene dose were increased up to 500 µg/plate the TA100 strain showed a decreasing number of revertants, which likely reflects the loss of viable cells due to the toxicity of PAHs, rather than a reduced proportion of revertants in the viable cell population. Likewise, in this study, that the number of revertants was lower for TA98 and slightly higher for TA100 in the presence of PAHs or the laccase-treated PAHs compared to control likely reflects the toxic effect to both strains. The addition of 100-1000 µg/plate of phenanthrene reduced the revertants into 1.82-fold and 3.7-fold for both strains (TA98 and TA100) compared to control (DMSO) (Bücker et al., 1979). The addition of pyrene up to 5 mg/plate showed positive result on TA98, while TA100, only gave a weak positive response of between 1.5 and 2 times, and this only at doses of 33 g/plate for phenanthrene (Smith et al., 2013). Most mutagens are harmful to bacteria at various concentrations, as evidenced by a reduction in the number of revertant colonies with increasing mutagen concentration as a result of cell death (Godefroy et al., 2005).

Pagnout et al. (2006) tested the AMES assay toward pyrene, fluoranthene and phenanthrene along with their degraded products by *Mycobacterium* sp. using TA98 and TA100 strains. The result showed that the Ames genotoxicity test on pyrene, fluoranthene, phenanthrene, and their metabolites revealed that the genotoxic

potential vanished nearly entirely after biodegradation. Genotoxicity was found only in strain TA100 for phenanthrene degradation products, both without the liver microsome extract (S9 fraction).



CHAPTER V

CONCLUSION

During the study period, 50 basidiocarps of white-rot fungi were collected from dead trees, braches that had fallen, and living trees. Thirty isolates were assigned to the Ganodermataceae, Hymenochaetaceae, Meripilaceae Phanerochaeteceae, Polyporaceae, and Schizophyllaceae families. Two new records of resupinate fungi (Basidiomycota) were discovered and reported for Indonesia: *Ceriporia inflata* and *Ceriporia lacerata*.

Furthermore, this study provides the basis for a four-step screening protocol to select WRF, which combines easily applicable technique of bioassessment. The protocols including guaiacol agar plate assay (Step 1), 2,2-azinobis(3-ethylbenzthiazholine-6-sulfonate) (ABTS) agar plate assay (Step 2), and assays for tolerance to three individual PAHs—phenanthrene, fluoranthene, and pyrene (Step 3), and degradation of PAHs in submerged medium (Step 4). According to these stepwise protocols, *Trametes polyzona* PBURU 12 was selected, based on its superior performance among the 30 isolates.

T. polyzona PBURU 12 was studied further for optimal laccase production. For screening multiple factors at once, the Plackett-Burman design was used. The results indicated that glucose, peptone, CuSO_4 , and pH had the greatest positive effects on laccase production by PBURU 12. These factors were then chosen for further investigation using response surface methodology (RSM). The results showed that the optimized medium increased laccase activity by nearly three-fold when compared to the basal medium.

Laccase from this fungus was purified and characterized. SDS-PAGE revealed that the laccase has a molecular mass of approximately 70 kDa. The optimum pH and pH stability were found to be 4.5 and 5.0, respectively. PBURU 12 laccase acted in a wide temperature range of 20-70°C and remained stable at 20-40°C for 60

minutes. Cu^{2+} was found to stimulate laccase activity, whereas Fe^{2+} and NaN_3 were found to be potent inhibitors.

Degradation of PAHs using live mycelia and crude laccase of PBURU 12 showed that both conditions were able to degrade PAHs up to 50% within 24 hours. PAHs degradation was increased when ABTS was added, and when laccase concentration was increased to the medium. The crude laccase was capable to degrade PAHs mixture up to 70%.

The genotoxicity experiment using *Allium cepa* revealed that the laccase-treated PAHs was less toxic compared to the untreated ones. The results of the AMES test with *Salmonella typhimurium* revealed that strain TA98 had no mutagenic activity for both untreated and laccase-treated PAHs. While revertant numbers for fluoranthene and pyrene for strain TA100 were increased. For both untreated mixed-PAHs and treated-PAHs, no growth was observed in either strain.

Trametes polyzona PBURU 12 is emerging as a promising candidate for bioremediation of recalcitrant pollutants, according to the findings of this study. Moreover, this strain could have potential in industrial applications such as pulp and paper due to its laccase activities and characteristics.

REFERENCES

- Abdel-Hamid, A. M., Solbiati, J. O., & Cann, I. K. O. (2013). Chapter One - Insights into lignin degradation and its potential industrial applications. *Advances in Applied Microbiology*, 82: 1-28: doi:<https://doi.org/10.1016/B978-0-12-407679-2.00001-6>
- Abdel-Shafy, H. I., & Mansour, M. S. M. (2016). A review on polycyclic aromatic hydrocarbons: Source, environmental impact, effect on human health and remediation. *Egyptian Journal of Petroleum*, 25(1): 107-123: doi:10.1016/j.ejpe.2015.03.011
- Achten, C., & Hofmann, T. (2009). Native polycyclic aromatic hydrocarbons (PAH) in coals – A hardly recognized source of environmental contamination. *Science of The Total Environment*, 407(8): 2461-2473: doi:<https://doi.org/10.1016/j.scitotenv.2008.12.008>
- Afrida, S., Tamai, Y., & Osaki, M. (2009). Screening of Indonesian white rot fungi for *Acacia* wood lignin degradation. *Tropics*, 18(2): 57-60: doi:10.3759/tropics.18.57
- Agrawal, N., Barapatre, A., Shahi, M. P., & Shahi, S. K. (2021). Biodegradation Pathway of Polycyclic Aromatic Hydrocarbons by Ligninolytic Fungus *Podoscypha elegans* Strain FTG4 and Phytotoxicity Evaluation of their Metabolites. *Environmental Processes*: doi:10.1007/s40710-021-00525-z
- Agrawal, N., & Shahi, S. K. (2017). Degradation of polycyclic aromatic hydrocarbon (pyrene) using novel fungal strain *Coriolopsis byrsina* strain APC5. *International Biodeterioration & Biodegradation*, 122: 69-81: doi:10.1016/j.ibiod.2017.04.024
- Agrawal, N., Verma, P., & Shahi, S. K. (2018). Degradation of polycyclic aromatic hydrocarbons (phenanthrene and pyrene) by the ligninolytic fungi *Ganoderma lucidum* isolated from the hardwood stump. *Bioresources and Bioprocessing*, 5(1): doi:10.1186/s40643-018-0197-5
- Alexopoulos, C. J., Mims, C. W., & Blackwell, M. (1996). *Introductory mycology*. New York: John Wiley and Sons.

- Alonso, D. M., Wettstein, S. G., & Dumesic, J. A. (2012). Bimetallic catalysts for upgrading of biomass to fuels and chemicals. *Chemical Society Reviews*, 41(24): 8075-8098: doi:10.1039/C2CS35188A
- Ang, T. N., Ngoh, G. C., & Chua, A. S. M. (2011). A quantitative method for fungal ligninolytic enzyme screening studies. *Asia-Pacific Journal of Chemical Engineering*, 6(4): 589-595: doi:<https://doi.org/10.1002/apj.451>
- Antecka, A., Blatkiewicz, M., Boruta, T., Górak, A., & Ledakowicz, S. (2019). Comparison of downstream processing methods in purification of highly active laccase. *Bioprocess and Biosystems Engineering*, 42(10): 1635-1645: doi:10.1007/s00449-019-02160-3
- Arora, D. S., & Gill, P. K. (2005). Production of ligninolytic enzymes by *Phlebia floridensis*. *World Journal of Microbiology and Biotechnology*, 21(6): 1021-1028: doi:10.1007/s11274-004-7655-2
- Asgher, M., Noreen, S., & Bilal, M. (2017). Enhancement of catalytic, reusability, and long-term stability features of *Trametes versicolor* IBL-04 laccase immobilized on different polymers. *International Journal of Biological Macromolecules*, 95: 54-62: doi:<https://doi.org/10.1016/j.ijbiomac.2016.11.012>
- Ayuso-Fernández, I., Martínez, A. T., & Ruiz-Dueñas, F. J. (2017). Experimental recreation of the evolution of lignin-degrading enzymes from the Jurassic to date. *Biotechnology for Biofuels*, 10(1): 67: doi:10.1186/s13068-017-0744-x
- Baborová, P., Möder, M., Baldrian, P., Cajthamlová, K., & Cajthaml, T. (2006). Purification of a new manganese peroxidase of the white-rot fungus *Irpex lacteus*, and degradation of polycyclic aromatic hydrocarbons by the enzyme. *Research in Microbiology*, 157(3): 248-253: doi:<https://doi.org/10.1016/j.resmic.2005.09.001>
- Bagewadi, Z. K., Mulla, S. I., & Ninnekar, H. Z. (2017). Optimization of laccase production and its application in delignification of biomass. *International Journal of Recycling of Organic Waste in Agriculture*, 6(4): 351-365: doi:10.1007/s40093-017-0184-4
- Baldrian, P. (2006). Fungal laccases – occurrence and properties. *FEMS Microbiology Reviews*, 30(2): 215-242: doi:10.1111/j.1574-4976.2005.00010.x
- Batista-Garcia, R. A., et al. (2017). Simple screening protocol for identification of potential mycoremediation tools for the elimination of polycyclic aromatic hydrocarbons

- and phenols from hyperalkalophile industrial effluents. *J Environ Manage*, 198(Pt 2): 1-11: doi:10.1016/j.jenvman.2017.05.010
- Bezalel, L., Hadar, Y., & Cerniglia, C. E. (1996). Mineralization of polycyclic aromatic hydrocarbons by the white rot fungus *Pleurotus ostreatus*. *Applied and Environmental Microbiology*, 62(1): 292-295: doi:10.1128/AEM.62.1.292-295.1996
- Bezalel, L., Hadar, Y., Fu, P. P., Freeman, J. P., & Cerniglia, C. E. (1996). Metabolism of phenanthrene by the white rot fungus *Pleurotus ostreatus*. *Applied and Environmental Microbiology*, 62(7): 2547-2553: doi:10.1128/AEM.62.7.2547-2553.1996
- Bhattacharya, S. S., Garlapati, V. K., & Banerjee, R. (2011). Optimization of laccase production using response surface methodology coupled with differential evolution. *New Biotechnology*, 28(1): 31-39: doi:<https://doi.org/10.1016/j.nbt.2010.06.001>
- Biko, O. D. V., Viljoen-Bloom, M., & van Zyl, W. H. (2020). Microbial lignin peroxidases: Applications, production challenges and future perspectives. *Enzyme and Microbial Technology*, 141: 109669: doi:<https://doi.org/10.1016/j.enzmictec.2020.109669>
- Bilal, M., et al. (2017). Immobilized ligninolytic enzymes: An innovative and environmental responsive technology to tackle dye-based industrial pollutants – A review. *Science of The Total Environment*, 576: 646-659: doi:<https://doi.org/10.1016/j.scitotenv.2016.10.137>
- Bolhassan, M. H., et al. (2012). Diversity and distribution of Polyporales in Peninsular Malaysia. *Sains Malaysiana*, 41: 155-161:
- Bortolotto, T., et al. (2009). Evaluation of the toxic and genotoxic potential of landfill leachates using bioassays. *Environmental Toxicology and Pharmacology*, 28(2): 288-293: doi:<https://doi.org/10.1016/j.etap.2009.05.007>
- Bourbonnais, R., & Paice, M. G. (1990). Oxidation of non-phenolic substrates: An expanded role for laccase in lignin biodegradation. *FEBS Letters*, 267(1): 99-102: doi:[https://doi.org/10.1016/0014-5793\(90\)80298-W](https://doi.org/10.1016/0014-5793(90)80298-W)

- Bryjak, J., & Rekuć, A. (2010). Effective purification of *Cerrena unicolor* laccase using microfiltration, ultrafiltration and acetone precipitation. *Applied Biochemistry and Biotechnology*, 160(8): 2219-2235: doi:10.1007/s12010-009-8791-9
- Bücker, M., et al. (1979). Mutagenicity of phenanthrene and phenanthrene K-region derivatives. *Mutation Research/Genetic Toxicology*, 66(4): 337-348: doi:[https://doi.org/10.1016/0165-1218\(79\)90044-2](https://doi.org/10.1016/0165-1218(79)90044-2)
- Buswell, J. A., Cai, Y., & Chang, S.-t. (1995). Effect of nutrient nitrogen and manganese on manganese peroxidase and laccase production by *Lentinula (Lentinus) edodes*. *FEMS Microbiology Letters*, 128(1): 81-87: doi:[https://doi.org/10.1016/0378-1097\(95\)00087-L](https://doi.org/10.1016/0378-1097(95)00087-L)
- Cabana, H., Jones, J. P., & Agathos, S. N. (2007). Elimination of endocrine disrupting chemicals using white rot fungi and their lignin modifying enzymes: A review. *Engineering in Life Sciences*, 7(5): 429-456: doi:10.1002/elsc.200700017
- Cajthaml, T., Möder, M., Kačer, P., Šašek, V., & Popp, P. (2002). Study of fungal degradation products of polycyclic aromatic hydrocarbons using gas chromatography with ion trap mass spectrometry detection. *Journal of Chromatography A*, 974(1): 213-222: doi:[https://doi.org/10.1016/S0021-9673\(02\)00904-4](https://doi.org/10.1016/S0021-9673(02)00904-4)
- Camarero, S., Ibarra, D., Martínez, M. J., & Martínez, Á. T. (2005). Lignin-derived compounds as efficient laccase mediators for decolorization of different types of recalcitrant dyes. *Applied and Environmental Microbiology*, 71(4): 1775-1784: doi:10.1128/AEM.71.4.1775-1784.2005
- Cañas, A. I., & Camarero, S. (2010). Laccases and their natural mediators: Biotechnological tools for sustainable eco-friendly processes. *Biotechnology Advances*, 28(6): 694-705: doi:<https://doi.org/10.1016/j.biotechadv.2010.05.002>
- Carlile, M. J., Watkinson, S. C., & Gooday, G. W. (2001). *The fungi* (2 ed.). Amsterdam: Elsevier Academic Press.
- Cerniglia, C. E. (1992). Biodegradation of polycyclic aromatic hydrocarbons. *Biodegradation*, 3: 351-368: doi:<https://doi.org/10.1007/BF00129093>
- Cerniglia, C. E. (1997). Fungal metabolism of polycyclic aromatic hydrocarbons: past, present and future applications in bioremediation. *Journal of Industrial Microbiology and Biotechnology*, 19(5): 324-333: doi:10.1038/sj.jim.2900459

- Cerniglia, C. E., & Sutherland, J. B. (2010). Degradation of polycyclic aromatic hydrocarbons by fungi. In K. N. Timmis (Ed.), *Handbook of Hydrocarbon and Lipid Microbiology* (pp. 2079-2110). Berlin, Heidelberg: Springer Berlin Heidelberg.
- Chairin, T., et al. (2014). Purification and characterization of the extracellular laccase produced by *Trametes polyzona* WR710-1 under solid-state fermentation. *J Basic Microbiol*, 54(1): 35-43: doi:10.1002/jobm.201200456
- Chen, D., Feng, Q., Liang, H., Gao, B., & Alam, E. (2018). Distribution characteristics and ecological risk assessment of polycyclic aromatic hydrocarbons (PAHs) in underground coal mining environment of Xuzhou. *Human and Ecological Risk Assessment: An International Journal*, 25(6): 1564-1578: doi:10.1080/10807039.2018.1489715
- Christopher, L. P., Yao, B., & Ji, Y. (2014). Lignin Biodegradation with Laccase-Mediator Systems. *Frontiers in Energy Research*, 2(12): doi:10.3389/fenrg.2014.00012
- Çifçi, D. İ., Atav, R., Güneş, Y., & Güneş, E. (2019). Determination of the color removal efficiency of laccase enzyme depending on dye class and chromophore. *Water Science and Technology*, 80(1): 134-143: doi:10.2166/wst.2019.255
- Claus, H. (2004). Laccases: structure, reactions, distribution. *Micron*, 35(1): 93-96: doi:<https://doi.org/10.1016/j.micron.2003.10.029>
- D'Souza, T. M., Merritt, C. S., & Reddy, C. A. (1999). Lignin-modifying enzymes of the white rot Basidiomycete *Ganoderma lucidum*. *Applied and Environmental Microbiology*, 65(12): 5307-5313: doi:10.1128/AEM.65.12.5307-5313.1999
- da Silva Vilar, D., et al. (2021). Lignin-modifying enzymes: a green and environmental responsive technology for organic compound degradation. *Journal of Chemical Technology & Biotechnology*: doi:<https://doi.org/10.1002/jctb.6751>
- Dai, Y.-C. (2012). Polypore diversity in China with an annotated checklist of Chinese polypores. *Mycoscience*, 53(1): 49-80: doi:<https://doi.org/10.1007/s10267-011-0134-3>
- Daisy, B. H., et al. (2002). Naphthalene, an insect repellent, is produced by *Muscodora vitigenus*, a novel endophytic fungus. *Microbiology (Reading, England)*, 148(Pt 11): 3737-3741: doi:10.1099/00221287-148-11-3737

- de Rainho, R. C., Machado Correa, S., Luiz Mazzei, J., Alessandra Fortes Aiub, C., & Felzenszwalb, I. (2013). Genotoxicity of polycyclic aromatic hydrocarbons and nitro-derived in respirable airborne particulate matter collected from urban areas of Rio de Janeiro (Brazil). *Biomed Res Int*, 2013: 765352: doi:10.1155/2013/765352
- Dhakar, K., & Pandey, A. (2013). Laccase production from a temperature and pH tolerant fungal strain of *Trametes hirsuta* (MTCC 11397). *Enzyme Research*, 2013: 869062: doi:10.1155/2013/869062
- Dhouib, A., et al. (2005). Screening for ligninolytic enzyme production by diverse fungi from Tunisia. *World Journal of Microbiology and Biotechnology*, 21: 1415-1423: doi:10.1007/s11274-005-5774-z
- Donk, M. A. (1964). A conspectus of the families of Aphylllophorales. *Persoonia*, 3: 199-324:
- Doyle, E., Muckian, L., Hickey, A. M., & Clipson, N. (2008). Chapter 2 - Microbial PAH degradation. In A. I. Laskin, S. Sariaslani, & G. M. Gadd (Eds.), *Advances in Applied Microbiology* (Vol. 65, pp. 27-66). San Diego: Academic Press.
- Erden, E., Ucar, C., Gezer, T., & Pazarlioglu, N. (2009). Screening for ligninolytic enzymes from autochthonous fungi and applications for decolorization of Remazole Marine Blue. *Brazilian Journal of Microbiology*, 40: doi:10.1590/S1517-83822009000200026
- Eugenio, M., Carbajo, J., Martin, J., González, A., & Villar, J. (2009). Laccase production by *Pycnoporus sanguineus* under different culture conditions. *Journal of Basic Microbiology*, 49: 433-440: doi:10.1002/jobm.200800347
- Evans, H. C., Fröhlich, J., & Shamoun, S. F. (2001). Biological control of weeds. In (pp. 349-401). Hong Kong: Fungal Diversity Press.
- Ezike, T. C., Ezugwu, A. L., Udeh, J. O., Eze, S. O. O., & Chilaka, F. C. (2020). Purification and characterisation of new laccase from *Trametes polyzona* WRF03. *Biotechnology Reports*, 28: e00566: doi:<https://doi.org/10.1016/j.btre.2020.e00566>
- Ezike, T. C., et al. (2021). Substrate specificity of a new laccase from *Trametes polyzona* WRF03. *Heliyon*, 7(1): e06080: doi:<https://doi.org/10.1016/j.heliyon.2021.e06080>
- Fazenda, M. L., Seviour, R., McNeil, B., & Harvey, L. M. (2008). Submerged culture fermentation of “higher fungi”: The macrofungi. In S. S. a. G. M. G. Allen I. Laskin

- (Ed.), *Advances in Applied Microbiology* (Vol. 63, pp. 33-103). San Diego: Academic Press.
- Forootanfar, H., Faramarzi, M. A., Shahverdi, A. R., & Yazdi, M. T. (2011). Purification and biochemical characterization of extracellular laccase from the ascomycete *Paraconiothyrium variable*. *Bioresource Technology*, 102(2): 1808-1814: doi:<https://doi.org/10.1016/j.biortech.2010.09.043>
- Gallery, R. E. (2014). Ecology of tropical rain forests. In R. K. Monson (Ed.), *Ecology and the Environment* (pp. 247-272). New York, NY: Springer New York.
- Gao, B., Feng, Q., Zhou, L., Wu, H., & Alam, E. (2019). Distributions of polycyclic aromatic hydrocarbons in coal in China. *Polish Journal of Environmental Studies*, 28(3): 1665-1674: doi:10.15244/pjoes/89899
- Gates, G. (2009). Coarse woody debris, macrofungal assemblages, and sustainable forest management in a *Eucalyptus obliqua* forest of southern Tasmania.
- Geremias, R., De Fávère, V. T., Pedrosa, R. C., & Fattorini, D. (2011). Bioaccumulation and adverse effects of trace metals and polycyclic aromatic hydrocarbons in the common onion *Allium cepa* as a model in ecotoxicological bioassays. *Chemistry and Ecology*, 27(6): 515-522: doi:10.1080/02757540.2011.602972
- Ghosal, D., Ghosh, S., Dutta, T. K., & Ahn, Y. (2016). Current state of knowledge in microbial degradation of polycyclic aromatic hydrocarbons (PAHs): A review. *Frontiers in Microbiology*, 7(1369): doi:10.3389/fmicb.2016.01369
- Gianfreda, L., Xu, F., & Bollag, J.-M. (1999). Laccases: A useful group of oxidoreductive enzymes. *Bioremediation Journal*, 3(1): 1-26: doi:10.1080/10889869991219163
- Glen, M., et al. (2014). Identification of basidiomycete fungi in Indonesian hardwood plantations by DNA barcoding. *Forest Pathology*, 44(6): 496-508: doi:<https://doi.org/10.1111/efp.12146>
- Godefroy, S. J., Martincigh, B., & Salter, L. F. (2005). Measurements of polycyclic aromatic hydrocarbons and genotoxicity in soot deposited at a toll plaza near Durban, South Africa. *South African Journal of Chemistry*, 58: 61-66:
- Goltapeh, E. M., Danesh, Y. R., & Varma, A. (2013). *Fungi as bioremediators*. In *Soil biology*. Heidelberg: Springer.

- Gramss, G. (1987). R. L. Gilbertson and L. Ryvarden, North American Polypores. Volume 1: Abortiporus — Lindtneria. 433 S., 209 Abb. Oslo 1986. Fungiflora A/S. Journal of Basic Microbiology, 27(5): 282-282: doi:<https://doi.org/10.1002/jobm.3620270513>
- Greenberg, B. M. (2003). PAH interactions with plants: uptake, toxicity and phytoremediation. In PAHs: An Ecotoxicological Perspective (pp. 263-273).
- Hadibarata, T. (2013). Effect of metals on amaranth decolorization by white-rot fungus *Pleurotus eryngii* sp. F019. Journal of Biological Sciences, 13: 550-554: doi:10.3923/jbs.2013.550.554
- Hadibarata, T., & Kristanti, R. A. (2013). Biodegradation and metabolite transformation of pyrene by basidiomycetes fungal isolate *Armillaria* sp. F022. Bioprocess and Biosystems Engineering, 36(4): 461-468: doi:10.1007/s00449-012-0803-4
- Hadibarata, T., Kristanti, R. A., Fulazzaky, M. A., & Nugroho, A. E. (2012). Characterization of pyrene biodegradation by white-rot fungus *Polyporus* sp. S133. Biotechnology and Applied Biochemistry, 59(6): 465-470: doi:10.1002/bab.1048
- Hadibarata, T., & Tachibana, S. (2010). Characterization of phenanthrene degradation by strain *Polyporus* sp. S133. Journal of Environmental Sciences, 22(1): 142-149: doi:10.1016/s1001-0742(09)60085-1
- Hakura, A., et al. (2005). *Salmonella*/human S9 mutagenicity test: a collaborative study with 58 compounds. Mutagenesis, 20(3): 217-228: doi:10.1093/mutage/gei029
- Hall, B. G. (2013). Building phylogenetic trees from molecular data with MEGA. Molecular Biology and Evolution, 30(5): 1229-1235: doi:10.1093/molbev/mst012
- Hammel, K. E., Gai, W. Z., Green, B., & Moen, M. A. (1992). Oxidative degradation of phenanthrene by the ligninolytic fungus *Phanerochaete chrysosporium*. Applied and Environmental Microbiology, 58(6): 1832-1838: doi:10.1128/aem.58.6.1832-1838.1992
- Han, M.-J., Choi, H., & Song, H.-G. (2004). Degradation of phenanthrene by *Trametes versicolor* and its laccase. Journal of microbiology, 42: 94-98:
- Hariharan, S., & Nambisan, P. (2012). Optimization of lignin peroxidase, manganese peroxidase, and laccase production from *Ganoderma lucidum* under solid state fermentation of Pineapple Leaf. BioResources, 8: doi:10.15376/biores.8.1.250-271

- Hashem, M. A. (2019). Estimation of aboveground biomass carbon stock and carbon sequestration using uav imagery at kebun raya unmul Samarinda education forest, East Kalimantan, Indonesia. (Master), University of Twente, Enschede, The Netherlands.
- Hatakka, A. (1994). Lignin-modifying enzymes from selected white-rot fungi: production and role from in lignin degradation. *FEMS Microbiology Reviews*, 13(2-3): 125-135: doi:<https://doi.org/10.1111/j.1574-6976.1994.tb00039.x>
- Hatakka, A. (2001). Lignin, humic substances and coal. In M. Hofrichter (Ed.), *Biopolymers Online*. Weinheim: Wiley-Blackwell.
- Hatakka, A., & Hammel, K. (2010). Fungal biodegradation of lignocelluloses. In M. Hofrichter (Ed.), *The Mycota (Industrial Application)* (Vol. 10, pp. 319-340). Berlin: Springer.
- Hattori, T. (2017). Biogeography of polypores in Malesia, Southeast Asia. *Mycoscience*, 58(1): 1-13: doi:<https://doi.org/10.1016/j.myc.2016.09.004>
- Hermiati, E., et al. (2013). Biological pretreatment of oil palm frond fiber using white-rot fungi for enzymatic saccharification. *MAKARA Journal of Technology Series*, 17: doi:10.7454/mst.v17i1.1926
- Hibbett, D., et al. (2014). Agaricomycetes. In (Vol. 7, pp. 373-429).
- Hibbett, D. S. (2006). A phylogenetic overview of the Agaricomycotina. *Mycologia*, 98(6): 917-925: doi:10.1080/15572536.2006.11832621
- Hjortstam, K., & Ryvarden, L. (2007). Checklist of corticioid fungi (Basidiomycotina) from the tropics, subtropics and the southern hemisphere. In L. Ryvarden (Ed.), *Synopsis Fungorum* (Vol. 22). Oslo: Fungiflora.
- Hofrichter, M. (2002). Review: lignin conversion by manganese peroxidase (MnP). *Enzyme and Microbial Technology*, 30(4): 454-466: doi:[https://doi.org/10.1016/S0141-0229\(01\)00528-2](https://doi.org/10.1016/S0141-0229(01)00528-2)
- Hyde, K. D., et al. (2019). The amazing potential of fungi: 50 ways we can exploit fungi industrially. *Fungal Diversity*, 97(1): 1-136: doi:10.1007/s13225-019-00430-9
- Iqbal Md, A., Anand, K., & Md, I. K. (2015). Characteristics and impact of different industrial effluents from coal mines with a biotechnological approach of using green algae

- for waste water treatment-an appraisal. *International Journal of Current Research*, 07: 14884-14888:
- Janusz, G., et al. (2017). Lignin degradation: microorganisms, enzymes involved, genomes analysis and evolution. *FEMS Microbiology Reviews*, 41(6): 941-962: doi:10.1093/femsre/fux049
- Jegatheesan, M., & Eyini, M. (2015). Response surface methodology mediated modulation of laccase production by *Polyporus arcularius*. *Arabian Journal for Science and Engineering*, 40(7): 1809-1818: doi:10.1007/s13369-014-1499-3
- Jepson, P., & van Noord, H. (2002). A review of the efficacy of the protected area system of East Kalimantan Province, Indonesia. *Natural Areas Journal*, 22: 28:
- Jia, B.-S., & Cui, B.-K. (2013). Two new species of *Ceriporia* (Basidiomycota, Polyporales) with a key to the accepted species in China. *Mycotaxon*, 121(1): 305-312: doi:10.5248/121.305
- Jia, B.-S., Zhou, L.-W., Cui, B.-K., Rivoire, B., & Dai, Y.-C. (2013). Taxonomy and phylogeny of *Ceriporia* (Polyporales, Basidiomycota) with an emphasis of Chinese collections. *Mycological Progress*, 13(1): 81-93: doi:10.1007/s11557-013-0895-5
- Juckpech, K., Pinyakong, O., & Rerngsamran, P. (2012). Degradation of polycyclic aromatic hydrocarbons by newly isolated *Curvularia* sp. F18, *Lentinus* sp. S5, and *Phanerochaete* sp. T20. *ScienceAsia*, 38(2): doi:10.2306/scienceasia1513-1874.2012.38.147
- Justo, A., & Hibbett, D. (2011). Phylogenetic classification of *Trametes* (Basidiomycota, Polyporales) based on a five-marker dataset. *TAXON*, 60: 1567-1583: doi:10.1002/tax.606003
- Justo, A., et al. (2017). A revised family-level classification of the Polyporales (Basidiomycota). *Fungal Biology*, 121(9): 798-824: doi:<https://doi.org/10.1016/j.funbio.2017.05.010>
- Kameshwar, A. K. S., & Qin, W. (2017). Qualitative and quantitative methods for isolation and characterization of lignin-modifying enzymes secreted by microorganisms. *Bioenergy Research*, 10(1): 248-266: doi:10.1007/s12155-016-9784-5
- Karyati, S. A., Muhammad Syafrudin (2016). Fluktuasi iklim mikro di hutan pendidikan fakultas kehutanan universitas Mulawarman. *AGRIFOR*, 15(1): 83-92:

- Kiiskinen, L.-L., Rättö, M., & Kruus, K. (2004). Screening for novel laccase-producing microbes. *Journal of Applied Microbiology*, 97(3): 640-646: doi:<https://doi.org/10.1111/j.1365-2672.2004.02348.x>
- Kirk, T., & Cullen, D. (1998). Enzymology and molecular genetics of wood degradation by white-rot fungi. In A. M. Young RA (Ed.), *Environmentally friendly technologies for the pulp and paper industry*. New York: Wiley.
- Kolb, M., & Harms, H. (2000). Metabolism of fluoranthene in different plant cell cultures and intact plants. *Environmental Toxicology and Chemistry*, 19(5): 1304-1310: doi:<https://doi.org/10.1002/etc.5620190512>
- Kong, W., et al. (2016). Characterization of a novel manganese peroxidase from white-rot fungus *Echinodontium taxodii* 2538, and its use for the degradation of lignin-related compounds. *Process Biochemistry*, 51(11): 1776-1783: doi:<https://doi.org/10.1016/j.procbio.2016.01.007>
- Kummerová, M., & Kmentová, E. (2004). Photoinduced toxicity of fluoranthene on germination and early development of plant seedling. *Chemosphere*, 56(4): 387-393: doi:<https://doi.org/10.1016/j.chemosphere.2004.01.007>
- Laessøe, T., & Lincoff, G. (2002). *Mushrooms*. New York: DK Pub.
- Larsson, K.-H. (2007). Re-thinking the classification of corticioid fungi. *Mycological Research*, 111(9): 1040-1063: doi:<https://doi.org/10.1016/j.mycres.2007.08.001>
- Lee, A. H., et al. (2020). A proposed stepwise screening framework for the selection of polycyclic aromatic hydrocarbon (PAH)-degrading white rot fungi. *Bioprocess and Biosystems Engineering*: doi:10.1007/s00449-019-02272-w
- Lee, H., et al. (2014). Biotechnological procedures to select white rot fungi for the degradation of PAHs. *Journal of Microbiological Methods*, 97: 56-62: doi:<https://doi.org/10.1016/j.mimet.2013.12.007>
- Lee, Y., et al. (2006). Effect of nutrients on the production of extracellular enzymes for decolorization of reactive blue 19 and reactive black 5. *Journal of microbiology and biotechnology*, 16: 226-231:
- Leme, D. M., & Marin-Morales, M. A. (2009). *Allium cepa* test in environmental monitoring: A review on its application. *Mutation Research/Reviews in Mutation Research*, 682(1): 71-81: doi:<https://doi.org/10.1016/j.mrrev.2009.06.002>

- Levin, L., Forchiassin, F., & Ramos, A. M. (2002). Copper induction of lignin-modifying enzymes in the white-rot fungus *Trametes trogii*. *Mycologia*, 94(3): 377-383: doi:10.1080/15572536.2003.11833202
- Li, S., et al. (2016). High-level production and characterization of laccase from a newly isolated fungus *Trametes* sp. LS-10C. *Biocatalysis and Agricultural Biotechnology*, 8: 278-285: doi:<https://doi.org/10.1016/j.bcab.2016.10.008>
- Li, X., et al. (2018). Emission characteristics of organic pollutants during coprocessing of coal liquefaction residue in Texaco coal–water slurry gasifier. *Energy & Fuels*, 32(2): 2605-2611: doi:10.1021/acs.energyfuels.7b03395
- Li, X., et al. (2010). Degradation of polycyclic aromatic hydrocarbons by crude extracts from spent mushroom substrate and its possible mechanisms. *Curr Microbiol*, 60(5): 336-342: doi:10.1007/s00284-009-9546-0
- Lindblad, I. (2001). Diversity of poroid and some Corticoid wood-inhabiting fungi along the rainfall gradient in tropical forests, Costa Rica. *Journal of Tropical Ecology*, 17(3): 353-369:
- Lueangjaroenkit, P., et al. (2019). Two manganese peroxidases and a laccase of *Trametes polyzona* KU-RNW027 with novel properties for dye and pharmaceutical product degradation in redox mediator-free system. *Mycobiology*, 47(2): 217-229: doi:10.1080/12298093.2019.1589900
- Machuca, Á., Palfner, G., & Guillén, Y. (2011). Screening for lignocellulolytic enzymes and metal tolerance in isolates of wood-rot fungi from Chile. *Interciencia*, 36: 860-868:
- Maiti, D., Ansari, I., Rather, M. A., & Deepa, A. (2019). Comprehensive review on wastewater discharged from the coal-related industries – characteristics and treatment strategies. *Water Science and Technology*, 79(11): 2023-2035: doi:10.2166/wst.2019.195
- Manavalan, T., Manavalan, A., Thangavelu, K. P., & Heese, K. (2013). Characterization of optimized production, purification and application of laccase from *Ganoderma lucidum*. *Biochemical Engineering Journal*, 70: 106-114: doi:<https://doi.org/10.1016/j.bej.2012.10.007>
- Mardji, D., & Noor, M. (2009). Keanekaragaman jenis jamur makro di hutan lindung Gunung Lumut. *JURNAL KEHUTANAN TROPIKA HUMIDA*, 2(2): 143-155:

- Martani, F., Beltrametti, F., Porro, D., Branduardi, P., & Lotti, M. (2017). The importance of fermentative conditions for the biotechnological production of lignin modifying enzymes from white-rot fungi. *FEMS Microbiology Letters*, 364(13): doi:10.1093/femsle/fnx134
- Mikiashvili, N., Wasser, S. P., Nevo, E., & Elisashvili, V. (2006). Effects of carbon and nitrogen sources on *Pleurotus ostreatus* ligninolytic enzyme activity. *World Journal of Microbiology and Biotechnology*, 22(9): 999-1002: doi:10.1007/s11274-006-9132-6
- Millis, C. D., Cai, D., Stankovich, M. T., & Tien, M. (1989). Oxidation-reduction potentials and ionization states of extracellular peroxidases from the lignin-degrading fungus *Phanerochaete chrysosporium*. *Biochemistry*, 28(21): 8484-8489: doi:10.1021/bi00447a032
- Mohammed, C. L., Rimbawanto, A., & Page, D. E. (2014). Management of basidiomycete root- and stem-rot diseases in oil palm, rubber and tropical hardwood plantation crops. *Forest Pathology*, 44(6): 428-446: doi:<https://doi.org/10.1111/efp.12140>
- Moose, R. A., Schigel, D., Kirby, L. J., & Shumskaya, M. (2019). Dead wood fungi in North America: an insight into research and conservation potential. *Nature Conservation*, 32: 1-17:
- Mortelmans, K., & Zeiger, E. (2000). The Ames *Salmonella*/microsome mutagenicity assay. *Mutation Research/Fundamental and Molecular Mechanisms of Mutagenesis*, 455(1): 29-60: doi:[https://doi.org/10.1016/S0027-5107\(00\)00064-6](https://doi.org/10.1016/S0027-5107(00)00064-6)
- Mukhopadhyay, M., & Banerjee, R. (2015). Purification and biochemical characterization of a newly produced yellow laccase from *Lentinus squarrosulus* MR13. *3 Biotech*, 5(3): 227-236: doi:10.1007/s13205-014-0219-8
- Munusamy, U., et al. (2008). Biodegradation of polycyclic aromatic hydrocarbons by laccase of *Pycnoporus sanguineus* and toxicity evaluation of treated PAH. *Biotechnology(faisalabad)*, 7: 669-677:
- Naranjo-Ortiz, M. A., & Gabaldón, T. (2019). Fungal evolution: diversity, taxonomy and phylogeny of the fungi. *Biological Reviews*, 94(6): 2101-2137: doi:<https://doi.org/10.1111/brv.12550>

- Navada, K. K., & Kulal, A. (2021). Kinetic characterization of purified laccase from *Trametes hirsuta*: a study on laccase catalyzed biotransformation of 1,4-dioxane. *Biotechnology Letters*, 43(3): 613-626: doi:10.1007/s10529-020-03038-1
- Pagnout, C., Rast, C., Veber, A. M., Poupin, P., & Ferard, J. F. (2006). Ecotoxicological assessment of PAHs and their dead-end metabolites after degradation by *Mycobacterium* sp. strain SNP11. *Ecotoxicol Environ Saf*, 65(2): 151-158: doi:10.1016/j.ecoenv.2006.03.005
- Palvannan, T., & Sathishkumar, P. (2010). Production of laccase from *Pleurotus florida* NCIM 1243 using Plackett-Burman design and response surface methodology. *J Basic Microbiol*, 50(4): 325-335: doi:10.1002/jobm.200900333
- Park, K., & Park, S.-S. (2008). Purification and characterization of laccase from basidiomycete *Fomitella fraxinea*. *Journal of microbiology and biotechnology*, 18: 670-675:
- Park, N., & Park, S.-S. (2014). Purification and characterization of a novel laccase from *Fomitopsis pinicola* mycelia. *International Journal of Biological Macromolecules*, 70: 583-589: doi:<https://doi.org/10.1016/j.ijbiomac.2014.06.019>
- Patel, A. B., Shaikh, S., Jain, K. R., Desai, C., & Madamwar, D. (2020). Polycyclic aromatic hydrocarbons: Sources, toxicity, and remediation approaches. *Frontiers in Microbiology*, 11(2675): doi:10.3389/fmicb.2020.562813
- Permpornsakul, P., et al. (2016). Two new records of the resupinate polypore fungi, *Ceriporia cystidiata* and *Macrohyporia dictyopora*, in Thailand. *ScienceAsia*, 42(3): doi:10.2306/scienceasia1513-1874.2016.42.171
- Piontek, K., Smith, A. T., & Blodig, W. (2001). Lignin peroxidase structure and function. *Biochemical Society Transactions*, 29(2): 111-116: doi:10.1042/bst0290111
- Pointing, S. (2001). Feasibility of bioremediation by white-rot fungi. *Applied Microbiology and Biotechnology*, 57(1): 20-33: doi:10.1007/s002530100745
- Potter, C. L., et al. (1999). Degradation of polynuclear aromatic hydrocarbons under bench-scale compost conditions. *Environmental Science & Technology*, 33(10): 1717-1725: doi:10.1021/es9810336

- Pozdnyakova, N. N., et al. (2010). Influence of cultivation conditions on pyrene degradation by the fungus *Pleurotus Ostreatus* D1. *World Journal of Microbiology and Biotechnology*, 26(2): 205-211: doi:10.1007/s11274-009-0161-9
- Pozdnyakova, N. N., Nikiforova, S. V., Makarov, O. E., & Turkovskaya, O. V. (2011). Effect of polycyclic aromatic hydrocarbons on laccase production by white rot fungus *Pleurotus ostreatus* D1. *Applied Biochemistry and Microbiology*, 47(5): 543: doi:10.1134/S0003683811050103
- Punnapayak, H., Prasongsuk, S., Messner, K., Danmek, K., & Lotrakul, P. (2009). Polycyclic aromatic hydrocarbons (PAHs) degradation by laccase from a tropical white rot fungus *Ganoderma lucidum*. *African Journal of Biotechnology*, 8(21): 5897-5900: doi:10.4314/ajb.v8i21.66070
- Putra, I., Nasrullah, M., & Dinindaputri, T. (2019). Study on diversity and potency of some macro mushroom at Gunung Gede Pangrango National Park. *Buletin Plasma Nutfah*, 25(2): 1-14: doi:10.21082/blpn.v25n2.2019.p1-14
- Rahmawati, L. R., Tanti NY (2018). Jenis-jenis jamur makroskopis anggota kelas *Basidiomycetes* di Hutan Bayur, Kabupaten Landak, Kalimantan Barat. *Jurnal Mikologi Indonesia*, 2(2): 56-65: doi:<http://doi.org/10.46638/jmi.v2i2.35>
- Reddy, C. A., & D'Souza, T. M. (1994). Physiology and molecular biology of the lignin peroxidases of *Phanerochaete chrysosporium*. *FEMS Microbiology Reviews*, 13(2-3): 137-152: doi:10.1111/j.1574-6976.1994.tb00040.x
- Revankar, M. S., & Lele, S. S. (2006). Increased production of extracellular laccase by the white rot fungus *Coriolus versicolor* MTCC 138. *World Journal of Microbiology and Biotechnology*, 22(9): 921-926: doi:10.1007/s11274-006-9136-2
- Riva, S. (2006). Laccases: blue enzymes for green chemistry. *Trends in Biotechnology*, 24(5): 219-226: doi:<https://doi.org/10.1016/j.tibtech.2006.03.006>
- Rojas, E., et al. (1993). Mitotic index and cell proliferation kinetics for identification of antineoplastic activity. *Anti-Cancer Drugs*, 4: doi:10.1097/00001813-199312000-00005
- Ryvarden, L., & Johansen, I. (1980). A preliminary Polypore flora of East Africa. Oslo: Fungiflora.

- Sadhasivam, S., Savitha, S., Swaminathan, K., & Lin, F.-H. (2008). Production, purification and characterization of mid-redox potential laccase from a newly isolated *Trichoderma harzianum* WL1. *Process Biochemistry*, 43(7): 736-742: doi:<https://doi.org/10.1016/j.procbio.2008.02.017>
- Sambrook, J., & Russell, D. W. (2006). Purification of nucleic acids by extraction with phenol:chloroform. *CSH protocols*, 2006(1). Retrieved from doi:10.1101/pdb.prot4455
- Sánchez, C. (2009). Lignocellulosic residues: Biodegradation and bioconversion by fungi. *Biotechnology Advances*, 27(2): 185-194: doi:<https://doi.org/10.1016/j.biotechadv.2008.11.001>
- Schnitz, A. R., Squibb, K. S., & Oconnor, J. M. (1993). Time-varying conjugation of 7,12-dimethylbenz[a]anthracene metabolites in Rainbow Trout (*Oncorhynchus mykiss*). *Toxicology and Applied Pharmacology*, 121(1): 58-70: doi:<https://doi.org/10.1006/taap.1993.1129>
- Schützendübel, A., Majcherczyk, A., Johannes, C., & Hüttermann, A. (1999). Degradation of fluorene, anthracene, phenanthrene, fluoranthene, and pyrene lacks connection to the production of extracellular enzymes by *Pleurotus ostreatus* and *Bjerkandera adusta*. *International Biodeterioration & Biodegradation*, 43(3): 93-100: doi:[https://doi.org/10.1016/S0964-8305\(99\)00035-9](https://doi.org/10.1016/S0964-8305(99)00035-9)
- Shraddha, Shekher, R., Sehgal, S., Kamthania, M., & Kumar, A. (2011). Laccase: microbial sources, production, purification, and potential biotechnological applications. *Enzyme Research*, 2011: 217861-217861: doi:10.4061/2011/217861
- Si, J., Peng, F., & Cui, B. (2013). Purification, biochemical characterization and dye decolorization capacity of an alkali-resistant and metal-tolerant laccase from *Trametes pubescens*. *Bioresource Technology*, 128: 49-57: doi:<https://doi.org/10.1016/j.biortech.2012.10.085>
- Singh, J., & Kapoor, R. (2014). Microbial laccases: a mini-review on their production, purification and applications.
- Siswanto, H., Arifin, Z., & Ariyanto, A. (2018). Dinamika menuju kesatuan pengelolaan hutan produksi (kphp) Samarinda “sebuah harapan dan tantangan”. *Ulin, Journal Hutan Tropika*, 1(2): doi:10.32522/ujht.v1i2.775

- Smith, K. E. C., Heringa, M. B., Uytewaal, M., & Mayer, P. (2013). The dosing determines mutagenicity of hydrophobic compounds in the Ames II assay with metabolic transformation: Passive dosing versus solvent spiking. *Mutation Research/Genetic Toxicology and Environmental Mutagenesis*, 750(1): 12-18: doi:<https://doi.org/10.1016/j.mrgentox.2012.07.006>
- Somtrakoon, K., & Chouychai, W. (2013). Phytotoxicity of single and combined polycyclic aromatic hydrocarbons toward economic crops. *Russian Journal of Plant Physiology*, 60(1): 139-148: doi:10.1134/S1021443712060155
- Stone, K. M., Roche, F. W., & Thornhill, N. F. (1992). Dry weight measurement of microbial biomass and measurement variability analysis. *Biotechnology Techniques*, 6(3): 207-212: doi:10.1007/BF02439345
- Sugiura, M., Hirai, H., & Nishida, T. (2003). Purification and characterization of a novel lignin peroxidase from white-rot fungus *Phanerochaete sordida* YK-624. *FEMS Microbiology Letters*, 224(2): 285-290: doi:[https://doi.org/10.1016/S0378-1097\(03\)00447-6](https://doi.org/10.1016/S0378-1097(03)00447-6)
- Suhara, H., et al. (2003). A new species, *Ceriporia lacerata*, isolated from white-rotted wood. *Mycotaxon*, 86: 335-347:
- Sutherland, J. B., Selby, A. L., Freeman, J. P., Evans, F. E., & Cerniglia, C. E. (1991). Metabolism of phenanthrene by *Phanerochaete chrysosporium*. *Applied and Environmental Microbiology*, 57(11): 3310:
- Taranath, T. C., Patil, B. N., Santosh, T. U., & Sharath, B. S. (2015). Cytotoxicity of zinc nanoparticles fabricated by *Justicia adhatoda* L. on root tips of *Allium cepa* L.-- a model approach. *Environ Sci Pollut Res Int*, 22(11): 8611-8617: doi:10.1007/s11356-014-4043-9
- Teerapatsakul, C., Parra, R., Bucke, C., & Chitradon, L. (2007). Improvement of laccase production from *Ganoderma* sp. KU-Alk4 by medium engineering. *World Journal of Microbiology and Biotechnology*, 23(11): 1519-1527: doi:10.1007/s11274-007-9396-5
- Teerapatsakul, C., Pothiratana, C., Chitradon, L., & Thachepan, S. (2017). Biodegradation of polycyclic aromatic hydrocarbons by a thermotolerant white rot fungus

- Trametes polyzona* RYNF13. *J Gen Appl Microbiol*, 62(6): 303-312: doi:10.2323/jgam.2016.06.001
- Tekere, M., Zvauya, R., & Read, J. S. (2001). Ligninolytic enzyme production in selected sub-tropical white rot fungi under different culture conditions. *Journal of Basic Microbiology*, 41(2): 115-129: doi:10.1002/1521-4028(200105)41:2<115::AID-JOBM115>3.0.CO;2-S
- Terrazas-Siles, E., Alvarez, T., Guieysse, B., & Mattiasson, B. (2005). Isolation and characterization of a white rot fungus *Bjerkandera* sp. strain capable of oxidizing phenanthrene. *Biotechnology Letters*, 27(12): 845-851: doi:10.1007/s10529-005-6242-4
- Thongkred, P., Lotrakul, P., Prasongsuk, S., Imai, T., & Punnapayak, H. (2011). Oxidation of polycyclic aromatic hydrocarbons by a tropical isolate of *Pycnoporus coccineus* and its laccase. *ScienceAsia*, 37(3): doi:10.2306/scienceasia1513-1874.2011.37.225
- Tianara, A., Susan, D., & Sjamsuridzal, W. (2020). New recorded species of polypore for Indonesia found in Universitas Indonesia Depok Campus. *IOP Conference Series: Earth and Environmental Science*, 457: 012010: doi:10.1088/1755-1315/457/1/012010
- Ting, W. T. E., Yuan, S. Y., Wu, S. D., & Chang, B. V. (2011). Biodegradation of phenanthrene and pyrene by *Ganoderma lucidum*. *International Biodeterioration & Biodegradation*, 65(1): 238-242: doi:10.1016/j.ibiod.2010.11.007
- Tišma, M., Zelić, B., & Vasic-Racki, D. (2010). White-rot fungi in phenols, dyes and other xenobiotics treatment – a brief review. *Croatian Journal of Food Science and Technology*, 2(2): 34-47:
- Torres-Farrada, G., et al. (2019). Biodegradation of polycyclic aromatic hydrocarbons by native *Ganoderma* sp. strains: identification of metabolites and proposed degradation pathways. *Appl Microbiol Biotechnol*, 103(17): 7203-7215: doi:10.1007/s00253-019-09968-9
- Tortella, G., Durán, N., Rubilar, O., Parada, M., & Diez, M. C. (2015). Are white-rot fungi a real biotechnological option for the improvement of environmental health?

Critical Reviews in Biotechnology, 35(2): 165-172:
doi:10.3109/07388551.2013.823597

Trimurti, S., & Lariman (2018). Differences of basidiomycotina types in natural forest arboretum gardens unmul Samarinda. International Journal of Scientific and Technology Research, 7: 164-168:

Tropenbos International Indonesia, P. (2005). Biodiversity assessment : Gunung Lumut protection forest Balikpapan: Tropenbos International Indonesia Programme.

Tuisel, H., et al. (1990). Lignin peroxidase H₂ from *Phanerochaete chrysosporium*: Purification, characterization and stability to temperature and pH. Archives of Biochemistry and Biophysics, 279(1): 158-166: doi:[https://doi.org/10.1016/0003-9861\(90\)90476-F](https://doi.org/10.1016/0003-9861(90)90476-F)

Türkoğlu, Ş. (2007). Genotoxicity of five food preservatives tested on root tips of *Allium cepa* L. Mutation Research/Genetic Toxicology and Environmental Mutagenesis, 626(1): 4-14: doi:<https://doi.org/10.1016/j.mrgentox.2006.07.006>

Vaithanomsat, P., Waraporn, A., Oncheera, P., & Jirawate, C. (2010). Production of ligninolytic enzymes by white-rot fungus *Datronia* sp. KAPI0039 and their application for reactive dye removal. International Journal of Chemical Engineering, 2010: doi:10.1155/2010/162504

Valentín, L., Feijoo, G., Moreira, M. T., & Lema, J. M. (2006). Biodegradation of polycyclic aromatic hydrocarbons in forest and salt marsh soils by white-rot fungi. International Biodeterioration & Biodegradation, 58(1): 15-21: doi:<https://doi.org/10.1016/j.ibiod.2006.04.002>

Viswanath, B., Chandra, M., Pallavi, H., & Rajasekhar Reddy, B. (2010). Screening and assessment of lacasse producing fungi isolated from different environment samples. African Journal of Biotechnology (ISSN: 1684-5315) Vol 7 Num 8, 7:

Viswanath, B., Rajesh, B., Janardhan, A., Kumar, A. P., & Narasimha, G. (2014). Fungal laccases and their applications in bioremediation. Enzyme Research, 2014: 21: doi:10.1155/2014/163242

Wang, Q., Qian, Y., Ma, Y., & Zhu, C. (2018). A preliminary study on the newly isolated high laccase-producing fungi: screening, strain characteristics and induction of


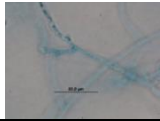
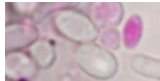

- laccase production. *Open Life Sciences*, 13(1): 463-469: doi:10.1515/biol-2018-0055
- Wang, S.-S., et al. (2017). Purification, characterization, and cloning of an extracellular laccase with potent dye decolorizing ability from white rot fungus *Cerrena unicolor* GSM-01. *International Journal of Biological Macromolecules*, 95: 920-927: doi:<https://doi.org/10.1016/j.ijbiomac.2016.10.079>
- Wariishi, H., Valli, K., & Gold, M. H. (1992). Manganese(II) oxidation by manganese peroxidase from the basidiomycete *Phanerochaete chrysosporium*. Kinetic mechanism and role of chelators. *Journal of Biological Chemistry*, 267(33): 23688-23695: doi:[https://doi.org/10.1016/S0021-9258\(18\)35893-9](https://doi.org/10.1016/S0021-9258(18)35893-9)
- Watanabe, T., Shirai, N., Okada, H., Honda, Y., & Kuwahara, M. (2001). Production and chemiluminescent free radical reactions of glyoxal in lipid peroxidation of linoleic acid by the ligninolytic enzyme, manganese peroxidase. *European Journal of Biochemistry*, 268(23): 6114-6122: doi:10.1046/j.0014-2956.2001.02557.x
- Waterborg, J. H., & Matthews, H. R. (1984). The Lowry method for protein quantitation. In J. M. Walker (Ed.), *Proteins* (pp. 1-3). Totowa, NJ: Humana Press.
- White, T., et al. (1990). Amplification and direct sequencing of fungal ribosomal RNA genes for phylogenetics. In *Pcr Protocols: a Guide to Methods and Applications* (Vol. 31, pp. 315-322). San Diego: Academic Press.
- Whittaker, R. H. (1969). New concepts of kingdoms of organisms. *Science*, 163(3863): 150: doi:10.1126/science.163.3863.150
- Winqvist, E. (2014). The potential of ligninolytic fungi in bioremediation of contaminated soils. (Doctoral Dissertation), Aalto University Helsinki
- Wirasnita, R., & Hadibarata, T. (2016). Potential of the white-rot fungus *Pleurotus pulmonarius* F043 for degradation and transformation of fluoranthene. *Pedosphere*, 26(1): 49-54: doi:10.1016/s1002-0160(15)60021-2
- Wu, Q., et al. (2019). Assessing pollution and risk of polycyclic aromatic hydrocarbons in sewage sludge from wastewater treatment plants in China's top coal-producing region. *Environ Monit Assess*, 191(2): 102: doi:10.1007/s10661-019-7225-6


- Xu, F. (1997). Effects of redox potential and hydroxide inhibition on the pH activity profile of fungal laccases. *Journal of Biological Chemistry*, 272(2): 924-928: doi:<https://doi.org/10.1074/jbc.272.2.924>
- Yadav, A., et al. (2019). Phytotoxicity, cytotoxicity and genotoxicity evaluation of organic and inorganic pollutants rich tannery wastewater from a Common Effluent Treatment Plant (CETP) in Unnao district, India using *Vigna radiata* and *Allium cepa*. *Chemosphere*, 224: 324-332: doi:<https://doi.org/10.1016/j.chemosphere.2019.02.124>
- Yamashita, S., Hattori, T., Ohkubo, T., & Nakashizuka, T. (2009). Spatial distribution of the basidiocarps of aphyllphoraceous fungi in a tropical rainforest on Borneo Island, Malaysia. *Mycological Research*, 113(10): 1200-1207: doi:<https://doi.org/10.1016/j.mycres.2009.08.004>
- Yang, J., Lin, Q., Ng, T. B., Ye, X., & Lin, J. (2014). Purification and characterization of a novel laccase from *Cerrena* sp. HYB07 with dye decolorizing ability. *PLoS One*, 9(10): e110834: doi:10.1371/journal.pone.0110834
- Yang, S., et al. (2013). Understanding the factors controlling the removal of trace organic contaminants by white-rot fungi and their lignin modifying enzymes: A critical review. *Bioresource Technology*, 141: 97-108: doi:<https://doi.org/10.1016/j.biortech.2013.01.173>
- Yin, L., Ye, J., Kuang, S., Guan, Y., & You, R. (2017). Induction, purification, and characterization of a thermo and pH stable laccase from *Abortiporus biennis* J2 and its application on the clarification of litchi juice. *Bioscience, Biotechnology, and Biochemistry*, 81(5): 1033-1040: doi:10.1080/09168451.2017.1279850
- Zhang, H., et al. (2016). Characterization of a manganese peroxidase from white-rot fungus *Trametes* sp.48424 with strong ability of degrading different types of dyes and polycyclic aromatic hydrocarbons. *J Hazard Mater*, 320: 265-277: doi:10.1016/j.jhazmat.2016.07.065
- Zhang, S., et al. (2015). Contrasting characteristics of anthracene and pyrene degradation by wood rot fungus *Pycnoporus sanguineus* H1. *International Biodeterioration & Biodegradation*, 105: 228-232: doi:<https://doi.org/10.1016/j.ibiod.2015.09.012>

- Zhou, X., et al. (2014). Effects of azide on electron transport of exoelectrogens in air-cathode microbial fuel cells. *Bioresource Technology*, 169: 265-270: doi:<https://doi.org/10.1016/j.biortech.2014.07.012>
- Zhou, X., Wen, X., & Feng, Y. (2007). Influence of glucose feeding on the ligninolytic enzyme production of the white-rot fungus *Phanerochaete chrysosporium*. *Frontiers of Environmental Science & Engineering in China*, 1: 89-94: doi:10.1007/s11783-007-0017-1
- Zhu, C., Bao, G., & Huang, S. (2016). Optimization of laccase production in the white-rot fungus *Pleurotus ostreatus* (ATCC 52857) induced through yeast extract and copper. *Biotechnology & Biotechnological Equipment*, 30(2): 270-276: doi:10.1080/13102818.2015.1135081
- Zhuo, R., & Fan, F. (2021). A comprehensive insight into the application of white rot fungi and their lignocellulolytic enzymes in the removal of organic pollutants. *Science of The Total Environment*, 778: 146132: doi:<https://doi.org/10.1016/j.scitotenv.2021.146132>

APPENDIX A

Fungal record sheet

<p>No Isolate PBURU 12</p> 	Date of Collection	13 May 2012
	Name	<i>Trametes polyzona</i>
	Family	Polyporaceae
	Class	Basidiomycetes
<p>Macroscopic Characters</p>	Shape	Annual to perennial
	Size	single pilei up to 10 cm wide and 15 cm long
	Texture	Flexible to corky
	Pileus	yellowish-ochraceous when fresh, soon darker, fulvous, ochraceous-brown or greyish-brown, margin thin
	Stipe	-
	Context	Duplex, ochraceous to yellowish-brown
	Pore surface	Cream to beige
	Pores	Angular to round (2-3 mm)
	Tube layer(s)	Concolorous with pore surface
	Color	Cream to beige (fresh); darkens to yellowish-brown (old)
	Hymenophore	Round
	Fruiting body	fused laterally to elongated lobed fruitingbodies
<p>Macroscopic Characters</p>	Hyphal system	Trimitic <ul style="list-style-type: none"> - Skeletal hyphae: 3-5 μm - Generative hyphae with clamps: 1-3 μm - Binding hyphae: 3-5 μm
	Cystidia	-
	Clamp connection	Present 
	Sterile element	-
	basidiospores	Oblong to ellipsoid, smooth thin walled 3-7 \times 2-3 μ m 
	basidia	Clavate with 4 sterigmata 
<p>H a p i t e</p>	Substrate/host	Dead tree, falling tree

	Seasonality	All year
	Type of decay	White rot
Biochemical Tests 	Water (control)	No color
	KOH	Not turn to black
	MELZER REAGENT	Inamyloid
	Lugol	-
Notes		
References		Norw. J. Bot. 19(3-4):230, 1972



APPENDIX B

Culture medium

The basal medium for LMEs production (Revankar & Lele, 2006)

Per one liter of basal medium was prepared by mixing solutions given below:

1. Glucose	20 g
2. KH_2PO_4	1 g
1 $\text{MgSO}_4 \cdot 7\text{H}_2\text{O}$	0.5 g
2 CaCl_2	0.01 g
3 $\text{FeSO}_4 \cdot 7\text{H}_2\text{O}$	0.01 g
4 $\text{MnSO}_4 \cdot 4\text{H}_2\text{O}$	0.001 g
5 $\text{ZnSO}_4 \cdot 7\text{H}_2\text{O}$	0.001 g
6 $\text{CuSO}_4 \cdot 5\text{H}_2\text{O}$	0.002 g

The pH was adjusted to 5.0 after sterilization at 121°C for 15 minutes.

Potato dextrose agar (PDA)

Glucose	20	gram
Fresh potato	200	gram
Agar	20	gram
Distilled H ₂ O to	1	liter

All the components were mix together. Sterilization was conducted at 120 °C, for 15 minutes.

Malt extract agar (MEA)

Glucose	20	gram
Malt extract broth	20	gram
Agar	20	gram
Distilled H ₂ O to	1	liter

All the components were mix together. Sterilization was conducted at 120 °C, for 15 minutes.

APPENDIX C

Enzyme calculation

Lignin modifying enzymes assays

Lignin peroxidase, manganese peroxidase and laccase activities was calculated by using the same equation as follow

$$\text{Enzyme activity} = \frac{\text{Absorbance of enzyme} \times \text{standard factor}}{\text{time of incubation (minute)}}$$

Whereas

$$\text{Standard factor} = \frac{\text{Concentration } (\frac{\mu\text{mol}}{\text{ml}})}{\text{Absorbance}}$$

$$A = \epsilon \times l \times c$$

Where A = Absorbance

ϵ = coefficient

c = concentration

l = path length

จุฬาลงกรณ์มหาวิทยาลัย
CHULALONGKORN UNIVERSITY

Laccase assay

A total of 1 ml laccase assay mixture contained:

Enzyme solution	0.10 ml
5 mM ABTS	0.10 ml
100 mM sodium acetate buffer (pH 5.0)	0.80 ml

Manganese peroxidase assay

A total of 1 ml Manganese peroxidase assay mixture contained:

Enzyme solution	0.10 ml
0.2 mM 2, 6 Dimethoxy phenol	0.10 ml
0.5 mM MnSO ₄	0.10 ml
25 mM sodium tartrate buffer (pH 5.0)	0.65 ml
0.1 mM H ₂ O ₂	0.05 ml

The reaction was started by addition of H₂O₂



APPENDIX D

Protein determination and purification

1. Lowry protein assay

- Solution A

CuSO ₄	0.5 g
Na ₂ C ₄ H ₄ O ₆ ·2H ₂ O	1.0 g
Distilled H ₂ O to	100 ml

The solution was kept in dark bottle at room temperature

- Solution B

Na ₂ CO ₃	20.0 g
NaOH	4.0 g
Distilled H ₂ O to	1.0 l

The solution was kept in dark bottle at room temperature

- Solution C

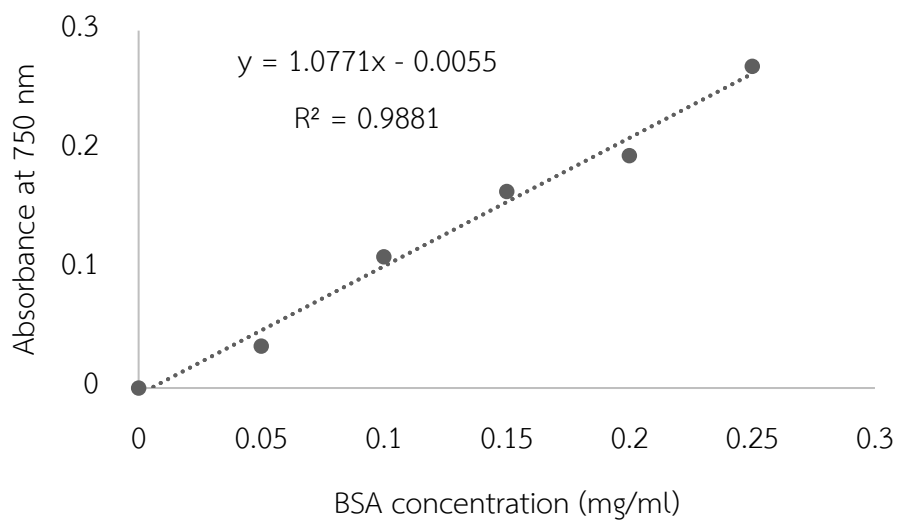
Solution A (5 ml) + Solution B (500 ml) ratio (1:100)

- Solution D

Folin-Ciocalteu reagent	10 ml
(prepared fresh)	
Distilled H ₂ O	10 ml

Protocol:

Add 0.5 enzyme sample to 5 ml test tube, then add 2.5 ml solution C. Vortex the solution and incubate at room temperature for 10 minutes. Add 0.25 ml solution D and vortex. Incubate the solution for 30 minutes, measure the absorbance at 750 nm. Standard curve was prepared by diluting BSA in 6 concentrations (0-0.25 mg/ml).



APPENDIX E

Optimization of laccase production

Plackett-burman experimental design matrix for screening of laccase production

Run	X1	X2	X3	X4	X5	X6	X7	X8	X9	X10	X11
1	+1	-1	-1	-1	+1	-1	+1	+1	-1	+1	+1
2	-1	-1	-1	+1	-1	+1	+1	-1	+1	+1	+1
3	+1	-1	+1	+1	-1	+1	+1	+1	-1	-1	-1
4	+1	+1	+1	-1	-1	-1	+1	-1	+1	+1	-1
5	-1	-1	+1	-1	+1	+1	-1	+1	+1	+1	-1
6	+1	+1	-1	+1	+1	+1	-1	-1	-1	+1	-1
7	-1	+1	+1	-1	+1	+1	+1	-1	-1	-1	+1
8	-1	+1	+1	+1	-1	-1	-1	+1	-1	+1	+1
9	+1	+1	-1	+1	+1	-1	+1	+1	+1	-1	-1
10	-1	-1	-1	-1	-1	-1	-1	-1	-1	-1	-1
11	+1	+1	-1	-1	-1	+1	-1	+1	+1	-1	+1
12	+1	-1	+1	+1	+1	-1	-1	-1	+1	-1	+1

APPENDIX F

AMES TEST PROTOCOL (*Salmonella typhimurium*)

The strain TA98 and TA100 were maintained in 2% (v/v) commercial nutrient broth (NB) medium:

1. Nutrient broth 20 g
2. Distilled H₂O up to 1 liter

Mix and dissolve them completely. Sterilize by autoclaving at 121°C for 15 minutes.

Ames test medium (Mortelmans & Zeiger, 2000):

1. Vogel-Bonner medium (VB)

Ingredients per 500 ml

Warm distilled H₂O 335 ml

MgSO₄·7H₂O 5 g

Citric acid monohydrate 50 g

K₂HPO₄ 250 g

NaNH₄HPO₄·4H₂O 87.5 g

- Salts are added to the warm water in a flask. Place the flask on a hot plate.
- After each salt dissolves entirely, transfer the solution into glass bottles and autoclave for 15 min at 121°C.
- When the solution gets cool, cap the bottle tightly.
- Store the solution at 4°C.

2. 0.5 mM histidine/biotin solution

Ingredients Per 125 ml

- D-Biotin (F.W. 247.3) 15.45 mg
- L-Histidine·HCl (F.W. 191.7) 12.0 mg
- Distilled H₂O 125 ml

Dissolve the biotin in hot distilled water. The solution is autoclaved for 15 min, at 121°C and then stored at 4°C.

3. Minimal glucose agar (MGA)

Ingredients Per 500 ml

- Agar 7.5 g
- Distilled H₂O 465 ml
- VB salts (Recipe 1) 10 ml
- 40% glucose 25 ml

Add agar in 465 ml of distilled water and autoclave for 15 min, at 121°C. After cooling, add the salts and glucose gently.

4. 0.2 M sodium phosphate buffer, pH 7.4

Ingredients Per 250 ml

- 0.2 M NaH₂PO₄·H₂O 30 ml (6.9 g/250 ml)
- 0.2 M Na₂HPO₄ 220 ml (7.1 g/250 ml)

Adjust pH to 7.4. Sterilize the buffer by autoclaving for 15 min at 121°C.

5. Procedures:

- Bacteria culture was grown in 2% nutrient broth medium.
- Preparation of minimal glucose agar (MGA) plates: mix the medium of MGA and pour 25 ml into each petri dish.
- To the 2 ml sterile Eppendorf tubes, add the following:
 - a. 0.1 ml fresh bacteria culture (TA98 and TA100)

- b. 0.2 ml of His/Bio solution
 - c. 0.5 ml sodium phosphate buffer
 - d. 0.1 ml test sample
 - e. Make it up to 1 ml using autoclaved distilled H₂O.
- Mix the contents of Eppendorf tube and pour onto petri dish and spread using spreader on the surface of MGA plates.
 - Incubate for 48 hours at 37°C while inverted.
 - Count the spontaneous revertants colonies that appear and clearly visible with unaided eyes.



APPENDIX G

Fasta format of internal transcribed spacers (ITS) of white-rot fungi

>*Trametes polyzona* PBURU 12

```
CCCTGGCGGGAAGGATCATTAAACGAGTTTTGAAATGGGTTGTAGCTGGCCTTCCGAGGCATGTG
CACACCCTGCTCATCCACTTTACACCTGTGCACTTACTGTAGGTTGGCGTGGGCTTCGGACCTC
CGGGTTCGAGGCATTCTGCCGGCCTATGTACAATACAACTCCGAAGTAACAGAATGTAAACGC
GTCTAACGCATCTTAATACAACCTTTCAGCAACGGATCTCTTGGCTCTCGCATCGATGAAGAACG
CAGCGAAATGCGATAAGTAATGTGAATTGCAGAATTCAGTGAATCATCGAATCTTTGAACGCAC
CTTGCGCTCCTTGGTATTCCGAGGAGCATGCCTGTTTGAGTGTGCATGGAATTCTCAACCCATAG
ATCCTTGTGGTCTACGGGCTTGGATTTGGAGGCTTGCCGGCCCTTACACGGGGTCCGGCTCCTCT
TGAATGCATTAGCTTGATTCCGTGCGAATCGGCTCTCAGTGTGATAATTGTCTACGCTGTGGCC
GTGAAGCGTTTGGCGAGCTTCTAACCGTCCGTTAGGACAACCTTCTTGACATCTGACCTCAAATC
AGGTAGGACTACCCGCTGAACTTAAGC
```

APPENDIX H
Taxa used for phylogenetic study

Species name	Sampel no.	ITS GenBank accession number
<i>Coriolopsis polyzona</i>	Cof143	FJ904854
<i>Coriolopsis polyzona</i>	Dai9468	FJ627248
<i>Coriolopsis polyzona</i>	Dai9495	FJ627247
<i>Coriolopsis polyzona</i>	BR311	GQ141700
<i>Phellinus igniarius (outgroup)</i>	BRNM 714866	GQ383710
<i>Trametes conchifer</i>	KUC20121123-36	KJ668445
<i>Trametes conchifer</i>	Dai8359	KC848278
<i>Trametes ectypa</i>	Cui 2580	KX880637
<i>Trametes ectypa</i>	FP103976sp	JN164961
<i>Trametes elegans</i>	28	EU661879
<i>Trametes elegans</i>	BCC23751	BCC23751
<i>Trametes gibbosa</i>	Cui7390	KC848302
<i>Trametes gibbosa</i>	CFMR:RF5JR	KU668971
<i>Trametes hirsuta</i>	Dai9586	KC848300
<i>Trametes hirsuta</i>	XSD-65	EU326211
<i>Trametes junipericola</i>	-	AY684171
<i>Trametes junipericola</i>	145295(O)	KC017758
<i>Trametes maxima</i>	UOC KAUNP MK78b	KR907875
<i>Trametes maxima</i>	Dai12274	KC848310
<i>Trametes membranacea</i>	X668	KF573010
<i>Trametes membranacea</i>	CRM125	JN164956
<i>Trametes ochracea</i>	Dai2005	KC848272
<i>Trametes ochracea</i>	CIRM-BRFM 632	FJ349624
<i>Trametes polyzona</i>	PBURU 12	KY234233
<i>Trametes polyzona</i>	IPBCC	LC412113

Species name	Sampel no.	ITS GenBank accession number
<i>Trametes polyzona</i>	WR710-1	JN848329
<i>Trametes polyzona</i>	BKW01	JN164980
<i>Trametes polyzona</i>	OH272sp	JN164979
<i>Trametes polyzona</i>	RYNF13	KT281117
<i>Trametes pubescens</i>	Cui7569	KC848292
<i>Trametes pubescens</i>	KUC20121102-13	KJ668443
<i>Trametes suaveolens</i>	Dai8290	KC848284
<i>Trametes suaveolens</i>	KUC20121109-10	KJ668441
<i>Trametes versicolor</i>	XSD-4	EU273523
<i>Trametes versicolor</i>	4490	AY968080
<i>Trametes villosa</i>	CBS 678.70	MH859898
<i>Trametes villosa</i>	BKO25	MK020684



จุฬาลงกรณ์มหาวิทยาลัย
CHULALONGKORN UNIVERSITY

VITA

NAME Retno Wulandari

DATE OF BIRTH 13 December 1983

PLACE OF BIRTH Samarinda

INSTITUTIONS ATTENDED Mulawarman University

HOME ADDRESS Baansuan Apartment, 67 Pracha Uthit 69 Rd, Thung Khru, Bangkok, 10140

PUBLICATION Wulandari, R., Lotrakul, P., Amirta, R., Kim, S., Punnapayak, H., & Prasongsuk, S. (2018). First record of *Ceriporia inflata* and *Ceriporia lacerata* (Phanerochaetaceae, Basidiomycota) from Indonesian tropical forest. *Agriculture and Natural Resources*, 52. doi:10.1016/j.anres.2018.10.017

Wulandari, R., Lotrakul, P., Punnapayak, H., Amirta, R., Kim, S. W., & Prasongsuk, S. (2021). Toxicity evaluation and biodegradation of phenanthrene by laccase from *Trametes polyzona* PBURU 12. 3 *Biotech*, 11(1), 32. doi:10.1007/s13205-020-02556-z